AD_____

METABOLISM, SEIZURES, AND BLOOD FLOW IN BRAIN FOLLOWING ORGANOPHOSPHATE EXPOSURE: MECHANISMS OF ACTION AND POSSIBLE THERAPEUTIC AGENTS

Final Summary Report

Lester R. Drewes, Ph. D.
Professor of Biochemistry

January 31, 1991

Supported by

U.S. ARMY MEDICAL RESEARCH AND DEVELOPMENT COMMAND
Fort Detrick, Frederick, Maryland 21702-5012

Contract No. DAMD17-86-C-6036

Department of Biochemistry and Molecular Biology
School of Medicine
University of Minnesota
Duluth, Minnesota 55812

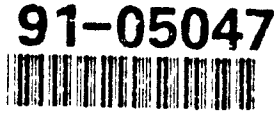

Unclassified
SECURITY CLASSIFICATION OF THIS PAGE

REPORT DOCUMENTATION PAGE

Form Approved OMB No. 0704-0188

1a. REPORT SECURITY CLASSIFICATION: Unclassified	1b. RESTRICTIVE MARKINGS
2a. SECURITY CLASSIFICATION AUTHORITY	3. DISTRIBUTION/AVAILABILITY OF REPORT: Approved for public release; distribution unlimited.
2b. DECLASSIFICATION/DOWNGRADING SCHEDULE	
4. PERFORMING ORGANIZATION REPORT NUMBER(S)	5. MONITORING ORGANIZATION REPORT NUMBER(S)
6a. NAME OF PERFORMING ORGANIZATION: University of Minnesota, Duluth; 6b. OFFICE SYMBOL (If applicable)	7a. NAME OF MONITORING ORGANIZATION
6c. ADDRESS (City, State, and ZIP Code): Duluth, Minnesota 55812-2487	7b. ADDRESS (City, State, and ZIP Code)
8a. NAME OF FUNDING/SPONSORING ORGANIZATION: U.S. Army Medical Research and Development Command; 8b. OFFICE SYMBOL (If applicable)	9. PROCUREMENT INSTRUMENT IDENTIFICATION NUMBER: Contract No. DAMD17-86-C-6036
8c. ADDRESS (City, State, and ZIP Code): Fort Detrick, Frederick, Maryland 21702-5012	10. SOURCE OF FUNDING NUMBERS: PROGRAM ELEMENT NO. 61102A; PROJECT NO. 3M1 61102BS10; TASK NO. EF; WORK UNIT ACCESSION NO. 408

11. TITLE (Include Security Classification): Metabolism, Seizures, and Blood Flow Following Organophosphate Exposure: Mechanisms of Action and Possible Therapeutic Agents. (Unclassified)

12. PERSONAL AUTHOR(S): Lester R. Drewes

13a. TYPE OF REPORT	13b. TIME COVERED	14. DATE OF REPORT (Year, Month, Day)	15. PAGE COUNT
Final Report	FROM 10/21/85 TO 7/20/90	1991 January 31	114

16. SUPPLEMENTARY NOTATION

17. COSATI CODES			18. SUBJECT TERMS (Continue on reverse if necessary and identify by block number)
FIELD	GROUP	SUB-GROUP	
06	01		soman; sarin; brain; vasodilation; seizure; protein synthesis cholinergic; phospholipids; phospholipase D; muscarinic;
06	15		metabolism; phosphatidylcholine; blood flow; (continued)

19. ABSTRACT (Continue on reverse if necessary and identify by block number)

Acute neurotoxicity of the organophosphorus (OP) compounds soman and sarin was investigated using the isolated, perfused canine brain preparation under constant perfusion pressure conditions. This model allows comprehensive study of metabolic (biochemical) and physiologic (vascular, electrical) responses to neurotoxicants. Intracarotid administration of soman (100 μg) or sarin (400 μg) produced cerebral vasodilation and synchronization of brain electrical activity prior to seizure genesis. OP-induced changes in cerebral blood flow and vasodilation were extensive. Increased neuronal discharge is associated with dramatic increases in cerebral oxygen and glucose metabolism. Regional autoradiography using D-[6-^{14}C]glucose showed increased glucose metabolism in all brain regions. Metabolite transport systems of brain microvasculature were uninhibited by OP exposure. Studies using L-[1-^{14}C]leucine and autoradiography showed protein synthesis that was greatest in cortical gray

20. DISTRIBUTION/AVAILABILITY OF ABSTRACT: ☐ UNCLASSIFIED/UNLIMITED ☒ SAME AS RPT ☐ DTIC USERS	21. ABSTRACT SECURITY CLASSIFICATION: Unclassified
22a. NAME OF RESPONSIBLE INDIVIDUAL: Mrs. Virginia Miller	22b. TELEPHONE (Include Area Code): 301/663-7325; 22c. OFFICE SYMBOL: SGRD-RMI-S

DD Form 1473, JUN 86 — Previous editions are obsolete. — SECURITY CLASSIFICATION OF THIS PAGE: Unclassified

Block 18, Subject Terms, continued.
nitric oxide; perfusion

Block 19, Abstract, continued.

matter, hippocampus, cerebellar gray matter, and some regions of brain stem was reduced by an average of ~60% after OP exposure. Based on results with cholinergic antagonists, the development of seizure activity and OP-induced vasodilation are separate, independent responses; simple involvement of cholinergic nicotinic, dopaminergic, or adrenergic mechanisms in OP-induced vasodilation is excluded. Nitric oxide, a recently identified endothelium-derived vasodilator, is a potent cerebrovasodilator, and OP compounds may cause vasodilation by mechanisms of its action on smooth muscle cells or stimulation of nitric oxide formation. Brain choline (Ch) levels rise following exposure to acetylcholinesterase inhibitors. Increased Ch levels during OP exposure, despite inhibition of acetylcholine (ACh) hydrolysis, suggest another means of Ch production. Blood-brain transport of lysophosphatidylcholine is not a significant source of Ch or phospholipid precursors. A phospholipase D capable of hydrolyzing phosphatidylcholine (PC) to free Ch was detected and characterized. It was discovered that a muscarinic ACh receptor is coupled to PC phospholipase D via a cholera toxin-sensitive G protein and this mechanism couples the neuronal muscarinic receptor to cellular responses.

Editor and preparer of final report: Carolyn Clark

AD_____

METABOLISM, SEIZURES, AND BLOOD FLOW IN BRAIN FOLLOWING ORGANOPHOSPHATE EXPOSURE: MECHANISMS OF ACTION AND POSSIBLE THERAPEUTIC AGENTS

Final Summary Report

Lester R. Drewes, Ph. D.
Professor of Biochemistry

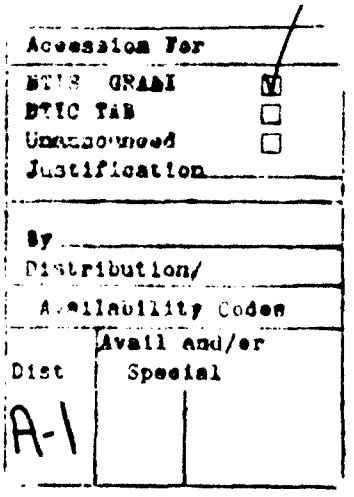

January 31, 1991

Supported by

U.S. ARMY MEDICAL RESEARCH AND DEVELOPMENT COMMAND
Fort Detrick, Frederick, Maryland 21702-5012

Contract No. DAMD17-86-C-6036

Department of Biochemistry and Molecular Biology
School of Medicine
University of Minnesota
Duluth, Minnesota 55812

SUMMARY

The acute neurotoxicity of the organophosphorus (OP) compounds soman and sarin was investigated using the isolated, perfused canine brain preparation. This experiment model allows a comprehensive study of the metabolic (biochemical) and physiologic (vascular and electrical) responses to neurotoxicants because extracerebral tissues and influences are absent, biochemical and physiological parameters without significant alterations in baseline data may be determined for experimental periods (≤120 min), and blood and tissue samples may be readily collected for quantitative biochemical analyses.

Administration of soman (100 μg) or sarin (400 μg) produced cerebral vasodilation and synchronization of brain electrical activity (measured by electroencephalogram) for 4-6 min prior to seizure onset. OP-induced changes in cerebral blood flow and vasodilation were determined by regional distribution of the radiolabeled blood flow tracer iodoantipyrine. Increases were manifested extensively and, with the exception of the caudate nucleus, white matter, and pituitary, were approximately doubled. Variations observed may reflect either a region-specific dilation response or a variable, maximal blood flow capacity of contributing vessels. Increased brain electrical activity (seizure) is associated with rapid, large increases in cerebral metabolic rates for glucose, oxygen, lactate, and carbon dioxide. The regional autoradiographic method using D-[6-^{14}C]glucose showed glucose metabolism to be increased in all brain regions. Infusion of L-[1-^{14}C]leucine and subsequent autoradiography of brain sections clearly revealed brain regions with active protein synthesis, with the greatest rates occurring in cortical gray matter, hippocampus, cerebellar gray matter, and some regions of the brain stem. OP exposure reduced brain protein synthesis by 40-60% in all brain regions examined.

Previous experiments with cholinergic antagonists atropine and scopolamine and with cholinergic agonists oxotremorine and arecoline have established the involvement of a cholinergic muscarinic mechanism in OP-induced seizure, but not in OP-induced vasodilation. To evaluate the possible involvement of other transmitter mechanisms in these events, experiments were conducted with specific antagonists: scopolamine, mecamylamine, propranolol, pimozide, and cimetidine. It was concluded that the development of seizure activity and the vasodilation induced by OP agents are separate and independent responses. Consequently, independent mechanisms must exist for OP-induced cerebral vasodilation.

Blood-brain transport studies indicated that a small increase in metabolite (glucose, leucine, glycine, and choline [Ch]) influx occurred during the first 20 min of OP exposure. This may result from the increase in vasodilation (increased vascular surface area) or from direct activation of transporters by a regulatory mechanism. Blood-brain transport studies also indicated that influx of [^{3}H]lysophosphatidylcholine (lysoPC) into all areas of the brain investigated was low when compared to blood-borne metabolic substrates, such as glucose and amino acids. It is concluded that blood-brain transport of lysoPC does not serve as a significant source of brain Ch or brain phospholipid precursors.

The permeability of the brain vasculature to palmitate and oleate was relatively low (2-43 ml/g·sec·10^{5}; pituitary, 71 ml/g·sec·10^{5}), but varied significantly among regions, with white matter being least permeable and cerebrum most permeable. Transport of oleic acid into brain was significantly greater (threefold) than palmitic acid transport. Following soman exposure, blood-brain transport of palmitate, but not oleate, increased two- to threefold. The metabolic fates of the free fatty acids after they entered the brain were determined by regional analysis of brain lipids. In control experiments, 40-60% of the radioactive palmitic acid was recovered in phosphatidylcholine (PC), with the remainder distributed in the free fatty acid fraction and in other phospholipid fractions. Following soman exposure, the pattern of [^{3}H]palmitate labeling, but not [^{3}H]oleate, was dramatically changed. The total radioactivity of the extracted lipid was significantly increased and resulted from a two- to eightfold increase in the radioactivity of the free fatty acid fraction. This increase was at the expense of incorporation into all the other lipids, which consistently had decreased amounts of labeled fatty acids. These results indicate that the metabolism, but not transport, of palmitate is drastically altered by soman exposure and during soman-induced seizure. The data further suggest that the rate of

phospholipid synthesis is decreased, or the rate of phospholipid degradation is increased, or both. The pathway and mechanism for breakdown of phospholipids and production of unesterified Ch during OP intoxication were investigated with brain enzyme preparations (microsomal and synaptosomal) and radioactive substrates. The hydrolytic activity of microsomal phospholipase D from canine cerebral cortex was measured by a radiochemical assay using 1,2-dipalmitoyl-*sn*-glycerol-3-phosphoryl[^{3}H]choline and analysis of released [^{3}H]Ch. Of several detergents tested, Triton X-100 was found to be the most effective in allowing expression of phospholipase D hydrolytic activity. The microsomal phospholipase D does not require any metal ion for its hydrolytic activity. Calcium and magnesium were slightly inhibitory, causing a loss of more than 90% activity at the 4 mM concentration. Nonhydrolyzable guanine nucleotide analogues, such as GTPγS and GMPPCP, but not GDPβS, at micromolar concentrations, were persistently able to stimulate phospholipase D hydrolytic activity. GDPβS was capable of partially blocking GTPγS stimulation of phospholipase D. Aluminum fluoride was also able to cause a two- to threefold increase in hydrolytic activity of phospholipase D. Cholera toxin had a stimulatory effect on hydrolytic activity of phospholipase D, whereas islet-activating protein pertussis toxin had no effect. These studies with canine cerebral cortex synaptosomes demonstrate that the guanine-nucleotide-binding protein- (G protein) regulated phospholipase D is directly linked to a muscarinic acetylcholine (ACh) receptor and that this pathway may be responsible for the rapid accumulation of phosphatidic acid and Ch in the central nervous system during OP intoxication. Our evidence demonstrates that a muscarinic ACh receptor is coupled to PC phospholipase D via a cholera toxin-sensitive G protein and that this mechanism is a novel signal transduction process coupling the neuronal muscarinic receptor to cellular responses. Furthermore, it is suggested that this pathway plays an important role in brain Ch metabolism and that these enzymes and regulatory proteins may be important targets of OP agents. The significance of this regulated process for supplying free Ch in the brain is especially evident when hydrolysis of ACh to Ch is blocked by acetylcholinesterase inhibitors. Further investigations of this newly discovered phospholipase D pathway will be of great benefit to our understanding of mechanisms of signal transduction and regulation of Ch and phospholipid metabolism in the central nervous system and the roles that these pathways play during periods of OP intoxication and therapeutic recovery. It is also believed that activation of phospholipases may be responsible for membrane degradation and eventually cell death. Soman, physostigmine, and diisopropylfluorophosphate were used to examine the direct effects of inhibitors on the hydrolysis of exogenous [^{3}H]PC by synaptosomes prepared from canine cerebral cortex. Soman and physostigmine had slight stimulatory effects on hydrolysis, but diisopropylfluorophosphate did not.

To evaluate the possible involvement of neurotransmitter systems other than the cholinergic muscarinic type in seizure genesis, experiments were conducted with specific receptor antagonists. None of the selected antagonists prevented the characteristic responses to soman exposure. Results indicate that simple involvement of cholinergic nicotinic, dopaminergic, adrenergic, or histaminergic mechanisms in OP-induced vasodilation and seizure may be excluded. In addition, pretreatment with the anticonvulsant valproic acid was ineffective in inhibiting soman-induced responses. Neither pyridostigmine nor HI-6 altered cerebral metabolism or, when administered prior to OP, prevented OP-induced convulsions, presumably because of their inability to cross the blood-brain barrier. Physostigmine, which is more lipid soluble, penetrated the blood-brain barrier, and its acute effects (vasodilation and seizure) were similar to the effects of soman. However, cholinergic antagonists blocked physostigmine responses; OP responses were not blocked. This is the clear distinction between the actions of OP compounds and carbamate anticholinesterases. However, when the brain was pretreated with scopolamine and physostigmine and then exposed to OP compounds, the vasodilation was blocked. This blocking of OP-induced vasodilation by the combination of physostigmine and scopolamine represents to our knowledge the first demonstration of the antagonism of this pathophysiological effect of OP agents. Neostigmine was able to prevent OP-induced vasodilation, but its presence precipitated seizure genesis. We tested the vasodilator activity of nitric oxide, proposed to be an endothelium-dependent relaxing factor in several tissues, on the cerebral vasculature and found it to be a potent dilator. Nitro blue tetrazolium, an inhibitor of nitric oxide, when present in the perfusate, blocked soman-induced vasorelaxation. This suggests that OP compounds may cause vasodilation by stimulating the formation of nitric oxide, and the pathway and mechanism may be targets for therapeutic intervention.

FOREWORD

This report describes the progress and results during a five-year research project. Appropriate comments are made by the principal investigator on the significance of the results and on their relevance to the comprehensive study. These comments are provided in the context of the overall goal of suggesting methods for preventing organophosphorus effects on human health.

In conducting the research described in this report, the investigators adhered to the "Guide for the Care and Use of Laboratory Animals," prepared by the Committee of the Institute of Laboratory Animal Resources on Care and Use of Laboratory Animals, National Research Council (DHEW Publication No. (NIH) 86-23, Revised 1985).

Citation of commercial organizations and trade names in this report does not constitute an official Department of the Army endorsement or approval of the products or services of these organizations.

TABLE OF CONTENTS

TABLE OF CONTENTS, continued

TABLES

FIGURES

FIGURES, continued

INTRODUCTION

Organophosphate (OP) compounds comprise a major class of chemicals used as insecticides, primarily by agricultural workers and in chemical warfare. These compounds are highly toxic, and an accidental overdose can result in confusion, loss of reflexes, seizure, coma, and, ultimately, death (1). The development of effective prophylactic or therapeutic intervention methods requires the thorough understanding of the mechanism(s) of action and the sequential events leading to the pathophysiological state. Because OP compounds are potent inhibitors of acetylcholinesterase (AChE), most previous work has focused on their actions at the neuromuscular junctions. In recent years, evidence has been growing to suggest that OP toxicity is not exclusively the result of inhibition of AChE, but also of a number of pathophysiological alterations occurring in the central nervous system (CNS) (2). In this report, we present studies using the isolated canine brain perfused at constant pressure to allow cerebral blood flow to vary freely in response to changes in vascular resistance. These studies are the conclusion of a research project designed to examine the effects of OP exposure on brain metabolism and blood flow with the goals of understanding the underlying mechanisms of OP intoxication and suggesting means of therapeutic intervention.

BACKGROUND

The isolated, perfused canine brain is an important tool for studying cerebral metabolism and blood-brain transport, and several reasons exist for using it in toxicity studies. Traditionally, investigations of neurotoxicants have centered on either *in vitro* studies with simple systems or *in vivo* studies using whole animal systems. With *in vitro* systems, many membrane barriers are demolished and enzymes are exposed to unfamiliar substrates and unusual concentrations of natural substrates. In addition, the methods of preparing brain slices, homogenates, or various cell organelles involve periods of anoxia or ischemia that may result in adverse and irreversible changes. After obtaining data from such systems and making appropriate corrections for artifacts resulting from preparation, one is confronted with the task of relating experimental results to the naturally occurring processes of the intact organ. *In vivo* preparations would simplify this task were it not for physiologic and metabolic interference from other tissues. A properly prepared isolated organ overcomes the stated disadvantages of both *in vitro* and *in vivo* systems. When care is taken to maintain the brain in a physiologic environment before and after isolation, it serves as an excellent tool for the comprehensive study of the metabolic and physiologic responses to neurotoxicants, such as the OPs. A closed, extracorporeal perfusion system permits the control of perfusate composition and flow rate, and constant arterial pressure can be sustained. Both arterial and venous blood samples may be obtained without contamination from other organs. Quantification of solute uptake is permitted because both flow rate and brain weight can be measured directly. Metabolic and physiologic studies can be readily related to *in vivo* processes because the brain is maintained in an active, functioning state, and the blood-brain barrier remains intact. At any time during an experiment, frozen tissue samples are easily obtained from the brain through a craniotomy. A final, but important, feature of the isolated canine brain is the economy that results from the ability to collect a large quantity of data and perform more than one experiment using a single preparation.

SPECIFIC AIMS

1. Monitor changes in brain electrical activity, blood flow, and cerebral metabolism in isolated brain under constant-pressure, control conditions and after organophosphate exposure.

2. Determine regional distribution of cerebral blood flow after organophosphate exposure.

3. Determine regional utilization of glucose in control and in organophosphate-exposed brain.

4. Determine regional protein synthesis in control and in organophosphate-exposed brain.

5. Investigate the blood-brain transport of various metabolites in control and in organophosphate-exposed brain.

6. Examine the cerebral metabolism of acetylcholine, choline, and choline depots (choline-containing lipids) after organophosphate exposure.

7. Identify the source and mechanism of choline production in organophosphate-exposed brain and determine phospholipase activity, phospholipid content, and the identity of choline-labeled phospholipid products.

8. Determine the kinetics of labeling of choline in phospholipids of various cellular fractions. Determine the regional blood-brain transport of the fatty acid palmitate (C16) and determine the kinetics of fatty acid incorporation into choline-containing brain phospholipids.

9. Examine the effects of organophosphorus compounds on labeling of phosphatidylcholine and on receptor-mediated choline turnover.

10. Determine changes in catecholamines and other neurotransmitters in organophosphate-exposed brain.

11. Examine the effects of α-methyl-*p*-tyrosine on cerebral blood flow, brain electrical activity, cerebral metabolism, and turnover of biogenic amines in control and in organophosphate-exposed brain.

12. Examine the effects of receptor family antagonists on cerebral blood flow, brain electrical activity, and cerebral metabolism in control and in organophosphate-exposed brain.

13. Examine the effects of a nicotinic agonist on receptor–mediated release of choline from phospholipids. Test the hypothesis that the muscarinic receptor-regulated phosphatidylcholine phospholipase D and phosphatidic acid phosphatase pathway is important in signal transduction for generation of diacylglycerol from phosphatidylcholine in brain.

14. Examine the efficacy of scopolamine and valproate as protective agents against cerebral damage caused by organophosphate-induced seizure.

15. Examine the effects of HI-6 and pyridostigmine (and physostigmine and neostigmine), alone or in combination with other drugs, in control and in organophosphate-exposed brain.

16. Determine the effects of nitric oxide and nitro blue tetrazolium on blood flow, cerebral metabolism, and brain electrical activity in control and in organophosphate-exposed brain.

METHODS

Canine brain isolation and perfusion. The procedure for canine brain isolation (3) involves removal of the mandible, the snout, and all extracranial soft tissue, leaving only the brain case intact. A laminectomy at the level of the second cervical vertebra permits ligation and transection of the spinal cord, dura, and vertebral sinuses. Blood is supplied to the brain through the internal carotid arteries and the anastomotic branch of the internal maxillary segments of the external carotid arteries (4). A Luer connector, placed through the occipital bone into the confluence of sinuses, permits the return of venous blood to the oxygenator. All these procedures are conducted without interruption of blood or perfusate supply to the brain. Thus, at no time is the brain subject to anoxia or ischemia.

Arterial blood—hematocrit adjusted to 33% with high-molecular-weight dextran (Rheomacrodex, Pharmacia Laboratories, Piscataway, NJ)—is drawn from a reservoir (Fig. 1) by a variable speed roller pump and is propelled sequentially through a heat exchanger, bubble trap, and T-tubes placed into the common carotid arteries near the bifurcation of the internal and external carotid arteries. At the time of isolation, the pump is adjusted to deliver blood to the brain at a flow rate of approximately 65 ml/100 g·min. Perfusion pressure is held constant during experiments by adjusting the roller pump speed manually, maintaining the mean arterial pressure at 102 ± 20 mm Hg, and the average control cerebrovascular resistance (CVR) at 169 ± 7 torr·g·min/ml. CVR is determined by the equation: CVR = mm Hg·W/F, in which W is the brain weight (g), and F is the blood flow rate (ml/min). Under these conditions, the perfusion pressure provides adequate perfusion to the brain stem and to other posterior brain regions. Blood in the reservoir is continuously recirculated through a dacron wool filter (Abbott Laboratories, North Chicago, IL) and membrane oxygenator at a rate of 200 ml/min (Sci-Med Products, Minneapolis, MN) (4).

Arterial blood is frequently sampled, and the pH, pCO_2, and pO_2 are determined using a pH/blood gas analyzer (model 170, Corning Medical, Medfield, MA) and appropriately standardized electrodes. Blood in the reservoir is maintained at pH 7.40 and at a pCO_2 of 40 torr with sodium bicarbonate or by adjusting the oxygenator gas mixture (97% air and 3% CO_2). Blood glucose concentration is measured using a glucose analyzer (model 27, Yellow Springs Instruments, Inc., Yellow Springs, OH) and maintained at 5-6 mM (90-108 mg/dl) with addition of concentrated glucose solution. Blood temperature is maintained at 38°C. Total oxygen content is determined with a calibrated Lex-O_2-Con analyzer (Hospex Fiberoptics, Chestnut Hill, MA). Continuous monitoring of venous oxygen content is achieved by drawing a portion of the venous effluent from the confluence of sinuses through the flow cell of an oximeter (Waters Instruments, Rochester, MN). The oximeter, which measures O_2 saturation of hemoglobin, is calibrated with the Lex-O_2-Con analyzer. The cerebral metabolic rate (CMR) for oxygen consumption (CMR-O_2) is then calculated with the equation: CMR-O_2 = (A-V) x F/W, in which A-V is the arteriovenous difference (μmol/ml). When A, F, and W are constant, the venous oxygen content directly reflects oxygen consumption by the brain. The cerebral blood flow (CBF) rate is determined by measuring the volume of venous blood collected in a 1-min interval. Arterial perfusion pressure is measured by placing a cannula connected to a pressure transducer into the infraorbital branch of the carotid artery near the base of the Circle of Willis. Intracranial pressure is measured by insertion of a needle cannula into the cisterna magna. Silver electrodes are attached to the skull at temporal and occipital locations for monitoring electroencephalograph (EEG) activity. Heparinized blood is collected from an appropriate donor dog immediately prior to use in the brain perfusion experiments. Centrifugation of the blood from the donor and aspiration of the buffy coat (platelets, lymphocytes, and macrophages) have eliminated the frequent and variable rise in vascular resistance during perfusion periods of 0.5-5 hr. We suspect that vasoconstrictor substances are released by cells of this layer, and, therefore, removal of these cells is included in routine preparation of the perfusate.

Data analysis. Appropriate statistical tests were applied to determine the statistical significance of the results. Experimental results are reported as means ± S.D. or S.E.M. In most cases the results were evaluated by Student's unpaired, two-tailed *t*-test. A p value of <0.05 was usually required to establish statistical differences between means of two groups. When appropriate with additional groups of data, analysis of variance was applied.

Specific Aim 1. Monitor changes in brain electrical activity, blood flow, and cerebral metabolism in isolated brain under constant-pressure, control conditions and after organophosphate exposure.

Background. A major feature of OP toxicity is the immediate alteration in the EEG pattern (2, 5, 6). In acute high-dose exposures, the resulting EEG pattern is comparable to status epilepticus and is indicative of excessive neuronal activity. We have found in studies with the isolated perfused canine brain (7, 8) that a significant delay occurs between the time of OP exposure and the onset of brain seizure. This contrasts other seizure-inducing chemicals such as bicuculline, pentylenetetrazole (9, 10), and others that produce seizure simultaneously with their arrival at the brain. The delayed, predictable seizure onset (4 min for 100 μg of soman and 6 min for 400 μg of sarin under the

conditions of our experiments) provides the opportunity to study biochemical changes present pre-ictally, thus related to seizure genesis and cellular damage, and to differentiate them from those resulting from prolonged convulsions and concomitant metabolic derangements. In this study, EEG activity was monitored to provide the most sensitive indicator of altered neuronal activity or physiologically related function.

Our earlier studies have shown that administration of OP compounds to the isolated, perfused canine brain reduced the CVR, indicating vasodilation (11). Because of the potential significant pathological consequence of CBF alterations during OP intoxications, total and regional CBF were investigated in this study and reported in this aim and in Specific Aims 2, 11, 12, and 14-16. Other researchers have reported that cholinesterase inhibition (by physostigmine) increases CBF and causes vasodilation (12). The mechanism by which the anticholinesterase compounds altered CBF is not known. Many authors have interpreted changes in CVR to be a direct consequence of the increased CMR (13, 14). Howse *et al.* (15) proposed tissue pH as an important sampling factor with regard to cerebral metabolism and blood flow. Metabolic control of CVR by means of the vasodilator action of adenosine has been proposed by Rubio and Berne (16). Despite this evidence for the metabolic regulation of decrease in CVR, several workers failed to find direct correlation between CMR and CBF (17). In our studies, also, we did not find any relationship between OP-induced change in CVR and OP-induced seizure or change in CMR. This issue is addressed further in Specific Aims 2, 11, 12, and 14-16.

Cerebral oxygen and glucose consumption are reportedly elevated during epileptic-like seizure induced with chemicals or electroshock (9, 10, 17-19). This also now appears to be the case with the OP compounds soman and sarin (7, 8, 20-22). It has been suggested that brain lactate may play a role in the development of OP-induced neuropathological changes. It is known that brain lactate becomes elevated during seizure induced by OP or by other chemical convulsants. This is probably a result of increased metabolic activity of the glycolytic pathway or an increase in the NADH/NAD^+ ratio. Both of these effects will occur if the metabolic demands of the brain exceed the oxygen supply. Lactate accumulation in brain may be enhanced by hyperglycemia because elevated blood glucose provides additional substrate for brain glycolysis (23). The inability of the brain to remove lactate by transport into the blood is also an important factor in elevation of brain lactate.

One response to acute OP intoxication in experimental animals is hyperglycemia (24, 25). Thus, if respiratory distress is sufficient to produce hypoxia and if brain glucose supplies from hyperglycemia are in excess, then brain lactic acidosis would be expected. If the brain acidosis reaches an excessive level, then it would further be expected that the metabolic processes of the brain cells would be irreversibly damaged, and cell death would result. There is some evidence that this can occur under some circumstances because normoglycemic or hypoglycemic animals recover from severe hypoxia, but similarly treated animals made hyperglycemic do not (26). Brain lactate in the normoglycemic and hyperglycemic animals reaches about 15 µmol/g and 35 µmol/g, respectively. However, the elevation of brain lactate after OP intoxication has not been observed to reach these concentration levels. In addition, when blood flow and oxygenation are not compromised, evidence indicates that during seizure the supply of oxygen is not limiting for cerebral metabolism (27). The experiments included in this specific aim were designed to characterize some of the basic metabolic processes that occur in the CNS during acute OP exposure and to relate them to physiological functions such as EEG and CBF in order to identify the key events leading to the neuropathological consequences of OP exposure.

Method. Canine brains were isolated and perfused for 90 min as described in METHODS (Fig. 1). EEG tracings monitored the brain electrical activity continuously, and pressure tracings indicated variations in blood pressure. Arterial and venous samples (1 ml each) were taken at 10-min intervals or more frequently when appropriate and analyzed to determine the CMRs for oxygen, glucose (CMR-G), lactate (CMR-L), and carbon dioxide (CMR-CO_2).

After a control perfusion period of 30-40 min to establish steady-state conditions and to obtain baseline data, soman (100 µg) or sarin (400 µg) (28) was injected directly into an arterial cannula. Arterial and venous samples were taken every minute up to 10 min, at 5-min intervals up to 30 min,

and then at 10-min intervals up to 60 min. CMRs were measured, and pressure and EEG tracings were observed throughout the perfusion period.

Results. The data on total brain blood flow (Fig. 2) and CMRs (Figs. 3-6) are expressed as percents of control, with the control value considered to be 100%. When soman was injected, CBF increased slowly in the first minute and then rapidly in the second minute (Fig. 2A). The CBF remained steadily high at about 150% up to 20 min and then slowly returned to near control values after 40 min. The CVR decreased to 60% of control values within 2 min, remained low up to 15 min, and then gradually increased to near control values after 40 min. The CBF increased rapidly to 150% within 1 min after sarin injection (Fig. 2B) and reached a maximum of 155% in 3 min. The rate remained high up to 15 min and then gradually returned to near control levels after 40 min. CVR, calculated as a ratio of pressure to flow, showed corresponding rapid decreases within 1 min after OP injection, indicating the vasodilatory action of OP.

Patterns of brain electrical activity (measured by EEG) after OP treatment under constant pressure conditions are similar to those observed under constant flow (8) (Figs. 7, 8). As the OP reached the cerebral vasculature, the EEG was rapidly altered. The maximum amplitude decreased by half to about 35 μV, and the frequency increased. These ictal periods occurred after about 4 min for soman and after 5.6 min for sarin. The ictal periods lasted 30-60 sec and were repeated several times before becoming continuous. By 60 min after OP, higher and lower frequency waves appeared in the pattern.

The altered blood flow and EEG are associated with increased substrate (glucose, O_2) utilization. Soman administration (Fig. 3A) caused an increase in glucose utilization with a maximal value of 165% of control after 6 min and remained steady up to 20 min. After sarin administration, the CMR-G increased rapidly and linearly for 3 min and plateaued at 160% of control by 10 min (Fig. 3B). The CMR-G was then steady up to 20 min before declining. Oxygen consumption increased rapidly after OP exposure. Administration of soman (Fig. 4A) caused a steady increase in O_2 consumption, reaching a maximal value of 150% of control in about 7 min and remaining at that value up to 15 min. The CMR-O_2 gradually decreased toward control levels by 50 min. The CMR-O_2 increased to 160% of control within 5 min after sarin administration (Fig. 4B). It remained high up to 30 min and then declined to near control values by 50 min. Soman administration (Fig. 5A) caused increases in CO_2 production to approximately 160% of control in about 3 min, and production remained at that level for 15 min and then declined to control values at 50 min. Administration of sarin (Fig. 5B) resulted in a similar metabolism pattern. Lactate efflux after OP exposure is shown in Fig. 6, and a net increase can be noted during the 10- to 15-min period after soman injection (Fig. 6A) and during the 3- to 7-min period after sarin injection (Fig. 6B).

Comment. The results of these experiments demonstrated that isolation and perfusion procedures for canine brain under constant pressure conditions were standardized (4) and that the perfusion system was validated for measurement of metabolic and physiologic parameters for prolonged periods (≤ 90 min), with no significant alterations or drift in baseline data.

Experiments under constant pressure conditions, when compared to experiments with constant flow, had longer periods of seizure activity with fewer silent periods. OP exposure caused significant cerebrovasodilation and an increase in CBF. Differences in the length of seizure activity and the frequency of silent periods were probably the results of variation of blood flow. Greater blood flow in experiments with constant pressure allowed a larger supply of substrates (oxygen and glucose) for brain metabolism, which led to longer periods of neuronal hyperactivity (seizure activity). EEG patterns in experiments with soman or sarin were qualitatively similar.

Development of seizure was coupled to a significant increase in metabolism. The CMR-O_2 was slightly increased during the first several minutes, but was rapidly elevated during a concomitant epileptic-like seizure, which initiated after 4-6 min. The higher CMR-G after OP (160% of control) compared to CMR-O_2 (150% of control) indicates that all the glucose utilized may not be oxidized completely to CO_2 and H_2O. It is interesting to note that at about 20-30 min after OP there was a noticeable drop in CMR-G and CMR-O_2, followed by a rise at 30 min. The cause for this alteration is unknown. After 30 min, the CMR-CO_2 consistently increased again to reach a peak at 35 min and

then decreased to control values at 50 min. The overall pattern of CO_2 production is similar to that of glucose utilization; however, the initial burst of CO_2 production after sarin exposure (210% of control) far exceeded O_2 consumption and glucose utilization, indicating that the brain may metabolize some substrate(s) other than glucose. Small quantities of glucose may be metabolized to lactate via anaerobic glycolysis after OP exposure. High variability in the values does not allow a conclusion to be made about the lactate metabolism.

In contrast to cerebral oxidative metabolism, CBF and the associated vascular resistance both respond immediately to OP and do not change appreciably during the seizure phase of the response. Maximal CBF is reached about 1-3 min after OP exposure, and acceleration of metabolic activities occurs subsequently. Thus, CBF and metabolism become uncoupled during OP exposure. The significance of this observation is that OP-induced cerebrovasodilation, which permits increased delivery of blood-borne OP agents to the brain, is, therefore, a prime target of therapeutic strategies for preventing OP-induced injury.

Specific Aim 2. Determine regional distribution of cerebral blood flow after organophosphate exposure.

Background. The influence of OP compounds on CBF is only now becoming appreciated. It is well known that CBF is tightly coupled to metabolism in the normal physiological state. Under many circumstances, an increase in nutrient demand is accompanied by an increase in delivery; thus, increased regional blood flow parallels increased metabolism. During status epilepticus, large increases in CBF and metabolism have been reported (10), but this is generally believed to be associated with the increased metabolic demand (10). In studies with the isolated canine brain perfused at constant flow, we found that marked vasodilation occurred within seconds of the administration of soman or sarin into the arterial perfusate (7, 8). This decrease in CVR was maximal during the pre-ictal period and increased during during the 60 min following the onset of seizure. In the studies of this project, perfusion was conducted at constant pressure. Thus, both total and regional CBF were allowed to increase in response to OP-induced vasodilation similarly to the *in vivo* condition in which systemic blood pressure remains constant or increases. Although an increase in total CBF was observed, no information on regional changes was previously available. Such changes could be important, particularly if some areas of the brain were favored to receive the bulk of the increased flow and other areas received no or even reduced and compromising flows. The purposes of these studies were first to apply the regional autoradiographic methods to the perfused preparation and second to determine the regional distribution of CBF during the maximal OP-induced vasodilation and then to compare these flows to the control situation.

Method. A series of perfusion experiments were conducted to determine regional CBF under control conditions and after OP-induced vasodilation. These experiments were conducted under constant perfusion pressure conditions that allow CBF to increase when vasodilation occurs.

The autoradiographic methods for determining regional blood flow were applied to the perfused brain model. These methods are based on the principle originally developed by Kety (29). Radioactive tracer compounds are infused into the arterial perfusate, and the distribution in brain is evaluated by autoradiography of frozen tissue sections. Rates of blood flow are then calculated using appropriate mathematical models of transport and blood-tissue exchange.

Arterial and venous blood was sampled for blood gas/pH analyses and glucose and lactate determinations during the 30-min control perfusion period. Experiments were conducted under control conditions and after OP, and, in the experiments using OP, soman (100 µg) was injected to induce seizure. Immediately after the onset of high frequency and amplitude in the EEG tracing, characteristic of seizure, the [^{14}C]iodoantipyrine (IAP) tracer (25 µCi) in 250 µl of isotonic saline was infused over a 30-sec period, using a constant-rate infusion pump (Harvard Apparatus, South Natick, MA) at a constant rate without recirculation of the venous perfusate. Perfusion was stopped instantly; the brain was then removed, frozen (liquid nitrogen-cooled isopentane, -100°C to -150°C), and

prepared for autoradiography and tissue sampling. Samples of arterial perfusate and aliquots of the injectate were analyzed for levels of radioactivity. Regional CBF was calculated using the equation

$$CBF = C^*_b / \int_0^T C^*(t)dt,$$

in which C^*_b is the amount of radioactivity in brain (dpm/g), and the denominator is the amount of radioactivity injected (dpm) divided by the blood flow rate (ml/min). The application of this tracer to regional CBF studies in perfused dog brain was demonstrated previously (30).

Results. Regional CBF in the isolated canine brain appears to be distributed among the various brain regions in a physiological pattern (Fig. 9). No significant differences were observed between the left and right hemispheres. Those structures normally receiving high flows, such as the cerebral and cerebellar cortex, or low flows, such as the white matter, exhibited high and low flows, respectively. In addition, within the level of autoradiographic resolution there were no detectable focal areas of ischemia, as might be expected if microemboli had occurred in the perfusate and disrupted flow patterns. It was concluded that the method was successfully adapted and that reliable, reproducible, and excellent quality regional flow data were determined.

CBF in perfused brain was regionally variable with rates from 0.17 ml/g·min in cortical white matter to 1.14 ml/g·min in gray matter of parietal cortex (Table 1). The total blood flow rate in these experiments averaged 0.66 ml/g·min. The flow rates for specific regions were consistent and reproducible, as indicated by standard errors of less than 8% for most structures. After maximal vasodilation was induced by soman exposure, CBF increased by approximately 54%. Although in cortical gray matter structures the increase was more than 110%, in caudate nucleus, white matter, and pituitary, no significant increases occurred (Table 1). The CBF in the hippocampus increased after soman exposure, but to a lesser extent than in cortical regions.

Comment. The mechanisms involved in OP-induced vasodilation are manifested extensively in the brain and, with the exception of caudate nucleus, white matter, and pituitary, are uniformly activated in response to soman. Some regional variation was observed, which may reflect either the regional dilation response or the blood flow capacity of the contributing vessels.

Specific Aim 3. Determine regional utilization of glucose in control and in organophosphate-exposed brain.

Background. The use of ^{14}C-labeled D-glucose for regional glucose utilization studies has been proposed (31) and applied to experimental conditions in which the 2-deoxyglucose method is not applicable or is less reliable. There appears to be some question about the regional rates of glucose metabolism determined by the [^{14}C]2-deoxyglucose method of Sokoloff (32) because the plasma glucose concentration increases considerably and the tissue glucose concentration is not known during the 45-min experimental period (20-22). Both these factors influence the value of the "lumped constant" and should be considered carefully or reevaluated before interpreting the results of the Sokoloff method (33, 34). We have observed a small, significant increase in cerebral oxygen consumption of OP-exposed brain during the pre-ictal period (7, 8), but the consumption increases greatly during each seizure and decreases during each post-ictal silent period. In the studies of this project, regional glucose-use rates were determined with D-[^{14}C]glucose and a method developed by the principal investigator (8). Of consideration during studies with D-[^{14}C]glucose is the possible loss of radioactive label to the blood. D-[6-^{14}C]glucose was used in the present experiments because, in the brain, carbon in the 6th position is believed to be more stable when compared with the other positions (31), and the amount of $^{14}CO_2$ lost to the blood is small.

Method. Experiments were performed to study regional CMR-G. In the control experiments, to keep the specific activity of the arterial glucose constant, D-[6-^{14}C]glucose was infused intra-arterially at a constant rate for 10 min without recirculation of the venous perfusate. In the experiments using OP, soman (100 μg) was injected to induce seizure. Immediately after the onset of high frequency and amplitude in the EEG tracing, characteristic of seizure, D-[6-^{14}C]glucose was infused, again at a constant rate, without recirculation of the venous perfusate. Arterial and venous blood was sampled for blood gas/pH analyses and glucose and lactate determinations. After 10 min of isotope infusion, brains were quickly frozen in liquid nitrogen-cooled isopentane and stored at -70°C for later analysis of tissue samples and for the preparation of sections for autoradiography. CMR-G was measured in seven brain regions. Amino acids and lactate in the venous blood were separated by high-pressure liquid chromatography with electrochemical detection (HPLC-EC) and analyzed for radioactivity levels and for their rates of synthesis from D-[6-^{14}C]glucose.

Results. Regional cerebral glucose metabolism as visualized by autoradiography is shown in Fig. 10. The metabolic rates for glucose in the corpus callosum, the cerebellar cortex, and in five gray matter structures from control and OP-exposed brains are listed in Table 2. The CMR-G values dramatically increased during OP-induced seizure in all areas examined and were particularly significant in the gyrus cinguli and corpus callosum. During the infusion of D-[6-^{14}C]glucose, $^{14}CO_2$ released amounted to only 3% of the total activity taken up by the brain and was similar in control and OP-exposed tissues. [^{14}C]Lactate was the major metabolic product detected in the venous perfusate, and it accounted for about 5% of the total activity taken up by the brain. No detectable radioactivity was lost in the form of amino acids.

Comment. These results suggest that OP compounds increase the CMR-G in all brain regions and that D-[6-^{14}C]glucose appears to be a suitable tracer for regional CMR-G studies because the loss of radioactivity through other products was less than 10%. Because the accumulation of glucose metabolic products does not distinguish between lactate and Krebs cycle intermediates, the relative flux of glucose through anaerobic glycolysis and aerobic pathways cannot be determined.

Specific Aim 4. Determine regional protein synthesis in control and in organophosphate-exposed brain.

Background. Acute exposure to OP agents in mammals causes excessive neuronal discharges mimicking an epileptic seizure. Associated with these convulsions is increased cerebral energy metabolism, principally in the form of increased glucose and oxygen consumption (see Specific Aim 1). Although cerebral energy metabolism may return to control levels during periods following OP-induced seizure, sustained biochemical alterations also are believed to occur. This may include irreversible changes leading to cell death, especially in selected or regional cell populations. It remains unclear whether the pathophysiological results are related to all energy metabolism or are related to other complex cellular processes such as protein synthesis or phospholipid metabolism. In this series of experiments, regional protein synthesis was examined in the isolated canine brain during control and during OP exposure using L-[1-^{14}C]leucine in the arterial perfusate followed by autoradiography of coronal tissue sections. It was observed that OP-induced seizure dramatically reduced brain protein synthesis in all brain regions examined.

The autoradiographic techniques for evaluating regional brain metabolism have been applied successfully to regional protein synthesis rates (35-37). These methods demonstrate high rates of amino acid incorporation into proteins of the hippocampus, dentate gyrus, piriform cortex, and some thalamic nuclei. Incorporation into proteins of the brain stem and cerebellum are low. The incorporation is sensitive to altered metabolic conditions such as hypoglycemia, especially in those regions vulnerable to pathological damage. The effect of OP compounds on protein synthesis in whole brain is not known; however, evidence indicates significant effects of OPs on neuronal RNA (38) and, therefore, possibly protein synthesis. It is also known that OP compounds inhibit serine esterases other than cholinesterases (39, 40). If proteases of the serine esterase type are involved in

neuronal protein turnover or in the degradation (inactivation) of neuropeptide transmitters, then OPs may significantly alter protein or neuropeptide metabolism.

Method. Protein synthesis in brain occurs by the standard biological polymerization process involving polyribosomal translation of messenger RNAs and incorporation of amino acids from activated aminoacyl-tRNAs. Measurement of the extent of protein synthesis in brain, as determined by the incorporation of plasma-derived amino acids, has been previously demonstrated (41, 42) in rat brain by application of the regional autoradiographic method. This method, which is analogous to the 2-deoxyglucose method (32) for regional glucose metabolism, involves intravenous administration of a radioactive amino acid, determination of the history of amino acid radioactivity in the plasma, rapid fixation by freezing the brain at the end of the experimental period, and quantitative autoradiography. The perfused brain is a particularly good model for this regional method because the amino acid content and specific radioactivity of the plasma amino acids are constant and easily determined, and the blood flow rate is controlled and maintained.

Brain leucine is the precursor of leucyl-tRNA, the amino acyl donor of ribosomal protein synthesis, and it is assumed that the specific activity of this protein precursor also quickly reaches equilibrium with the plasma leucine specific activity. Any catabolism of L-[1-^{14}C]leucine is assumed to occur by transamination and subsequent decarboxylation of the α-keto acid, thus liberating $^{14}CO_2$ and forming nonradioactive metabolites. Regional protein synthesis, as well as free leucine and leucyl-tRNA, can be determined by differential autoradiography .

In these experiments, L-[1-^{14}C]leucine was infused at a constant rate into the arterial perfusate either during a 20-min control perfusion period or during a 20-min period immediately following exposure to OP (soman, 100 μg). The perfusate was not recirculated, and the specific activity of leucine was constant and was determined directly by amino acid analysis of arterial plasma samples.

After a brief control period (~30 min) to establish a steady state, 50-100 μCi of L-[1-^{14}C]leucine was infused at a constant rate into the carotid cannulae over a period of 20 min. The venous perfusate was not recirculated, and, therefore, the arterial perfusate contained constant specific activity of L-[1-^{14}C]leucine. At the end of the 20-min period, the brain was rapidly removed and frozen, and, on the following day, 20-μm thick coronal sections were prepared with a cryostat for autoradiography. After the first autoradiographic exposure, the tissue sections were wash-incubated in 10% trichloroacetic acid (TCA) to remove acid-soluble carbon-14 radioactivity and then exposed again to photographic films for a second autoradiography. The first autoradiograph represents total tissue radioactivity including free L-[1-^{14}C]leucine, ^{14}C-labeled metabolites, and ^{14}C-labeled protein. The second autoradiograph represents only acid-insoluble ^{14}C-iabeled protein and, therefore, represents protein synthesis during the 20-min infusion period.

Results. In preliminary experiments performed during Year 2 of the research project, we studied protein synthesis under control conditions and during oligemia (low perfusate flow) in order to develop and validate the method. The experimental conditions for the two regional protein synthesis experiments were identical except that the perfusate flow rate was reduced to 45% (0.30 ml/g·min) during oligemia (Table 3). This flow rate was used because a significant alteration in EEG occurred within 30 sec of attaining it. The EEG activity pattern changed to low frequency with high amplitude. Such an alteration in EEG is presumed to represent an alteration in cerebral metabolism. After 30 min, total accumulation of plasma-derived L-[1-^{14}C]leucine in brain was substantial, and the amount into acid-insoluble material was about 75% under control conditions (Table 3). However, under reduced flow conditions, the fraction of L-[1-^{14}C]leucine that accumulated in acid-insoluble material was reduced to about 40%. Although equal amounts of L-[1-^{14}C]leucine were infused during both control and oligemia experiments, the specific radioactivity of L-[^{14}C]leucine during oligemia was greater because of the reduced perfusate flow rate. Therefore, the total accumulated ^{14}C in brain during oligemia was greater than under control conditions (Table 3). Protein synthesis was significantly reduced in all brain regions during oligemia except in the hippocampus, which may have about the same relative incorporation into acid-insoluble material as controls (Figs. 11, 12).

In experiments recently completed, protein synthesis was studied after OP exposure. Radioactive leucine was transported into the brain through the vascular endothelium, and the specific activity of brain leucine rapidly approached the specific activity of plasma leucine. The examination of regional protein synthesis in control and OP-exposed brain involved perfusion with L-[1-^{14}C]leucine and subsequent autoradioagraphy of thin coronal sections of rapidly frozen brain. The regional incorporation of L-[1-^{14}C]leucine is apparent from the autoradiographs (Figs. 13, 14). The autoradiographic technique clearly shows regions of high protein synthesis in the cortical gray matter, hippocampus (dentate gyrus and CA1-CA4), brain stem, and cerebellar gray matter (Figs. 13, 14). Evaluation of the results indicate that substantial incorporation of leucine into brain protein of cerebral cortex occurred during the 20-min control experimental period (Table 4). Transport and incorporation were much greater in cortical gray matter than in white matter, and incorporation into different regions of gray matter also appeared to vary. Following OP (soman, 100 μg) exposure, protein synthesis was greatly reduced, and the amount of free L-[1-^{14}C]leucine was slightly increased (Table 5). Quantitatively, leucine incorporation into protein accounts for between 65 and 97% of the total radioactivity in control brains, but only 23-46% of the total radioactivity in OP-exposed brain undergoing seizure (Table 6).

Comment. It is evident from these studies that regional protein synthesis can be investigated using the perfused brain preparation. The relative fraction of radioactivity incorporated into protein (TCA insoluble) material agrees closely with the results obtained for the rat brain *in vivo* (43). The clarity and definition visible in the autoradiographs permit quantitation and identification of specific regions of high or low protein synthesis.

Under conditions of OP-induced seizure, transport of L-leucine into the brain appears unaltered. However, incorporation of the amino acid into protein was severely impeded, especially in those structures and cell layers that normally conduct protein synthesis at the highest rates. The reason for reduced protein synthesis may be because of a direct OP effect on some component of the protein synthesis process. Alternatively, excessive neuronal discharge and associated energy depletion may result in dissociation of the polyribosomal complexes and diminution of protein synthesis events. This hypothesis is supported by the similar results observed in oligemia situations, during which energy is compromised and gradients are disrupted.

Specific Aim 5. Investigate the blood-brain transport of various metabolites in control and in organophosphate-exposed brain.

Background. The brain endothelial cell, which lines the walls of all cerebral blood vessels and which forms tight junctions to restrict passive diffusion of blood-borne substances, performs the important function of selectively transporting essential substrates and products in and out of the brain. Although OP compounds cause profound changes in cerebral metabolism, it is not known whether they affect the blood-brain transport of metabolites under constant perfusion pressure conditions. In preliminary experiments (8), the unidirectional transport of glucose (glc), choline (Ch), leucine (leu), and glycine (gly) from blood to brain was measured during control periods and after soman exposure. During the influx measurements under high perfusate flow associated with soman exposure, there was an apparent slightly higher transport rate, although the increase was not significant because of the few measurements obtained. Additional measurements were conducted following OP-induced perfusate flow increases. The experiments in this section were designed to determine blood-brain transport (influx velocity, v_{in}) of glc, Ch, gly, and leu. For more complete investigation of the possible influence of flow rate, cholinergic agonists, and other cholinergic agents on blood-brain transport of glc, Ch, leu, and gly, additional influx measurements were made following exposure to carbachol, arecoline, oxotremorine, and AF64a.

Method. [^{3}H]Glc, [^{3}H]Ch, [^{3}H]leu, or [^{3}H]gly, along with an intravascular reference compound, [^{22}Na^{+}], which does not enter the brain significantly, was rapidly infused (1 sec) into the arterial blood stream (44). After injecting a labeled metabolite, venous blood samples were collected every second for 30 sec, by which time the radioactivity in the blood had reduced to nearly background levels. The

next compound was injected after 1 min, and venous blood samples were collected again for 30 sec. Radioactivity levels of the test compound and reference marker were measured in all the blood samples by liquid scintillation spectrometry. The maximum difference in radioactivity between the reference marker and test compound was a measure of the maximal influx of the metabolite (E_{max}). E_{max} for all the metabolites was determined in control and OP-exposed brains, and the v_{in} values were calculated using the formula $v_{in} = -(F/W)A \ln(1-E_{max})$, in which E_{max} = extraction maximum, A = arterial concentration (glc, 5 mmol/l; Ch, 5 µmol/l; gly, 0.17 mmol/l; and leu, 0.089 mmol/l), F = plasma flow rate (ml/min), and W is the brain weight (g).

Results. The control v_{in} values during an experiment determined at 50, 60, and 80 min after brain isolation did not vary significantly (data not shown). In the OP-exposed brain, the v_{in} values of metabolites were determined at 10 min and 50 min after injecting 100 µg of soman. The influx of glc, leu, and gly increased significantly during the elevated flow rate period following OP exposure (Tables 7-10), but Ch influx remained constant (Table 10). The increased glc transport also was generally elevated under conditions of high perfusate flow induced by other agents, including carbachol, arecoline, and a combination of carbachol and soman (Table 7). AF64a, an irreversible inhibitor of high-affinity, sodium-dependent Ch transporter of synaptosomes, did not alter the blood-brain transport of any of the ^{3}H-labeled substrates. High perfusate flow did not appear to alter blood-brain transport of leu, gly, or Ch (Tables 8-10).

Comment. Previously, we did not observe any change in the blood-brain transport of metabolites after OP exposure under constant flow conditions (8). In the present studies, under conditions of constant perfusion pressure, cerebral perfusion flow rate increased about 50% during the first 20 min after OP exposure (see Fig. 2). The calculated increase in metabolite influx during this period may be significant. Our results indicate that OP agents do not inhibit or impair the transporter for glc, amino acids, or Ch. In fact, the evidence suggests that the transport capacity for glc and amino acids may be increased. One explanation is that extensive vasodilation may increase or maximize the number of vessels that have blood (and substrates) flowing through them, and, therefore, the surface area or number of transport sites is increased. An alternative explanation is that there is an enhanced activity of the transport systems resulting from increased metabolic demands and activity. In either case, any effect of OP is a secondary response, and the cholinesterase inhibitors are not acting directly on the transporter system. It should be emphasized that the transport processes reported here are carrier-mediated systems specific for their specific substrates. Blood-brain barrier breakdown or opening of the blood-brain barrier is a separate phenomenon. Blood-brain barrier breakdown refers to the hypothesized physical opening of gaps or channels between or within the vascular endothelial cells. This event will allow nonspecific extravasation of blood-borne substituents (including high-molecular-weight proteins). It has been hypothesized that the blood-brain barrier opening *in vivo* may result from a combination of extensive cerebral vasodilation and concomitant hypertension in the first moments of OP intoxication. Transmission of elevated blood pressure (hydrostatic) to the small arterials and capillaries may result in physical rupture of vessel walls and production of foci of extravasation.

Specific Aim 6. Examine the cerebral metabolism of acetylcholine, choline, and choline depots (choline-containing lipids) after organophosphate exposure.

Background. Brain Ch plays a central role in the metabolism of at least two classes of brain constituents — as a precursor and degradation product of the neurotransmitter acetylcholine (ACh) and as a component of the membrane lipids phosphatidylcholine (PC) and sphingomyelin (45, 46). Although brain is capable of *de novo* Ch synthesis (47), this pathway appears minor, and most brain Ch is of hepatic or dietary origin, reaching the brain via the circulation in either free or possibly conjugated form (48, 49). A low-affinity Ch carrier has been described for the blood-brain transport of Ch (50). In brain, Ch is known to be produced from the inactivation and hydrolysis of ACh by AChE, an enzyme sensitive to inhibition by OP compounds. The toxicity of these agents is usually attributed to the accumulation of ACh in the brain and other tissues, which causes overstimulation of cholinoceptive neurons (2). However, other toxic influences have been reported (2). For example,

Ch levels are greatly elevated by some, but not all OP inhibitors of AChE (51, 52). Similar elevations of Ch are reportedly produced by direct cholinergic agonists such as oxotremorine (53, 54). Although the primary effect of OPs on brain ACh levels is well established, their additional primary and secondary effects on blood-brain transport and cerebral metabolism have not been elucidated. This series of experiments was focused on the effects of soman and sarin on 1) brain ACh and Ch levels, 2) unidirectional influx of blood Ch into the brain, and 3) the cerebral metabolic rate for free Ch (CMRCh) in isolated, perfused canine brain.

Method. The dog brain was isolated as described in METHODS and perfused for a control period (30 to 45 min) to establish a steady state and to obtain baseline data. Administration of either 100 µg of soman or 400 µg of sarin to the perfusate was accomplished by injection directly into an arterial cannula; thus, each brain served as its own control for physiologic and metabolic measurements.

Nonperfused controls. Adult mongrel dogs (10-25 kg) were anesthetized with 3% halothane and 70% N_2 and were maintained under anesthesia with 2% halothane. After the dog was anticoagulated with heparin and euthanized, the brain was removed from the skull and was dissected immediately. Cerebellum, brain stem, hippocampus, and cerebral cortex samples were frozen immediately after collection and stored at <-60°C for later analysis. The time required for sample collection before freezing was 2-3 min.

Perfused controls, recirculation. Dog brains were isolated and perfused, as described above. Venous perfusate was reoxygenated, returned to the reservoir, and allowed to recirculate through the pump/oxygenator system. Perfusion was stopped after either 5 or 90 min, the brain was rapidly removed, and samples were collected and stored as described above. Also during the 90-min perfusion experiments, arterial and venous blood samples were collected every 10 min for Ch analysis.

Perfused controls, nonrecirculation. The dog brains were isolated and perfused as described above, except the venous effluent from the brain was not returned to the pump-oxygenator system for recirculation. Perfusion was continued for 40 min, and brain samples were then rapidly collected, as described above, for later analysis.

Soman or sarin exposure, 5 min. The isolated brain was perfused for 30 min under recirculation conditions to establish a steady state, and then a bolus of 100 µg of soman or 400 of µg sarin was injected into the common carotid cannula. Perfusion of the brain was discontinued 5 min after the agent injection, and brain regions were dissected and stored, as described above.

Soman or sarin exposure, 60 min. The isolated brain was perfused for 30 min under recirculation conditions to establish a steady state, and then a bolus of 100 µg of soman or 400 µg of sarin was injected into the common carotid cannula. During the next 60 min, arterial and venous blood samples were collected at 10-min intervals for Ch analysis. At 60 min after OP administration, brain samples were collected, as described above, for later analysis.

Analysis of ACh and Ch. At the time of analysis, frozen brain samples were homogenized with formic acid/acetone (3:17), and blood samples were deproteinized with 0.3 mol/l perchloric acid. Each sample was centrifuged, and the clear supernatant was extracted and analyzed for ACh and Ch as described earlier (55). The CMRCh (nmol/g·min) was calculated by the equation Efflux = (A - V)F/W, in which A and V are the respective concentrations of Ch in the arterial and venous samples (nmol/ml), F is the blood flow rate (ml/min), and W is the brain weight (g).

Unidirectional Ch influx. The velocity of Ch influx was determined using the indicator dilution method for the perfused dog brain as described previously (44). A 50-µl solution containing 2 µCi of ^{22}Na, the intravascular marker, and 10 µCi of [methyl-^{3}H]choline, the test molecule, was injected into the arterial bloodstream of the common carotid artery. Immediately after the injection, 30 consecutive venous blood samples were collected at 1-sec intervals. Then, a 50-µl aliquot of each sample was decolorized with H_2O_2 and processed for dual-isotope liquid scintillation spectrometry. Data calculation and analysis (44) allowed the determination of the maximal fractional extraction, E, for Ch.

The rate of unidirectional Ch transport into the brain, u_{in}, was then calculated using the formula $u_{in} = EA \cdot F/W$, in which A is the plasma Ch concentration, F is the plasma flow rate, and W is the brain weight.

Statistics. The significant differences between controls and multiple comparisons were determined using Dunnett's procedure against two-sided alternatives (56), except in Table 11, for which Student's unpaired, two-tailed *t*-test was used.

Results. In this study, ACh levels in anesthetized dog brain were found to differ among brain regions. The concentrations were from 0.6 to 4.3 nmol/g tissue, with the lowest concentration in the cerebellum and the highest in the cerebral cortex (Table 11). No significant changes were detected in regional ACh concentrations during perfusion up to 90 min. ACh levels were not influenced by either recirculation or nonrecirculation of the perfusate (Table 11).

Ch levels in anesthetized dog brain ranged between 41 and 79 nmol/g tissue, with the lowest in the cerebral cortex. Isolation of the brain caused about a twofold increase in the brain concentration of Ch (Table 11). When the perfusate was recirculated, Ch continued to increase during the perfusion period, and it reached levels between 239 and 295 nmol/g tissue after 90 min (Table 11). When the perfusate was not recirculated, brain Ch remained at the same levels as at the beginning of perfusion in all areas of the brain except cortex, in which a small increase of 9% was detected (Table 11).

The CMRCh (Ch efflux) during a series of nonrecirculation and recirculation experiments was -1.1 ± 0.1 and -1.6 ± 0.4 nmol/g·min, respectively (Table 12). Although the level of perfusate Ch increased severalfold during recirculation experiments, the efflux of brain Ch was constant during the entire perfusion period (data not shown).

Blood-brain transport of plasma Ch was determined by measuring unidirectional influx of [^{3}H]choline. Before OP exposure, transport velocity was 0.49 ± 0.07 nmol/g·min, and this value did not change significantly for up to 40 min after either soman or sarin treatment (Table 13). Unidirectional transport of glc, leu, and gly were also similarly determined and found unaltered by OP exposure (data not shown).

Inhibition of AChE by administration of soman caused a large increase in ACh levels of between 10- and 50-fold within 5 min in all brain regions sampled except in the cerebellum, where the increase was small (Table 14). After 60 min of soman exposure, the levels of ACh in hippocampus and cerebellum were greater than after 5 min. Acute exposure to sarin (400 µg) also produced a substantial ACh increase in all brain regions (Table 14), although the rise was not as great after 5 min when compared to the concentrations after soman exposure. The ACh levels in cortex and hippocampus remained constant, but brain stem and cerebellum ACh continued to increase, reaching levels comparable to soman-exposed brain after 60 min.

Brain levels of Ch were also affected by OPs. Within 5 min after administration of soman, increases of 120-250% were observed in all brain regions except cerebral cortex, where the increase was ~70% (Table 15). Sixty minutes after acute soman exposure, the concentration of Ch decreased in all brain regions (Table 15). Acute exposure to sarin increased brain Ch concentrations after 5 min to levels similar to those for soman-exposed brain (Table 15). Sixty minutes after acute sarin exposure, the concentration of Ch decreased significantly in all brain regions (Table 15).

To assess the effect of OP compounds on Ch efflux from brain during soman or sarin exposure, the CMRCh was determined during a control period before and for 30 min after each treatment. In this group of experiments, the CMRCh was -1.58 ± 0.09 nmol/g·min during control perfusion periods, indicating net efflux of Ch. The efflux rate decreased toward zero (0.32 ± 0.07 nmol/g·min) after 30 min and returned to 60-70% of control rates by 60 min after exposure to either soman or sarin (Fig. 15).

Comment. In this study, when dog brain regions were compared, the concentrations of ACh and Ch were observed to differ substantially. Higher concentrations of ACh were observed in the cortex and in the brain stem than were observed in the hippocampus, and the least was detected in the cerebellum. Similar relative variations have been reported for other species (57), although dog brain ACh concentrations appear lower than those in most smaller species (58-62). The consistent levels of ACh in nonperfused and perfused brain of either short (5 min) or long (90 min) duration indicate that ACh metabolism remains in a steady state and is undisturbed by the isolation and perfusion procedure. This is consistent with numerous other observations of metabolism in the perfused brain preparation (63).

The higher Ch concentrations in brain regions of dog compared to rodents may reflect higher steady-state levels in dog, which may be an effect of anesthesia/surgery or may result from Ch formation during the brief (2-3 min) delay in collection and freezing of tissue samples. There is evidence that Ch increases substantially in ischemic or postmortem brain (64, 65). Because of the size of the dog brain, inactivation with microwave irradiation was impractical; however, introduction of an unnecessary variable was avoided by maintaining a consistent sampling protocol.

The CMRCh indicated that Ch production by the perfused brain was about 1.6 nmol/g·min. This net synthesis of unesterified Ch was constant during the perfusion period even when the blood Ch increased about 10-fold during recirculation of perfusate. Arteriojugular differences in Ch were reported previously (64, 66-68); however, because the cerebral blood flow rate was not determined, the CMRCh was not calculated accurately. The biochemical source of this Ch and the regulation of its synthesis are unknown, although it has been suggested that lipid-bound Ch (48), possibly lysophosphatidylcholine (lysoPC) (49), is the source.

The concentration of brain Ch appears to vary rapidly in accordance with the blood Ch concentration. This equilibration between the brain Ch pool and the blood Ch pool occurs via the Ch transporter of the brain capillary endothelial cell (Fig. 16). Blood-brain transport of Ch by a saturable, stereospecific, and carrier-mediated mechanism has previously been demonstrated in rat (50, 69). A unidirectional Ch influx of 0.49 ± 0.09 nmol/g·min was determined using [^{3}H]Ch under control conditions for the perfused brain. This value is similar to the calculated rate of Ch transport (0.18-0.34 nmol/g·min) into rat forebrain at physiological concentrations of plasma Ch (50). The Ch transporter was not inhibited by either of the OP compounds. Thus, it is unlikely that transport involves an essential serine at the active binding site, as do the serine esterases that can be inhibited by OPs. Hemicholinium and some quaternary amines are capable of inhibiting the Ch transporter (50).

Wurtman (70), Cohen and Wurtman (71), and Haubrich *et al.* (72) proposed that increasing the concentration of Ch will enhance the synthesis and concentration of ACh in brain. In the present study, no changes in brain ACh were observed over a wide range of blood and brain levels of Ch. These results support the suggestions of Jope (73) that regulatory mechanisms maintain a constant level of ACh even under increased availability of Ch to the brain. The effects of chronically elevated Ch were not investigated here.

The exposure to soman and sarin rapidly produced increases in both ACh and Ch. The rise in ACh is a result of the inhibition of AChE by OP compounds and synthesis by Ch acetyltransferase (74). The increase in Ch on a molar basis is considerably greater than the increase in ACh. Because AChE in cerebral cortex is 92-98% inhibited by OP under these experimental conditions (75), the rise in ACh during the first 5 min of soman exposure is calculated to be 12 nmol/g·min and represents synthetic capacity. A similar estimation of the rate of Ch production during the first 5 min of soman exposure yields a minimum rate of 25 nmol/g·min. Total net production of Ch, therefore, is 37.5 nmol/g·min, calculated by combining the increase in tissue Ch, plus the Ch used to form ACh, plus Ch lost to the blood (~0.5 nmol/g·min). Based on isotope incorporation studies, Chol *et al.* (66) calculated a Ch turnover rate of 28.4 nmol/g·min in rat brain under unstimulated conditions. This is slower than that reported here in brain stimulated to seizures by OP exposure (76). The source of this Ch is 1) uptake of lipid-bound Ch from blood, 2) *de novo* synthesis in the brain, or 3) from Ch-containing brain lipids, or 4) a combination of these.

Ch-containing lipids are a probable source of the elevated levels of brain Ch. Studies of brain free fatty acids (FFAs) suggest that brain lipids are rapidly hydrolyzed following acute alterations in cerebral metabolism. Brain FFAs are known to increase severalfold during the first few minutes of ischemia (77). Although this increase in FFA is partly attributed to hydrolysis of the phosphoinositides (78, 79), PC is also a readily available and abundant substrate for lipase activity. The product of PC hydolysis, lysoPC, would, therefore, be a source of both free Ch and additional FFA by the action of a phosphatase or lysophospholipase. In support of this hypothesis, lysoPC reportedly increases rapidly and undergoes active turnover at the onset of ischemia (80).

The efflux of Ch from brain after OP exposure declines despite the high levels of brain Ch, thus indicating that the tissue Ch pool in equilibration with blood Ch falls and approaches the blood concentration. It further suggests that brain Ch is sequestered in a pool unavailable for transport to blood and is probably intracellular (Fig. 16).

It is proposed that Ch in brain exists in two compartments, the intracellular, Ch_i, and the extracellular, Ch_e (Fig. 16). Ch_e is formed by the action of AChE (reaction 5) on ACh released from neurons. Ch_e is in steady-state equilibrium with plasma Ch, Ch_p, via the Ch transporter of the endothelial cell (reaction 1). Net efflux occurs when Ch_e is greater than Ch_p. Ch_i is the precursor of synaptosomal ACh and is derived from Ch transport (reaction 2) and synthesis from unidentified endogenous sources (reaction 6). When AChE is inhibited (reaction 5), Ch_e decreases, net efflux slows, and synthesis of Ch_i, by reaction 6, is stimulated by regulatory or receptor-mediated processes.

The metabolism of Ch in brain is complex because of Ch involvement in both ACh synthesis and phospholipid metabolism. However, it is evident that the implications of the effects of cholinesterase inhibitors on cholinergic neurotransmissions, on cholinergic mechanisms of cerebral blood flow regulation (81, 82), and on cerebral membrane lipid metabolism are significant.

Specific Aim 7. Identify the source and mechanism of choline production in organophosphate-exposed brain and determine phospholipase activity, phospholipid content, and the identity of choline-labeled phospholipid products.

Background. Ch serves as a direct precursor for ACh, PC, and sphingomyelin in brain. Although brain has been shown to synthesize Ch via a *de novo* pathway (46), the synthesized Ch accounts for less than 10% of the brain's requirement, with the rest originating from an unknown metabolic source or extracted from blood in a form other than free Ch. However, at any given time, the concentration of Ch in brain is higher than in blood, resulting in a net efflux of Ch from brain to blood (83, 84). Enhanced levels of Ch were observed in ischemic rat brain (65) as well as in the brains of rats treated with OP (52). Our results with isolated canine brain showed that administration of OP (100 µg of soman or 400 µg of sarin) resulted in a two- to fourfold increase in Ch and about a 10-fold increase in ACh levels in all brain regions studied (83). The mechanism for Ch production is not known. Since PC is a major Ch-containing phospholipid in brain, it is reasonable to assume that substantial amounts of Ch can be derived from PC hydrolysis. The OP-induced increase in Ch concentration can occur from the activation of catabolic enzymes on PC (or sphingomyelin) by OP directly or by increased ACh (resulting from AChE inhibition) acting through some regulatory mechanism.

Possible pathways and enzymes involved in Ch production are illustrated in Fig. 17. Phospholipase D [1] (bracketed numbers refer to the numbers shown in the figure) hydrolyzes PC to phosphatidic acid (PA) and free Ch. Phospholipase A_2 or A_1 [2] hydrolyzes fatty acid from the *sn*-2 or *sn*-1 position, respectively, of PC to form lysoPC. Lysophospholipase D [3] may hydrolyze lysoPC to lysoPA and free Ch. Rat brain was shown to contain lysophospholipase D which acts on lysoplasmalogens to produce lysoPA and free base (85, 86). LysoPC can be deacylated to glycerophosphocholine (GPC) by lysophospholipase [4]. GPC-phosphodiesterase [5] hydrolyzes GPC to glycerophosphate and free Ch. GPC can also be hydrolyzed by GPC-cholinephosphodiesterase [6] to yield phosphocholine. Phospholipase C [7] hydrolyzes PC to produce diacylglyceride and phosphocholine. Alkaline phosphatase [8] hydrolyzes phosphocholine to phosphate and free Ch. Sphingomyelin is another Ch-containing lipid which may also contribute to

Ch production. Sphingomyelinase [9] hydrolyzes sphingomyelin to ceramide and phosphocholine, which, in turn, can be hydrolyzed by alkaline phosphatase [8] to form Ch. Phospholipase D-type action on sphingomyelin is known to produce free Ch in *Corynebacterium ovis* (87), but it is not known whether an enzyme of this activity and specificity is present in canine brain or mammalian tissues. We have done a partial characterization of phospholipase D in the subcellular preparation of dog brain using [^{3}H]Ch-labeled PC as the substrate, and our procedure and results are presented below.

Method. Subcellular fractions from dog brain tissue were prepared essentially according to Whittaker and Barker (88) and modified as described (89). Briefly, the tissue was homogenized in 0.32 M sucrose (10% w/v) with a Potter-Elvehjem homogenizer. The homogenate was centrifuged initially at 1000 x g for 10 min, and the postnuclear supernatant was centrifuged at 22,000 x g for 30 min to obtain a crude membrane pellet which contained myelin, synaptosomes, and mitochondria. The supernatant, containing microsomes, was centrifuged at 100,000 x g for 1 hr to sediment the microsomes. The crude membrane pellet and the microsomes were washed once, and each preparation was resuspended in 0.32 M sucrose and stored at -20°C until use. The protein content was determined according to Lowry *et al.* (90).

Phospholipase D assay. The substrate 1,2-dipalmitoyl-*sn*-glycero-3-phosphoryl[^{3}H]choline (the specific activity of [^{3}H]PC adjusted to 1 x 10^4 dpm/nmol) in toluene/ethanol (1:1) was aliquoted into incubation tubes. The solvent was evaporated under a nitrogen stream, 5 µl of ethanol followed by buffer was added, and the tubes were vortexed to disperse the substrate. The incubation medium in 0.25 ml contained 132 µM [^{3}H]PC (3.3 x 10^5 dpm), 40 mM HEPES buffer at pH 7.4, 0.1% Triton X-100, and the crude brain membrane preparation (200-500 µg of protein). Incubations were carried out at 37°C for 30 min, with shaking. Reactions were stopped by adding methanol, and lipids were extracted as described by Bligh and Dyer (91). Control values were obtained by stopping the reaction immediately after adding the enzyme or by using boiled enzyme in the reaction mixture. The radioactivity levels in the water-soluble ^{3}H-labeled products (Ch, phosphocholine, and GPC) were measured in the upper phase after separation by thin-layer chromatography (TLC) (silica gel-H) (92) using methanol/0.6% NaCl/conc. ammonia (50:50:5). More than 90% of the radioactivity was recovered in the Ch fraction, and radioactivity released into this upper phase indicated phospholipase D activity.

In other experiments, the brain microsomal preparation was used as the enzyme source. Diisopropylfluorophosphate (DFP), an OP similar to sarin, was used to examine the effect of DIFP on phospholipase D in these dog brain preparations. Experimental details are given in Table 16.

To examine the effects of detergents on phospholipase D, different concentrations of sodium deoxycholate, sodium oleate, sodium linoleate, 3[(3-cholamidopropyl)dimethylammonio]-propane sulfonate (CHAPS), octylglucopyranoside, and Triton X-100 were added to the incubations. Experimental details are given in Table 17.

Results. Levels of phospholipase D activity in the subcellular fractions of control dog brain cortex are listed in Table 16. The activity was higher in the microsomal fraction when compared with the homogenate or the crude membrane fraction. Surprisingly, DFP did not affect phospholipase D activity (Table 16). This observation, however, is consistent with a recent report that DFP administration to rats did not increase brain Ch levels (52). The effects of detergents on phospholipase D are shown in Table 17. The data are expressed as percentages of control with the control activity (in the absence of detergents) considered to be 100%. Sodium deoxycholate, sodium oleate, and sodium linoleate were inhibitory at all concentrations studied (0.2 mg/ml to 2.0 mg/ml). CHAPS had marginal effects. Octylglucopyranoside was slightly stimulatory up to a concentration of 0.4 mg/ml, and higher concentrations were inhibitory. Triton X-100 showed concentration-dependent stimulation up to 2 mg/ml. Since Triton X-100 was most effective among the detergents tested, several different concentrations were used to determine an optimal concentration, and the results are shown in Fig. 18. The activity increased with increasing concentration, reaching a maximal stimulation of about 400% of control at 2 mg/ml before decreasing. Since many hydrolytic enzymes exhibit metal-ion dependency, it was of interest to examine the effects of metal ions on phospholipase D activity. For this purpose, the effects of $CaCl_2$, $MgCl_2$,

$ZnCl_2$, and the metal chelator EDTA were examined (Table 18). It appeared that the enzyme did not require any metal ion for its action. Even the addition of EDTA at a concentration of 4 mM had no effect. In fact, Ca^{2+} and Mg^{2+} were slightly inhibitory between concentrations of 1 and 4 mM, whereas Zn^{2+} was highly inhibitory, causing a loss of more than 90% of the activity at the 4 mM concentration.

Comment. Phospholipase D activity in mammalian tissues appears to be latent, and detergent exposure is an important treatment to allow expression of the enzymatic activity (93). Transphosphatidylation activity of phospholipase D from rat brain microsomes was enhanced severalfold by fatty acids (93). In our experiments, both sodium oleate and sodium linoleate were found to be ineffective in activating phospholipase D. However, Triton X-100 caused a fourfold increase in phospholipase D activity in dog brain microsomes.

It is concluded that a major pathway for the formation of free choline in brain is the action of phospholipase D on membranous phosphatidylcholine. Further, it appears that this enzyme is not a target for inactivation by OP agents such as sarin. These studies have been reported previously (94, 95), and further investigations of the regulation of phospholipase D following inhibition of AChE are reported in Specific Aims 9 and 13 below.

Specific Aim 8. Determine the kinetics of labeling of choline in phospholipids of various cellular fractions. Determine the regional blood-brain transport of the fatty acid palmitate (C16) and determine the kinetics of fatty acid incorporation into choline-containing brain phospholipids.

Background. We have previously hypothesized that the dynamic steady-state level of brain Ch is dependent on the neuronal uptake of Ch from degraded ACh, the activity of the enzyme Ch acetyltransferase, and the action of phospholipases (i. e., phospholipase D) on choline-containing lipids such as PC (83). In the steady state, the rate of PC synthesis must equal the rate of PC breakdown. The following studies were undertaken to investigate the synthesis of Ch lipids in the intact brain.

The initial objective of this study was to examine the metabolism of Ch-containing lipids under control conditions and during OP-induced seizure using radioactive Ch infused into the arterial perfusate. In preliminary experiments, [^{3}H]Ch was infused over a 15- to 30-min period, and the incorporation of [^{3}H]Ch into brain tissue and brain lipids was determined. Although [^{3}H]Ch was readily transported into brain, there was essentially no detectable radioactivity in PC, sphingomyelin, or in other phospholipids. This is probably the result of the low specific activity of the available radioactive Ch, a slow rate of Ch incorporation into phospholipids, or a combination of both. Consequently, to investigate phospholipid metabolism under control conditions and after OP exposure, the long-chain fatty acids palmitate (C16) and oleate (C18:1) were selected as alternative substrates for lipid biosynthesis. These fatty acids are both known to be incorporated into cellular phospholipids. Palmitate is commonly present at the *sn*-1 position of glycerophosphate, and the unsaturated oleate is commonly found in the *sn*-2 position. Based on preliminary infusion experiments, ^{3}H-labeled fatty acids appeared to be useful for examining OP effects on blood-brain transport of these compounds, as well as cerebral metabolism of phospholipids during OP-induced seizure, and the following studies were undertaken.

Method. Perfusion experiments were conducted in which the brain was allowed to reach equilibrium with the perfusate and to establish a metabolic steady state during an initial 30-min control period. The influx rate constants, K_{in}, for blood to brain transport of palmitic acid, a 16-carbon saturated fatty acid, and oleic acid, an 18-carbon unsaturated fatty acid, were determined.

[^{3}H]Palmitic acid or [^{3}H]oleic acid (1.2 mCi, New England Nuclear, Wilmington, DE) in ethanol was dried under nitrogen, resuspended in 250 µl of saline or plasma and infused at a constant rate into the arterial cannulae over a 5-min period. The brain was then rapidly removed, and tissue samples were collected from specific brain regions for digestion and determination of radioactivity levels by

liquid scintillation spectrometry. Additional tissue samples were collected, extracted with chloroform/methanol solvent, and subjected to TLC and quantitative phospholipid analysis. Isolated phospholipid fractions (free fatty acid, PC, phosphatidylinositol [PI], phosphatidylserine [PS], phosphatidylethanolamine [PE], and sphingomyelin) from the TLC were also analyzed for radioactivity and incorporation of [^{3}H]palmitate or [^{3}H]oleate.

Blood-brain transport of [^{3}H]palmitate was evaluated by the integral method, as described previously (96). The influx rate constant, K_{in}, is calculated from the relationship $C^*_{brain} = K_{in} \int_0^T C^*_{plasma}\, dt$, in which C^*_{brain} is the radioactivity (dpm/mg) in brain tissue, C^*_{plasma} is the radioactivity (dpm/ml) in arterial plasma, and T is the time of infusion (sec). Because the radioactivity in brain is measured, and the time and amount of infused radioactivity are known, the influx constant, K_{in}, is readily calculated. For calculation of net transport of palmitate and oleate, the relationship $v_{net} = 60(K_{in})(S)$, in which S is the plasma palmitate or oleate concentration, was employed. The perfusate concentrations of unesterified long-chain fatty acids were determined by extraction, derivatization (methyl ester), and gas chromatography.

Results. The permeability of the brain vasculature to palmitate and oleate was relatively low (Table 19). White matter was the least permeable (smallest K_{in} values) to palmitate, and midbrain and hippocampal regions had influx constants approximately twice the values for white matter. Cortical regions of the cerebrum and cerebellum had the highest influx constants, which were about four times the white matter values.

Transport of oleic acid into brain was significantly greater than palmitic acid transport in all areas of the brain examined (Tables 19, 20). In cerebral cortex, the K_{in} values were four to five times greater for oleate than palmitate. The K_{in} values of oleate and palmitate transport into the pituitary, a structure lacking a typical blood-brain barrier, were similar and were significantly greater than those in the other brain regions.

The concentrations of fatty acids in the perfusate (Table 21) were found to vary over a fivefold range and to be similar to those for the same fatty acids in plasma from fasted humans (97). The combination of palmitate and oleate represent about one-half of the total fatty acids. Because the concentrations of perfusate palmitate and oleate are about equal (80 μM), the net uptake of palmitate and oleate are about 0.4 nmol/g·min and 1.5 nmol/g·min, respectively.

When soman (100 μg) was administered acutely to the perfused brain by bolus injection into the carotid cannulae, an immediate increase occurred in CBF (~60%), and a grand mal-like seizure occurred after ~4 min. Blood-brain transport of palmitate but not oleate determined under those conditions increased two- to threefold over transport under control conditions (Tables 19, 20).

The metabolic fates of the free fatty acids after they entered the brain were determined by regional analysis of brain lipids (Tables 22, 23). In control experiments, 40-60% of the radioactive palmitic acid was recovered in PC (Table 22). The free fatty acid fraction contained 25-35% of the total radioactivity, and sphingomyelin labeling consisted of 12-20% of the total. Small and similar incorporations into PI, PS, and PE were detected. These results were similar in all of the eight structures examined except white matter (data not shown) in which all free fatty acid incorporations were low, a result consistent with the low blood-brain transport rates for white matter.

After soman exposure, the pattern of [^{3}H]palmitate labeling was drastically changed. The total radioactivity of the extracted lipids significantly increased and resulted from a two- to eightfold increase in the free fatty acid fraction. This increase was at the expense of incorporation into all the other lipids, which consistently had lower amounts of [^{3}H]palmitate (Table 23).

Metabolism of [^{3}H]oleic acid was markedly different. The majority of [^{3}H]oleate was recovered in the free fatty acid fraction (Table 24). Among the phospholipids, incorporation into PC was greatest, with incorporation into PE and PI about one-half and one-fourth that of PC, respectively. Only small

amounts were incorporated into sphingomyelin and PS. Similar results were observed in the various brain structures, with white matter having low incorporations (data not shown).

During soman-induced seizure, the amount of [^{3}H]oleate found in the phospholipids decreased by 50% or more. This result is similar to that observed for [^{3}H]palmitate (Table 25). Levels of [^{3}H]oleate in the free fatty acid pool did not change.

Positional analysis of the labeled PC showed that palmitate was predominantly incorporated into the *sn*-1 position and oleate into the *sn*-2 position. These results are in agreement with the natural distribution of saturated and unsaturated fatty acids in brain phospholipids (Fig. 19).

PC metabolism was also investigated using [^{3}H]Ch as a labeled precursor similarly to the fatty acid incorporation experiments. It was anticipated that Ch would be taken up by the brain and be incorporated into PC. This would then make it possible to study the metabolism of labeled PC and the effect of soman exposure on its metabolism. However, infusion of labeled Ch for 5 min did not result in extensive incorporation into PC. A repeat of the experiment yielded the same result. It is concluded that the incorporation of Ch into PC is relatively small or the specific activity of the intracellular pool of cholinesterase is too low to detect incorporation.

Comment. These studies demonstrate that phospholipid metabolism in brain is dynamic and surprisingly active—a finding that is in contrast to the notion that membranes and their lipids are substantially inert. These results also indicate that the metabolism, but not transport, of free fatty acid is drastically altered by soman exposure and during soman-induced seizure. The data further suggest that the rate of phospholipid synthesis is decreased or the rate of phospholipid degradation is increased or both. In addition, our results suggest possible effects of OP on carrier-mediated transport systems at the blood-brain interface. These effects may be the result of an increase in the surface area of the vasculature, resulting from extensive vasodilation.

These results parallel the findings of protein synthesis (Specific Aim 4, above), another major energy-requiring process that was greatly diminished by OP-induced seizure.

Specific Aim 9. Examine the effects of organophosphorus compounds on labeling of phosphatidylcholine and on receptor-mediated choline turnover.

Background. AChE inhibitors have been shown to cause rapid accumulation of ACh in brain because of their ability to block the hydrolysis of ACh to Ch and acetate. Unexpectedly, it has been observed that brain Ch levels also increase simultaneously (52-54, 83). The elevated Ch has been proposed to originate from hydrolysis of PC, a Ch-containing lipid, and may result directly from the effect of AChE inhibitors on PC hydrolysis or indirectly via ACh through muscarinic receptor stimulation of PC hydrolysis. It has been suspected that some AChE inhibitors may also interact with certain phospholipases to affect their activities and cause changes in Ch levels in brain. In this study, we investigated the direct effects of soman, physostigmine, and DIFP on the hydrolysis of PC by canine cerebral cortex synaptosomes.

Method. Experiments were conducted to examine the effects of anticholinesterase compounds on PC metabolism and the effects on receptor-mediated Ch release from Ch-containing lipids. Brains were isolated and perfused for a control period of 35-45 min to establish a steady state and to obtain baseline data. Administration of 100 µg of soman to the brain vasculature was accomplished by injection directly into the arterial cannulae. Perfusion of the brain was discontinued 15 min after the injection, brain cerebral cortex tissue was dissected, and subcellular microsomal and synaptosomal fractions were prepared essentially according to the following procedure.

Preparation of canine cerebral cortex synaptosomal fractions. The subcellular fractions from dog cerebral cortex were prepared according to Whittaker and Barker (88) and modified as described (89). Briefly, fresh dog cerebral cortex was minced and homogenized (10% w/v) with a Potter-Elvehjem

homogenizer in 0.32 M sucrose containing 1 mM EGTA. The homogenate was centrifuged initially at 1000 x g for 10 min, and the postnuclear supernatant was centrifuged at 22,000 x g for 30 min to obtain a crude membrane pellet that contained myelin, synaptosomes, and mitochondria. The crude membrane fraction was resuspended in 0.32 M sucrose and centrifuged with a Beckman SW-27 rotor at 53,000 x g for 1 hr on a discontinuous sucrose density gradient of 0.32 M, 0.85 M, and 1.2 M. The crude synaptosomal fraction was collected between the 0.85 and 1.2 M sucrose layer. The fraction containing the synaptosomes was diluted to a final sucrose concentration of 0.32 M and layered on top of a discontinuous sucrose gradient of 0.32, 0.85, and 1.2 M. After centrifugation at 75,000 x g for 30 min, the material at the interface of the 0.85 and 1.2 M sucrose layers was collected, diluted with 0.32 M sucrose, and centrifuged at 14,500 x g for 20 min to give the synaptosomal pellet. The pellet was then washed several times and resuspended in 0.32 M sucrose and stored at -20°C until use. The protein content was determined according to Lowry *et al.* (90).

Measurement of the choline-containing products of phosphatidylcholine hydrolysis. The exogenous substrate 1,2-dipalmitoyl-*sn*-glycerol-3-phosphoryl[^{3}H]choline (^{3}H-PC) (S.A. = 1 x 10^4 dpm/nmol) was used (95). Each incubation mixture in 0.25 ml contained 32 mM [^{3}H]PC (8.0 x 10^4 dpm), 40 mM HEPES buffer at pH 7.0, 0.1 mM $MgCl_2$, and 0.4% Triton X-100. The reaction was initiated by the addition of cerebral cortex synaptosomes (200-300 µg of protein) as the enzyme source and incubated at 37°C, with shaking for 30 min. Reactions were stopped by adding methanol containing 1% acetic acid, and lipids were extracted. The radioactive Ch and phosphorylcholine in the upper phase were separated with a Dowex-1 anion-exchange column or separated by TLC (silica gel-H) using methanol/0.6% NaCl/concentrated ammonia (50:50:5) (98). The radioactivity levels of the Ch fractions were measured using liquid scintillation spectrometry. The amount of [^{3}H]Ch released that was separated from phosphorylcholine represents the hydrolytic activity of phospholipase D. To eliminate [^{3}H]Ch as a product of the hydrolysis of phosphoryl[^{3}H]choline that may be produced by PC phospholipase C action, 5.0 mM cold phosphorylcholine or 5.0 mM *p*-nitrophenylphosphate, competitive inhibitors of alkaline phosphatase (95, 98), was present in all incubation mixtures. The radioactivity in the Ch fraction was consistently higher than 90% of the total radioactivity recovered in the aqueous phase after lipid extraction. On the other hand, less than 10% of the radioactivity was recovered in the phosphorylcholine fraction, and only a trace amount of radioactivity was recovered in the glycerophosphorylcholine fraction. The enzyme activity was linear with time and protein concentrations used in our experiments.

The direct effects of physostigmine, another AChE inhibitor, on PC hydrolysis by synaptosomes prepared from untreated dog brains were investigated using the same assay conditions as were used in the studies with soman.

To study the potential coupling between muscarinic receptors and phospholipase D, synaptosomes isolated from canine cerebral cortex were used. The hydrolytic activity of PC phospholipase D in the synaptosomes was measured using a radiochemical assay with 1,2-dipalmitoyl-*sn*-glycerol-3-phosphoryl[^{3}H]choline as the exogenous substrate. To examine the possible involvement of the G protein(s) in regulating PC phospholipase D activity, guanine nucleotide analogues were added to the incubation mixtures.

Results. *Organophosphate studies.* When the amounts of [^{3}H]Ch and phospho[^{3}H]choline released by synaptosomes prepared from two isolated dog brains that were perfused and treated with 100 µg of soman were compared with those of controls, a slightly higher (about 20% above the control value) but not statistically significant ($p > 0.05$, n = 4) amounts of radioactivity were released during the 30-min incubation time (Fig. 20). However, when various concentrations of soman (0.008 mg/ml - 0.16 mg/ml) were added to the incubation mixtures to examine the direct effects of OP on hydrolysis of PC by synaptosomes prepared from control dog brains, statistically significant ($p < 0.05$, n = 3), slight increases in [^{3}H]Ch and phospho[^{3}H]choline were observed (Fig. 21). The maximal stimulation reached 125% of the control value at 0.12 mg/ml; at the higher soman concentration of 0.16 mg/ml, PC hydrolysis was not affected.

Another organophosphate compound, DFP, was also used to examine the effects on PC hydrolysis by the control synaptosomal preparations. Under these conditions, DFP at concentrations between 0.005 mg/ml and 0.2 mg/ml did not affect PC breakdown ($p > 0.05$, n = 3, data not shown).

Physostigmine studies. The direct effects of physostigmine, another AChE inhibitor, on PC hydrolysis by control synaptosomes were investigated under the same assay conditions as were used in the soman studies. Physostigmine, similar to soman, also showed the statistically significant ($p < 0.05$, $n = 3$) but small stimulations at concentration ranges between 0.02 and 0.2 mg/ml when it was added to the reaction mixtures (Fig. 22). At concentrations higher than 0.2 mg/ml, physostigmine appeared to be ineffective.

Comment. Our previous studies (83) of the metabolism and blood-brain transport of Ch in perfused canine brain suggest that the production of Ch after organophosphate administration may involve hydrolysis of Ch-containing phospholipids. Brain Ch plays a central role in the metabolism of at least two classes of brain constituents: as a precursor and degradation product of the neurotransmitter ACh and as a component of the membrane lipids PC and sphingomyelin. We postulated that the dynamic interrelationship between the choline in ACh and Ch in membrane PC is highly regulated and balanced (92). A significant imbalance could arise as a consequence of chronic administration of AChE inhibitors that block the formation of Ch within synapses and thus reduce the amounts of Ch entering presynaptic terminals via high-affinity Ch uptake. PC is not only an important reservoir of Ch for ACh biosynthesis, but also is an integral part of the phospholipid component of neuronal membranes, comprising 30-60% of the total phospholipids. Since PC is a major Ch-containing phospholipid in brain, it can be postulated that substantial amounts of Ch can be derived from PC hydrolysis. Further, the increased Ch may result from the direct effects of AChE inhibitors on PC phospholipase D and/or phospholipase C or, indirectly, via cholinergic receptor-mediated PC hydrolysis. In studies of chicken heart, muscarinic stimulation enhanced the hydrolysis of Ch phospholipids and resulted in elevated Ch and phosphatidic acid (PA) levels (99). It was presumed that these results occurred via activation of phospholipase D (99). However, the biochemical mechanisms of action involved with Ch levels being increased by AChE inhibitors and cholinergic agonists were not understood until recently. Our findings (100) have demonstrated that a muscarinic ACh receptor regulates PC phospholipase D via the G protein(s) in canine cerebral cortex synaptosomes. It clearly suggests that the ability of AChE inhibitors to mobilize large amounts of Ch in brain is related to their effects on accumulation of ACh. This accumulation, in turn, results in a stimulation of a muscarinic ACh receptor, which causes the breakdown of membrane PC and a rapid elevation of Ch levels.

Our results here provide evidence that some AChE inhibitors, including physostigmine and soman, have slight stimulatory effects on the release of Ch and phosphocholine from PC, presumably via phospholipase D and phospholipase C mechanisms; however, DFP has no effect. Our studies with soman show that the concentration capable of inducing seizure and rapid elevation of Ch levels in perfused brain is 100-fold lower than the concentration capable of causing a statistically significant, but only slight, stimulation in *in vitro* incubation reactions. Therefore, we conclude that direct effects of AChE inhibitors on PC phospholipase D and phospholipase C do not play significant roles in elevating brain Ch levels, but may only partially, if at all, contribute to prolonged and slow elevation of Ch. Our results, from another aspect, support the hypothesis that a muscarinic ACh receptor-regulated PC phospholipase D plays a key role in rapid elevation of brain Ch levels after administration of AChE inhibitors.

Specific Aim 10. Determine changes in catecholamines and other neurotransmitters in organophosphate-exposed brain.

Background. Although it has been reported that exposure of animals to various convulsive and anticonvulsive drugs alters brain catecholamines levels, the roles of the adrenergic or dopaminergic systems in the etiology of seizure are not fully understood. Feldberg and Sherwood (101) and Jones and Roberts (102) found that intracerebral injection of norepinephrine (NE) into the brain accompanied anticonvulsant activity. Conversely, an intraventricular injection of 6-hydroxydopamine, which caused marked reduction in brain NE and dopamine (DA) levels, significantly lowered the seizure threshold (103). Banister and Singh (104), however, did not observe any change in the seizure threshold in rats whose NE level was reduced 50% by α-methyl-*p*-tyrosine (α-MPT). Several investigators have shown that monoamine oxidase (MAO) inhibitors, which would increase brain NE

levels, protected rats against the development of seizure (105-107). Contrarily, other workers did not detect such anticonvulsant activity of MAO inhibitors (108, 109). Beta-adrenergic-blocking agents are reported to have anticonvulsive effects (110), although Faiman *et al.* (111) found that propranolol failed to protect rats from OP-induced seizure. Despite the impressive evidence that brain NE participates in inhibitory functions essential for normal resistance to seizure, its role in the development of seizure is unclear.

Altering DA levels in the brain, either by DA or L-DOPA injections, also did not alter the seizure susceptibility (112-114). Apomorphine, which specifically activates DA receptors in the CNS, was found to elevate the threshold for electroshock seizure (115). Similar to NE, the role of DA in seizure etiology remains unclear.

To investigate the mechanisms that underlie the development of seizures and vasodilation during OP intoxication further, the catecholamines, a major class of CNS neurotransmitters, were examined in the perfused canine brain model. The primary aim was to determine whether significant changes in catecholamines occurred in response to acute OP exposure. As a followup study, the β-adrenergic blocker propranolol and the dopaminergic antagonist pimozide were included in the perfusate to ascertain if either of these types of receptors were involved in eliciting the OP responses despite the absence of gross alteration in the concentrations of their natural agonists, NE and DA. In addition to measurement of the catecholamines, the vascular and metabolic effects of these two antagonists are reported below in Specific Aim 12.

Method. Biogenic amines were determined using high performance liquid chromatography with electrochemical detection (HPLC-EC) analysis. In preliminary experiments, we found that direct injection of perchloric acid extracts into the HPLC analytical system results in the elution of several unidentified compounds at or near the solvent front and prior to elution of most biogenic amine compounds of interest. These earlier eluting substances reportedly can be eliminated by purifying and concentrating the biogenic amines with adsorption and elution from activated alumina columns. An evaluation was performed on this method of alumina purification before HPLC analysis. Our results indicated that although these chromatograms showed fewer peaks and higher values for NE and DA, other compounds such as serotonin (5-HT), 5-hydroxyindole-3-acetic acid (5-HIAA), and homovanillic acid (HVA) were lost during the process. The recoveries were also inconsistent. Therefore, it was decided to proceed with the method in which the perchloric acid-extracted tissue samples are injected directly onto the chromatography column without passage through an alumina column.

Perfusion experiments were conducted to collect tissue samples for analyses of catecholamines and other neurotransmitters. The canine brain was isolated as described in METHODS and perfused for a control period of approximately 30 min to allow establishment of a steady state. Sarin (400 μg) or soman (100 μg) was administered by direct injection into the common carotid cannulae. In separate experiments, propranolol (0.06 μM) or pimozide (2 μM) was added to the perfusate after a 30-min control period, and soman was injected ~15 min after propranolol or pimozide treatment. Ten to sixty minutes later, brain tissue was dissected from six different regions (cerebellum, frontal cortex, parietal cortex, brain stem, hippocampus, and hypothalamus) and immediately frozen in liquid nitrogen. The frozen samples were stored at -70°C until the biogenic amines were extracted from tissue (200 mg) with 1.0 ml of cold 0.05 M perchloric acid, and 100 μl were injected directly into the HPLC-EC system for analysis of NE, DA, 5-HT, HVA, and 5-HIAA. Dihydroxybenzylamine was used as the internal standard.

Results. Analysis of brain biogenic amines in perfused control brains revealed distinct regional variations in the respective compounds (Table 26). The hypothalamus and brain stem generally had lower catecholamine concentrations than the cerebellum or cortex, findings that are in general agreement with those reported for other species both qualitatively and quantitatively. The somewhat large variation in the data (large standard errors) is also reported by other workers and is often attributed to dissection, sampling, or individual test differences. Standard errors were not calculated for any of the experimental groups except the control because of the lack of sufficient numbers (n = 2) of valid data.

One hour after soman-induced seizure, the levels of DA appeared to be lower and NE higher in nearly all brain regions. No changes or trends were apparent for 5-HT, 5-HIAA, or HVA.

The presence of pimozide (DA receptor antagonist) appeared to diminish the soman-induced depletion of DA, whereas propranolol had no effect on this catecholamine (Table 26). Propranolol (β-blocker), however, tended to blunt the soman enhancement of NE. Neither antagonist appeared to affect the levels of 5-HT, 5-HIAA, or HVA.

Comment. Based on the analyses of biogenic amines in control brains, it is concluded that the perfusion model contains normal levels of the compounds measured. Soman exposure appears to cause depletion of DA, an effect that is antagonized by pimozide. This observation may suggest that a dopaminergic receptor is involved in either DA release or metabolism. DA depletion may be a result of its conversion to NE by DA hydroxylase. This is supported by the fact that NE is increased after soman exposure. A β-adrenergic receptor may be involved in this process because propranolol antagonized the response. Because of the lack of sufficient sampling size, no firm conclusions can be drawn.

Specific Aim 11. Examine the effects of α-methyl-*p*-tyrosine on cerebral blood flow, brain electrical activity, cerebral metabolism, and turnover of biogenic amines in control and in organophosphate-exposed brain.

Background. Catecholamines represent a major family of brain neurotransmitters and are derived by sequential metabolic steps from the amino acid L-tyrosine. It has been proposed that OP compounds such as soman or sarin may act by affecting biogenic amines or the respective functions that they regulate (e.g., cerebral blood flow, metabolism, etc., 116, 117). The compound α-MPT is a strong inhibitor of tyrosine hydroxylase, a rate-limiting enzyme early in the pathway of biosynthesis of DA, NE, and epinephrine. If OP agents alter the turnover of any of these catecholamines (increased or decreased degradation), then the catecholamine concentration should be significantly different in the presence and absence of the inhibitor (α-MPT). This was the hypothesis to be tested.

Method. Perfusion experiments were conducted to investigate the role of catecholamines in OP toxicity. Specifically, the involvement of DA was examined by depleting the brain DA with the inhibition of its synthesis by α-MPT. Analysis of catecholamines was with HPLC-EC.

Brains were isolated and perfused for an approximate 30-min control period. Then, α-MPT (300 mg/l) was added to the perfusate, and perfusion was continued for 60 min. This 60-min perfusion was conducted either in the absence of soman or following the administration of soman (100 μg) at the same time as the α-MPT. During this period, the brain electrical activity was constantly monitored by EEG, and blood samples were collected every 10 min and analyzed for metabolism rates. Following the OP exposure period, tissue samples from six brain regions (brain stem, cerebellum, cerebral cortex, motor cortex, hippocampus, and hypothalamus) were rapidly dissected and immediately frozen in liquid nitrogen. The frozen samples were stored at -70°C until the biogenic amines were extracted from tissue (200 mg) with 1.0 ml of cold 0.05 M perchloric acid. A 100-μl sample was then injected directly into the HPLC-EC system for analysis of NE, DA, 5-HT, HVA, and 5-HIAA. Dihydroxybenzylamine was used as the internal standard.

Results. Addition of α-MPT to the perfusate did not alter brain electrical activity or brain metabolism during the control period (Fig. 23A). This compound also was not vasoactive during the experimental period, indicated by an unaltered CVR (data not shown). Administration of soman after pretreatment with α-MPT produced the characteristic OP-induced effects, i.e., immediate vasodilation and increases in brain metabolism with the occurrence of seizure (Fig. 23B). The results of HPLC analysis (Table 27) indicated that the dog brain was rapidly depleted of DA when circulated with perfusate

containing α-MPT. The depletion was extensive, approaching the limits of detection (<4 ng/g of tissue) in cerebellum, cerebral cortex, and hippocampus, and about half the control values in brain stem and hypothalamus. The results also revealed no apparent differences, as determined by statistical analysis of variance, between depletion during control conditions or after OP exposure.

The response to α-MPT observed in these experiments was more rapid than previously observed during *in vivo* experiments in rats (109) and buttresses the previous evidence that α-MPT effectively blocks DA synthesis in brain. The results indicate that DA degradation in brain occurs at an average rate of at least 38 ± 12 (S.E.M.) ng/g/hr. The evidence also suggested that depletion of DA does not significantly alter the levels of NE, a major product of DA metabolism during the time frame of this study.

Comment. It is concluded that the inhibitor α-MPT quickly penetrates the blood-brain barrier and inhibits the formation of DA by blocking tyrosine hydroxylase. Mechanisms that involve DA utilization continue to be active during α-MPT exposure and result in DA depletion. However, depletion of DA did not significantly alter OP-induced vasodilation, OP-induced changes in brain metabolism, or the OP-induced seizure. No observable differences occurred between control and OP-exposed brain catecholamine levels. Thus, it does not appear that OP agents affect either the steady-state levels or the turnover of the measured biogenic amines.

Specific Aim 12. Examine the effects of receptor family antagonists on cerebral blood flow, brain electrical activity, and cerebral metabolism in control and in organophosphate-exposed brain.

Background. OPs are known to produce irreversible inhibition of AChE, which results in accumulation of ACh at the synaptic cleft. An excess of ACh overstimulates cholinergic receptors and disrupts neurotransmission, thus leading to toxic manifestation. The existence of cholinergic innervation and regulation of brain circulation has been extensively documented (81, 118). Using the isolated, perfused canine brain (3), Drewes and Singh (76) showed that OPs induce vasodilation and seizure, implicating cholinergic involvement in these events. Oxotremorine, another cholinergic agonist, did cause vasodilation, but did not produce fully developed seizure (119). Experiments with atropine (120) and scopolamine, both cholinergic muscarinic antagonists, resulted in the prevention of OP-induced seizure. Also, scopolamine blocked oxotremorine-induced vasodilation, but not OP-induced vasodilation. These results indicate involvement of independent or additional mechanisms in OP-induced vasodilation and OP-induced seizure.

Extensive studies on animals revealed the existence of adrenergic innervation parallel to cholinergic innervation and emphasized the significant role adrenergic innervation plays in cerebral vasomotor regulation (121). There is pharmacological evidence that this close relationship allows for an interaction mechanism by which the cholinergic nerves, through nicotinic receptors on the adjacent adrenergic fibers, can inhibit the release of NE and thereby promote a vasodilatory response during cholinergic nerve activation (122). This effect of NE is mediated through α-adrenergic receptors. It has been reported in another series of experiments that stimulation of noradrenergic neurons causes vasodilation of the cerebral arteries (123, 124). Lowe and Gilboe (125) observed that injection of NE into isolated, perfused brain caused vasodilation. Winquist *et al.* (126) noted that NE caused a relaxation in the porcine cerebral vessel *in vitro* and that the relaxation response to NE was blocked by β-adrenergic antagonists. These results indicate that NE exerts its effect on cerebral arteries by a β-adrenergic mechanism. DA is also reported to cause vasodilation and to increase CBF. McCulloch and Harper observed that stimulating dopaminergic receptors with apomorphine increased the CBF (127). Pimozide, a DA receptor blocking agent, prevented the apomorphine-induced increase in CBF (127). The existence of mast cells, located along the pial and intracerebral vessels (128), implicates the possible involvement of histamine in cerebral vasomotor regulation. Studies indicated that both H1 and H2 receptors are present in brain, with H2 receptors mainly responsible for vasomotor control.

In the following series of brain perfusion experiments, several antagonists were evaluated as potential agents to prevent OP-induced vasodilation and OP-induced alterations in metabolism. Additional experiments were conducted to test the vasoactive response of the cerebrovasculature to histamine and to characterize the response with the H2 antagonist cimetidine.

Method. *Neurotransmitter antagonists.* The mechanisms of OP-induced vasodilation and seizure genesis were investigated using the isolated, perfused canine brain preparation (3, 4). Brain tissues were isolated and prepared, and physiologic and metabolic measurements were determined as described in METHODS.

Previous experiments (for extensive review, see ref. 129) with cholinergic antagonists atropine and scopolamine and with cholinergic agonists oxotremorine and arecoline have established the involvement of a cholinergic muscarinic mechanism in OP-induced seizure, but not in OP-induced vasodilation. To evaluate the possible involvement of other transmitter mechanisms in these events, experiments were conducted with specific antagonists: scopolamine (cholinergic muscarinic antagonist, 1.6 μM), mecamylamine (nicotinic ganglionic blocker, 60 μM), propranolol (β-adrenergic blocker, 0.06 μM), pimozide (dopaminergic receptor blocker, 2 μM), and cimetidine (histaminergic H2 antagonist, 0.1 mM). These substances were used because of their potency, specificity, and their ability to penetrate the blood-brain barrier. They were dissolved in saline, and concentrations were calculated to be molar concentrations in the perfusate.

After a 30- to 45-min control perfusion period, specific antagonists were added to the perfusate, and arterial and venous blood samples were collected at regular intervals. Samples were analyzed to measure CMRs. Fifteen minutes after the antagonist was added, soman (100 μg) was injected directly into an arterial cannula, and blood flow was adjusted to maintain constant pressure. EEG was monitored to assess OP-induced effects on brain electrical activity after the respective pretreatments.

Histaminergic mechanisms. After a 30-min control period, 50-μl aliquots of histamine solution in a concentration range of 10^{-6} M to 10^{-1} M were injected via a carotid cannula. Injections were made after the vasodilatory response (CVR) returned to the control value. Cimetidine (10^{-5} or 10^{-4} M) was added to the perfusate in two experiments, and the series of histamine injections was repeated. The cerebrovascular response was calculated for each concentration point.

Results. Addition of scopolamine to the perfusate did not produce detectable changes in CVR or in brain metabolism, but did change brain electrical activity. Even though scopolamine alone did not prevent vasodilation induced by injection of OP, the effect was brief when compared to the duration of vasodilation induced by the addition of OP alone or addition of OP after the other antagonists (Fig. 24). Injection of OP produced an immediate decrease in perfusion pressure, characterized by a 25% decrease in CVR, and the pressure began to increase 5 min later (Fig. 24). Except for transitional disturbances in brain electrical activity, the EEG pattern retained scopolamine-induced characteristics throughout the experiment.

Addition of mecamylamine, pimozide, propranolol, or cimetidine to the perfusate had no effect on CVR (Fig. 24), brain metabolism (Fig. 25A-C), or brain electrical activity. Perfusion pressure was unchanged, CMRs for glucose, O_2, and CO_2 remained essentially the same as during the control period, and the EEG was unchanged. None of these antagonists, however, prevented the characteristic responses to soman exposure. Administration of soman was followed by an immediate decrease in perfusion pressure, manifested by a 25-40% decrease in CVR that remained low for 15 min, and seizure genesis occurred in all cases within 4-5 min. With the occurrence of seizure, the CMRs of glucose, O_2 and CO_2 increased 30 to 60% (data not shown).

In our experiments, histamine had a dose-dependent vasodilatory effect. This response was inhibited by cimetidine, a specific H2 antagonist, at submillimolar concentrations (data not shown).

Comment. Our observations excluded a cholinergic muscarinic mechanism as the sole factor in OP-induced vasodilation and suggest some additional mechanism(s) in this event. The initial (<1 min) event in OP-induced vasodilation may have different components from the later (>5 min) phase of

induced vasodilation. Even though pretreatment with scopolamine was not enough to prevent the occurrence of OP-induced vasodilation, a faster recovery of CVR during these experiments was evident (Fig. 24), which supports a cholinergic mechanism for a portion of the response. The observed vasodilation had the characteristics of OP-induced vasodilation and did not change in intensity or duration. Although histaminergic mechanisms appear not to be involved in OP-induced vasodilation, histamine was a potent vasoactive substance when administered to the cerebrovasculature. The response appears to be mediated via an H2 type histidine receptor.

The results of our experiments indicate that OP-induced vasodilation and seizure may be uncoupled, i.e., occur by separate, independent mechanisms. In addition, our studies exclude simple involvement of cholinergic muscarinic, cholinergic nicotinic, dopaminergic, adrenergic, or histaminergic mechanisms in OP-induced vasodilation. The cholinergic muscarinic mechanism plays some role in this vasodilation, but only as a part of a more complex process. Studies of involvement of the endothelium-derived relaxing factor (EDRF) may give some additional insight into the mechanism(s) of OP action.

In a parallel study we examined the possible role of NE using α-MPT (inhibitor of NE biosynthesis). These studies are reported in detail in Specific Aim 11.

Specific Aim 13. Examine the effects of a nicotinic agonist on receptor–mediated release of choline from phospholipids. Test the hypothesis that the muscarinic receptor-regulated phosphatidylcholine phospholipase D and phosphatidic acid phosphatase pathway is important in signal transduction for generation of diacylglycerol from phosphatidylcholine in brain.

Background. Diacylglycerol (DAG), an intracellular second messenger, plays an important role in cell signal transduction by activating protein kinase C that, in turn, phosphorylates a range of cellular proteins (130, 131). The well-established pathway for generation of DAG is via receptor-mediated stimulation of inositol phospholipid breakdown by specific phospholipase C action (132, 133). Recently, this classical scheme involving inositol phospholipids as the sole source of DAG has been challenged (134-136). Mounting evidence indicates that an important alternative mechanism for the agonist-induced generation of DAG may be through breakdown of PC (98, 137-141). The formation of DAG may occur either directly via PC phospholipase C or by the action of PC phospholipase D to yield PA that is further dephosphorylated to DAG by PA phosphatase. However, the actual biochemical mechanisms for agonist-stimulated DAG generation from PC have yet to be characterized and may indeed vary from receptor to receptor in different types of cell systems.

Our recent findings (100) revealed that a muscarinic ACh receptor regulates PC phospholipase D via a guanine-nucleotide-binding protein (G protein) in canine cerebral cortex synaptosomes and indicated that this muscarinic receptor-regulated PC phospholipase D is responsible for the rapid formation of Ch and PA. Since PA phosphatase is abundant in synaptic membranes (142), it can be inferred that PA formed by the phospholipase D activity on membrane PC might serve as a substrate for the PA phosphatase activity present in the synaptic membranes. Therefore, we postulate that muscarinic receptor-regulated PC phospholipase D and PA phosphatase comprise an important signal-transduction pathway for generation of Ch and DAG from PC in brain.

Method. *Preparation of [3H]PA.* The [^{3}H]PA was prepared from 1-palmitoyl-2-[9,10-^{3}H]palmitoyl-L-3-phosphocholine (Amersham Corp.) by action of phospholipase D from *Streptomyces chromofuscus* (Sigma). Incubation buffer contained 1 mM $MgCl_2$, 0.5 mM $CaCl_2$, 0.1% Triton X-100, and 40 mM HEPES, pH 7.4. Reactions were carried out for 60 min at 30°C, with shaking. Lipids were extracted as described (100) after the reactions were stopped. [^{3}H]PA was separated on Silica Gel G plates using the upper phase from a mixture of ethyl acetate/2,2,4-trimethylpentane/acetic acid/water (9:5:2:10) (143). PA was localized by brief exposure to iodine vapor. To allow the iodine to evaporate, plates were held at room temperature for 30 min before elution of [^{3}H]PA by methanol. The specific radioactivity of [^{3}H]PA was 57 Ci/mol.

PA Phosphatase assay. Synaptic membranes of cerebral cortex were prepared as described previously (100). Incubation mixtures (0.25 ml) contained 1 mM $MgCl_2$, [^{3}H]PA (4 x 10^6 dpm), 40 mM HEPES at pH 7.4, 0.4 mM $CaCl_2$, and 0.04% Triton X-100. In inhibitor testing studies, unlabeled PA was combined with [^{3}H]PA, or various concentrations of propranolol were added. Reaction mixtures were ultrasonicated on ice for 10 sec and then incubated for 20 min at 37°C, with shaking. Reactions were stopped with methanol containing 1% acetic acid, and the lipids were extracted (98) and separated on Silica Gel 60 using hexane/diethyl ether/acetic acid (65:35:4) (144). Lipids were localized by exposure to iodine vapors, the specific area of DAG was scraped into vials, and the radioactivity levels were determined using liquid scintillation spectrometry. The PA phosphatase activity was not measurably altered by the presence of detergent (0.04% Triton X-100).

Measurement of radioactive PC breakdown. Radioactive PC (1-palmitoyl-2-[9,10-^{3}H]palmitoyl-L-3-phosphocholine) was used as the exogenous synaptic membrane substrate for phospholipases. Incubation mixtures (0.25 ml) contained 0.25 µCi of PC (exogenous PC specific activity: 57 Ci/mol), 40 mM HEPES at pH 7.4, 1 mM $MgCl_2$, 0.4 mM $CaCl_2$, 0.04% Triton X-100, 0.5 µM GTPγS, 150 µg of synaptic protein, and the indicated concentration of ACh or muscarine. Incubation and lipid extraction procedures were the same as described above. For PA analysis, the extracted lipids were separated on Silica Gel 60 using ethyl acetate/2,2,4-trimethylpentane/acetic acid (45:25:10) (145) or on Silica Gel H plates (with 1% potassium oxalate) developed in a solvent system of chloroform/methanol/10 N HCl (87:13:0.5). DAG was separated as described above. Individual lipids were localized by exposure to iodine vapors, the specific areas were scraped into vials, and the radioactivity levels were determined using liquid scintillation spectrometry. [^{3}H]Phosphorylcholine and [^{3}H]Ch produced from another radioactive-labeled PC (1,2 dipalmitoyl-*sn*-glycerol-3-phospho[^{3}H]choline) were separated and determined as described (100). The activity of phospholipase C using either of the two radioactive substrates was not measurably affected by 0.04% Triton X-100.

Results. To test our hypothesis, initial experiments were conducted to determine the presence and characteristics of PA phosphatase in synaptic membranes isolated from canine cerebral cortex. [^{3}H]PA was used as the exogenous substrate to measure the conversion of [^{3}H]PA to [^{3}H]DAG as an indicator of PA phosphatase activity. The activity was linear with incubation time (up to 40 min) and the synaptosomal protein concentrations (up to 400 mg of protein) used in our experiments (Fig. 26A and B). Several compounds were tested for their ability to inhibit PA phosphatase. The amphiphilic cationic drug DL-propranolol, reported to be a PA phosphatase inhibitor (128), was examined. A concentration-dependent inhibition was observed (Fig. 26C). Propranolol, at a concentration of 3 mM, caused an inhibition greater than 90%. This amphiphilic cationic compound was postulated to interact with membrane PA by its positively charged substituted amino group (146), thus causing inhibition of PA phosphatase. However, propranolol is known also to be a nonselective β-adrenergic blocker. Although exogenous norepinephrine (NE) was absent from our assay system, we tested the effects of NE on PA phosphatase activity. With our experimental conditions, addition of NE had no effect on the conversion of [^{3}H]PA to [^{3}H]DAG. This result indicates further that inhibition of PA phosphatase by propranolol is unlikely to be related to its β-blocking activity. This β-blocking-independent inhibitory effect on PA phosphatase was also reported by several other groups (147-149). Another compound we tested was unlabeled exogenous PA (cold PA), and this compound caused a decrease in [^{3}H]DAG formation (Fig. 26D). As previously suggested, this apparent inhibition of PA phosphatase activity is the result of competition between cold PA and [^{3}H]PA as substrate for the enzyme (138). These two compounds, propranolol and cold PA, are useful tools for characterizing the mechanism of DAG generation.

To examine PA and/or DAG generation by cholinergic agonists, the following experiments were performed. When radioactive-labeled PC was used as the exogenous substrate for synaptic membrane phospholipases, the addition of cholinergic agonists ACh or muscarine in the presence of 0.5 mM GTPγS, caused a concentration-dependent stimulation of [^{3}H]PA formation (Fig. 27A). At the same time, a significant increase in [^{3}H]DAG was observed (Fig. 27B). The accumulation of [^{3}H]DAG may result either from direct PC phospholipase C action or from the combined actions of PC phospholipase D and PA phosphatase. To distinguish these possible biochemical mechanisms, we first measured the time course of [^{3}H]PA and [^{3}H]DAG generation from [^{3}H]PC after 1 mM ACh stimulation (Fig. 27C). [^{3}H]PA rapidly accumulated within 15 sec, whereas [^{3}H]DAG formation

showed a transient lag period before becoming elevated and then exceeding the amount of [^{3}H]PA. Second, the amounts of [^{3}H]phosphocholine and [^{3}H]Ch produced by synaptic membranes were measured by using another radioactive-labeled PC, 1,2 dipalmitoyl-*sn*-glycerol-3-phospho-[^{3}H]choline, as the exogenous substrate (100). Muscarine caused a concentration-dependent accumulation of [^{3}H]Ch, but not [^{3}H]phosphocholine (Fig. 27D). These results indicate that the generation of [^{3}H]DAG by cholinergic agonists is not a result of the direct action of PC phospholipase C, but is most likely derived from the PC phospholipase D—PA phosphatase pathway. The possibility that accumulation of [^{3}H]PA could be from phosphorylation of [^{3}H]DAG by a DAG kinase activity is excluded because in our experiments no DAG kinase activity was detected in the absence of exogenous ATP.

Additional experiments were conducted to support this PC phospholipase D—PA phosphatase pathway mechanism. In our previous study, zinc was shown to be a potent inhibitor of PC phospholipase D in canine brain (95, 100). In the current study, muscarine-induced accumulations of both [^{3}H]PA and [^{3}H]DAG were significantly inhibited by 2 mM zinc (Fig. 28). Another compound, *p*-chloromercuribenzoate (*p*CMB), has been shown to be a potent inhibitor of phospholipase D in brain and plant tissues (150, 151). Therefore, the effect of *p*CMB on muscarine-induced accumulation of [^{3}H]PA and [^{3}H]DAG was also examined. Once again, no accumulation of [^{3}H]PA or [^{3}H]DAG was observed (Fig. 28). Zinc, a heavy metal ion, and *p*CMB, a sulfhydryl residue-blocking reagent, may be nonspecific phospholipase D inhibitors and may also inhibit PC phospholipase C activity in the synaptic membranes. However, neither zinc nor *p*CMB had any effect on basal phospholipase C activity (Z. Qian and L. R. Drewes, unpublished observations). Thus, inhibition by zinc and *p*CMB appears to be relatively selective for PC phospholipase D over PC phospholipase C. The inhibitory effects of zinc and *p*CMB on accumulations of [^{3}H]PA and [^{3}H]DAG suggest that when PC phospholipase D is inhibited, generation of [^{3}H]PA is prevented and no [^{3}H]PA is available for dephosphorylation by PA phosphatase to form [^{3}H]DAG.

To validate the phospholipase D—PA phosphatase pathway further, muscarine was added to the incubation mixtures to stimulate breakdown of [^{3}H]PC in the presence of a PA phosphatase inhibitor, propranolol, or cold PA (Fig. 28). Muscarine caused significant additional accumulations of [^{3}H]PA. However, [^{3}H]DAG did not accumulate, and even decreased, when compared with the control. These results show that [^{3}H]PA produced by muscarine-stimulated PC phospholipase D cannot be further degraded to [^{3}H]DAG because the conversion of [^{3}H]PA to [^{3}H]DAG is blocked by propranolol or cold PA.

Comment. Our above results provide strong evidence that a muscarinic ACh receptor-regulated PC phospholipase D—PA phosphatase pathway does exist in the synaptic membranes of canine cerebral cortex and indeed is responsible for the accumulation of DAG in the CNS after ACh stimulation (152). PC is the major lipid component of all eukaryotic cells and comprises 30 to 60% of membrane phospholipids, including the synaptic membranes in brain. Furthermore, a large quantity of protein kinase C is also associated with synaptic membranes (153). It is reasonable to postulate that DAG generated in synaptic membranes by our newly discovered pathway plays an important role in activation of protein kinase C in brain. Since the fatty acid composition of DAG from PC often differs from that of the inositol phospholipids, the question of whether different species of DAG regulate different subspecies of protein kinase C in brain has yet to be resolved.

Specific Aim 14. Examine the efficacy of scopolamine and valproate as protective agents against cerebral damage caused by organophosphate-induced seizure.

Background. Acute exposure to OP agents produces neurological seizure and respiratory arrest. Neuropathological damage is readily detectable within 1 hr of exposure (119, 154), progresses for 24-48 hr, and is permanently established and evident weeks following exposure. The lesions detected by light and electron microscopy following acute OP exposure resemble lesions caused by hypoxia and ischemia and, therefore, may be related to the stimulated energy and metabolic demands of seizure. Some attempts have been made to correlate the pathological damage to the presence or absence of convulsions (155, 156). However, no clear answer has yet emerged to the

question of what damage is a result of seizure and the related cholinergic crises. If brain lesions can be significantly reduced by preventing seizure, then the use of anticonvulsants may be a useful strategy for preventing significant degeneration induced by OP seizure.

Extensive morphological alterations and edema are evident in the isolated perfused dog brain 1 hr following OP exposure and seizure (8, 154). Cholinergic antagonists (e.g., scopolamine and atropine) prevent seizure induction.

Valproic acid (VPA) is an anticonvulsant drug that has been successfully used to treat several forms of seizure (157, 158). VPA is related structurally to γ-aminobutyric acid (GABA), and even though it is thought to have a mechanism of action involving the enhancement of GABA-mediated neurotransmission (159), the precise mechanism is not known. Some researchers have reported that VPA causes a specific dose-related increase in potassium membrane conductance that leads to hyperpolarization of the resting membrane potential (160). No previous report describes the testing of VPA as an anticonvulsant following OP exposure. Experiments were conducted to examine the efficacy of VPA to act as an anticonvulsant to soman.

Method. After a 30-min control perfusion period, VPA was added to the perfusate at concentrations of 0.4-0.7 μM. These concentrations are at the upper range of pharmacological activity for VPA as an anticonvulsant in humans. The VPA was circulated through the perfusion system for 10-60 min, during which time the metabolism rates and brain electrical activity were examined, before the addition of soman (100 μg).

Perfusion experiments were conducted to examine the ability of cholinergic antagonists to protect the brain from OP-induced edema formation, which is thought to be the result of seizure activity. Each brain was perfused for a 30-min control period and for an additional 15 min with perfusate containing the muscarinic antagonist scopolamine (1.3 μM). This amount of scopolamine is sufficient to prevent OP-induced seizure. In one experiment, soman (100 μg) was administered and in another, sarin (400 μg); a third served as a scopolamine-treated control. Approximately 60 min after OP exposure or after 90 min of perfusion for the control experiment, brains were flushed briefly with saline to remove erythrocytes and other blood components. The brains were then perfusion fixed with appropriate preservation solutions, and tissues were prepared for light and electron microscopy.

Results. Addition of VPA to the perfusate did not produce observable changes in brain metabolism or in the diameter of brain vessels, which would have been detected by a change in perfusion pressure and CVR. CMR values and EEG patterns were unchanged from those of the control period. Injection of OP caused immediate vasodilation, but seizure occurrence was inconsistent. In two experiments, seizure was fully developed. In other experiments, EEG changes were nonspecific, ranging from near normal cortical electrical activity to activity exhibiting gradually smaller and smaller amplitudes.

The protective effects of scopolamine against OP-induced seizure are known from previous experiments. To evaluate protection from scopolamine on a cellular level, brains were fixed for light and electron microscopy. The results indicate that shifts in cellular osmolytes and water occurred despite scopolamine's inhibition of extensive neuronal firing (seizure). Although no seizure activity was apparent from the EEG, edema formation was pervasive and other morphological alterations were present. When compared to OP-exposed brain with no protection against seizure, the cellular alterations and edema were qualitatively similar, but appeared quantitatively somewhat less. However, in control brain tissue perfused and administered only the antagonist, significant signs of edema and morphological alterations were observed. Because scopolamine is commonly used clinically, this result was unexpected and may be an anomaly; however, it should not be ruled out until it is repeated.

Comment. It is concluded that under the conditions of these experiments, the anti-epileptic activity of valproate was ineffective in inhibiting soman-induced seizure, although all results were not in agreement. Because VPA was generally ineffective as an anticonvulsant, light and electron microscopy was not performed on VPA-exposed brains.

Results of the experiments with scopolamine suggest that the anti-epileptic effects on OP-induced seizure are not sufficient to prevent the neurological and neuropathological consequences of OP poisoning. Our studies suggest that mechanisms of cellular degeneration leading to necrosis are activated by OP agents in the absence of sustained seizure. Extensive lesioning, however, may be ameliorated by the action of effective anticonvulsants such as cholinergic antagonists. This may be an important observation for suggesting therapeutic strategies because anti-epileptic drugs, although not sufficient for preventing the specific toxic effects of OP poisoning, may be beneficial in substantially reducing the associated pathological consequences.

Specific Aim 15. Examine the effects of HI-6 and pyridostigmine (and physostigmine and neostigmine), alone or in combination with other drugs, in control and in organophosphate-exposed brain.

Background. In the classic treatment for poisoning by OP compounds, atropine is employed to counteract the muscarinic effects of ACh accumulation, and an oxime is used to reactivate the inhibited enzyme. However, with some OP compounds, such as soman, the inhibited enzyme undergoes an "aging" process that makes it resistant to the nucleophilic attack of oximes (161). In case of poisoning by soman and other similar compounds, conventional oximes are not effective treatment because 1) they are poor reactivators of inhibited AChE, 2) they are incapable of reactivating "aged" enzyme, and 3) most of these oximes do not pass the blood-brain barrier (162, 163). The bisquaternary mono-oximes (HS-6 and HI-6) have been shown to be effective against soman intoxication in rats (164). A number of previous studies have indicated that the AChE reactivation by oximes does not correlate well with their protective effects (165, 166). Lundy and Shih (167) proposed that OP-poisoning protection by HI-6 cannot be predicted solely from examining the brain ACh values. They also proposed that central-noncholinergic effects of HI-6 may be important in reducing the effect of OP. HI-6 has been reported to exert ganglionic (168) and antimuscarinic blockade (169).

Several carbamate anticholinesterase compounds have been found to be effective in protecting animals against soman poisoning (170). Since both carbamate and OP compounds inhibit the enzyme AChE by similar mechanisms, addition of the two compounds together would be expected to enhance the toxic action. Koster (171) proposed that carbamates provided protection against OP toxicity if their administration occurred before OP exposure. When carbamate was administered after the OP, however, additional toxic effects were observed (171). The mechanism for this apparent paradox is not known. Berry and Davis (170) and Gordon *et al.* (172) have shown that protection given by physostigmine and other carbamates against soman poisoning was optimum if the interval between administration of the two drugs was about 30-60 min. They also observed that the dose of carbamate was not critical and protection was essentially constant for doses ranging from half to four times the maximum dose. The duration of the protective action of a single intramuscular injection of carbamates was greater than 2 hr, pyridostigmine being the largest (172). Dirnhuber *et al.* (173) showed that doses of pyridostigmine that produced 50 or 30% inhibition in AChE activity had essentially the same protection against soman poisoning. Harris *et al.* (174) have shown that the mean ACh concentrations in physostigmine-treated rats were higher than in those animals treated with both physostigmine and soman. In the present studies, the combined effect on OP exposure of a carbamate AChE inhibitor, pyridostigmine (or physostigmine, neostigmine), with a cholinergic antagonist (scopolamine) was investigated. Because pyridostigmine is a charged molecule and does not readily penetrate the blood-brain barrier, the efficacy of opening the barrier by pretreatment with hyperosmolar urea or mannitol was also tested. Finally, HI-6, a potential reactivator of inhibited AChE, was investigated for its ability to ameliorate the CNS response to OP exposure.

Method. After a control period of 30-35 min, we added pyridostigmine (10 mg/l), physostigmine (0.03 mM), neostigmine (0.16 mM), or HI-6 (12.5 mg/l) to the perfusate and observed the EEG patterns, perfusion pressure, blood flow, and cerebral metabolism. Following an additional perfusion period of 10-30 min, OP (100 μg of soman) was rapidly administered via the arterial cannulae. Physostigmine under the above conditions was itself found to be convulsant; therefore, in two experiments the lipid-soluble muscarinic antagonist scopolamine (1.3 μM) preceded the

administration of physostigmine to block the cholinergic convulsant and vasodilatory actions of this reversible cholinesterase inhibitor. In two experiments with pyridostigmine, the brain was treated for 30 sec by infusion of either 1.2 M mannitol in saline or 2 M urea in saline to permeabilize the cerebrovasculature to the carbamate.

Results. Our results indicate that the cholinesterase inhibitors that are unable to penetrate the cerebrovascular endothelial layer are unable to induce vasodilation or substantial EEG and metabolic alterations. Pyridostigmine and HI-6, both very hydrophilic and ionic, are limited to the blood and do not cause vasodilation, induce seizure, or alter metabolism. Furthermore, when the brain vasculature was altered by hyperosmolar agents to allow penetration of pyridostigmine, no major alterations in blood flow, EEG, or metabolism were observed. In contrast, when physostigmine was added to the perfusate, the initial brain electrical activity pattern was altered, and strong vasodilation occurred immediately (Fig. 29). The initial characteristic change noted in the EEG was synchronization of electrical activity or the appearance of waves of low voltage and high frequency. Seizure occurred after ~5 min, and cerebral metabolism increased accordingly (Fig. 30). This pattern was similar to that observed with soman or sarin. However, when scopolamine was pre-administered to the perfusate, no dilation (Fig. 29) or seizure occurred; CMRs were unchanged (Fig. 30). Additional injection of soman during these experiments did not produce further changes in EEG, blood flow (Fig. 29), or metabolism of glucose, O_2, or CO_2 (data not shown).

In the first experiment with neostigmine, we progressively increased the concentration of the inhibitor in the perfusate from 0.02 mM to a final concentration of 0.1 mM. During this experiment, neostigmine did not produce changes in vasodilation or in glucose, O_2, or CO_2 metabolism. The EEG showed gradual changes with a decrease in amplitude and an increase in frequency. The remaining experiments were performed with a final neostigmine concentration of 0.16 mM. This concentration produced slow and sustained vasodilation with the same changes in EEG as previously described, with no effect on brain metabolism. Neostigmine was allowed to circulate for 15 min before soman (100 µg) was injected. OP did not produce additional vasodilation, except in one experiment in which the vasodilation was about 18% greater. The most consistent change was the reduction in the time of seizure genesis from 4-5 min to 2-3 min after OP injection. The development of seizure was followed by the typical increase in brain metabolism.

Administration of HI-6 (12.5 mg/l) into the perfusate during four separate experiments resulted in no changes in physiologic or metabolic parameters of the perfused brain. Brain electrical activity, monitored by EEG, blood flow, and glucose, lactate, and oxygen metabolism were unchanged. Following about 20 min of HI-6 exposure, OP (sarin, 400 µg) was administered, and no detectable difference was observed when compared to the response in the absence of HI-6.

Comment. With regard to the acute effects of the oxime-type cholinesterase inhibitors on the CNS, our results basically corroborate studies indicating that the brain endothelium is a major barrier to the entry and action of these agents. Compounds that are more lipid soluble, such as the tertiary amine physostigmine, are able to act centrally, but lipid-insoluble (water soluble) compounds such as pyridostigmine and HI-6 are not active centrally. However, our results also suggest "opening" the blood-brain barrier with hyperosmolar agents may not be effective for the blood-borne pyridostigmine compound.

In contrast to soman exposure, scopolamine prevented the physostigmine-induced dilation and seizure. Thus, a major distinction between OP agent mechanisms and physostigmine mechanisms was indicated. Neostigmine, as a quaternary ammonium drug, does not cross the blood-brain barrier easily. Although neostigmine, at elevated levels, was able to prevent OP-induced vasodilation, the occurrence of OP-induced seizure was precipitated. Because seizure genesis is dependent upon penetration of certain substances into the brain, a low accumulation of neostigmine (and subsequent elevation of ACh) within the brain tissue was not enough to produce seizure, but was enough to lower the seizure threshold. Under the conditions of our experiments, it appears that HI-6 in the CNS is poor in its protection or rapid reactivation from OP exposure.

The blocking of OP-induced vasodilation by the combination of physostigmine and scopolamine represents, to our knowledge, the first demonstration of the antagonism of this pathophysiological

effect of OP agents. Thus, the distinction between OP agent mechanisms and physostigmine mechanisms suggests the potential usefulness of this regimen for preventing a toxic effect from soman. These observations led to additional hypotheses involving the effect of OP agents on cerebrovascular blood flow regulating factors and are detailed further in Specific Aim 16 below.

Specific Aim 16. Determine the effects of nitric oxide and nitro blue tetrazolium on blood flow, cerebral metabolism, and brain electrical activity in control and in organophosphate-exposed brain.

Background. One of the neuropathologic consequences of OP toxicity is extensive vasodilation of the cerebral vasculature. To prevent or reverse this response by pharmacological means requires a better understanding of the underlying mechanisms. Previous studies (129, 175) have eliminated several potential mechanisms involving neurotransmitters as major contributors to the OP-induced vasodilation. Recent studies of blood flow regulation in cerebral arteries and in arteries from numerous other sources indicate that endothelial cells produce a factor that diffuses to the adjacent smooth muscle cell and causes the smooth muscle cell to relax (176). This so-called EDRF (endothelium-derived relaxing factor) is short lived ($T_{1/2}$ = 6 sec), anionic, and hydrophobic (177). Some reports indicate that EDRF is nitric oxide (NO) and is derived from the amino acid arginine (178). To examine the possible role of NO (the putative EDRF) in the cerebral vasculature during soman exposure, NO was first tested as a vasoactive chemical in the perfused brain preparation. The oxidizing agent nitro blue tetrazolium was then tested for its ability to block soman-induced vasorelaxation.

Method. *Vasoactivity of NO.* The canine brain was perfused for a minimum of 30 min to establish control and steady-state conditions. NO (0.001 M $NaNO_2$ in 0.01 N HCl) was then administered by injection into the arterial cannulae, and the perfusion pressure was observed for >5 min to monitor the CVR. The most dilute concentrations of NO were tested first, followed by increasingly higher concentrations. The CVR was allowed to return to constant control levels between NO administrations.

Nitro blue tetrazolium (NBT) experiments. NBT was dissolved in a minimum of 30% ethanol in saline and added slowly with mixing to the perfusate to a final concentration of 0.5 to 1 mM. Perfusion was maintained for 6-8 min before soman (100 µg) was administered rapidly as a bolus into the arterial perfusate. Perfusion and determination of vascular resistance were continued for 15 min.

Results. NO was a potent and effective vasodilator in the canine cerebrovasculature when injected into the carotid arterial perfusate (data not shown). The response was immediate, concentration dependent, and reversible within approximately 5 min.

Cerebral metabolism and blood flow were minimally affected by NBT in the perfusate. However, when soman was administered with the inhibitor NBT present in the perfusate, the typically rapid vasorelaxation response was completely blocked (Fig. 31).

Comment. These findings indicate that NO has strong vasoactive relaxation properties in the cerebral circulation and corroborates previous reports (177, 179, 180). Furthermore, the data suggest that NO plays an important role in the pathophysiological vasodilation response to OP agents. This is the first such demonstration and suggests that OP-induced, noncholinergic vasodilation occurs by the EDRF pathway and that EDRF may be NO. OPs thus cause vasodilation by stimulating the formation of EDRF (NO). The pathway by which EDRF is formed and the signal transduction mechanism by which EDRF causes smooth muscle relaxation are, therefore, targets for therapeutic drugs aimed at preventing or minimizing the neurotoxicity of OP agents.

Table 1. Regional Cerebral Blood Flow in Perfused Canine Brain and the Effect of Soman Exposure. Regional blood flow in the perfused canine brain was determined using [^{14}C]iodoantipyrine as described in the Method of Specific Aim 2 and the legend to Fig. 9. The data are averages (± S.E.M.) of five control experiments and four soman (100 µg) exposure experiments. The total CBF in control brain was 0.67 ± 0.02 ml/g·min and in soman-exposed brain was 1.03 ± 0.10 ml/g·min.

	Control (ml/g·min)	S.E.M.	After Soman (ml/g·min)	S.E.M.	Increase (%)
Pituitary gland	1.01	±0.13	1.11	±0.28	10
Olfactory	0.77	±0.13	0.84	±0.14	9
Frontal cortex	1.12	±0.04	1.83	±0.18	64
Parietal cortex	1.14	±0.11	2.49	±0.26	118
Temporal cortex	1.04	±0.07	2.04	±0.24	96
Occipital cortex	0.88	±0.05	1.89	±0.12	115
Cerebral cortex	0.82	±0.08	1.37	±0.07	67
Vermis	0.81	±0.10	1.15	±0.08	42
Pons	0.49	±0.12	0.96	±0.08	96
Inferior colliculus	0.97	±0.06	1.73	±0.29	78
Midbrain	0.58	±0.03	1.29	±0.16	123
Rostral hippocampus	0.45	±0.03	0.70	±0.05	56
Caudal hippocampus	0.51	±0.03	0.76	±0.05	50
Thalamus	0.85	±0.10	1.68	±0.41	98
Caudate nucleus	0.92	±0.05	1.05	±0.08	14
White matter	0.17	±0.01	0.18	±0.02	4
Cerebellar white matter	0.32	±0.09	0.62	±0.10	95
Corpus callosum	0.39	±0.16	0.32	±0.03	-18

Table 2. Effects of Soman on Regional Utilization of Glucose. D-[6-^{14}C]Glucose was infused into the arterial cannulae of control brains or brains with seizure activity induced by injecting 100 µg of soman. Ten minutes after isotope infusion, brains were quickly removed and frozen in liquid nitrogen-cooled isopentane. To measure radioactivity levels, brain sections (~25 µm) from the different regions were prepared and subjected to autoradiography.

	CMR-G (µmol/g·min)	
Brain Region	Control conditions (n = 3)	Seizure conditions (n = 3)
Gyrus cinguli	0.64 ± 0.13	1.32 ± 0.21*
Striatum	0.78 ± 0.07	1.34 ± 0.34
Gyrus coronalis	0.68 ± 0.11	1.33 ± 0.13**
Corpus callosum	0.18 ± 0.05	0.56 ± 0.11*
Hippocampus	0.46 ± 0.20	0.67 ± 0.14
Gyrus suprasilvius	0.68 ± 0.14	1.29 ± 0.24**
Cortex cerebellum	0.51 ± 0.11	1.02 ± 0.25

*$p < 0.05$ when compared to control values.
**$p < 0.1$ when compared to control values.

Table 3. L-[1-^{14}C]Leucine Incorporation into Brain. Experiment conditions are as follows: perfusate flow, 0.66 and 0.30 ml/g·min for control conditions and during oligemia, respectively; plasma leucine, 54 nmol/ml; L-[1-^{14}C]leucine infused, 100 μCi; L-[1-^{14}C]leucine specific activity, 1.22 and 2.46 nCi/nmol for control conditions and during oligemia, respectively.

	Control	Oligemia
Brain radioactivity (nCi/g)		
Total	99.5	285.1
Acid insoluble	71.2	122.5
Leucine		
Integrated plasma specific activity (μCi·sec/ml)	176	332
Brain concentration (nmol/mg)	0.15	0.15

Table 4. Uptake of L-[1-^{14}C]Leucine by Perfused Canine Brain Under Control Conditions. L-[1-^{14}C]Leucine (50-100 μCi) was infused into the arterial perfusate at a constant rate for 20 min. The brain vasculature was rapidly cleared (~10 sec) of radioactive perfusate with ice-cold saline before the brain was removed, sliced into five coronal slabs, and frozen. Twenty-micron thick sections were prepared and subjected to a first autoradiography. Following this initial exposure, the sections were washed with hot 5% TCA to remove unincorporated L-[1-^{14}C]leucine and acid-soluble metabolites. The sections were dried and subjected to a second autoradiography. Both films were exposed for 20 days. The first autoradiogram represents protein synthesis plus primary free L-[1-^{14}C]leucine. The second autoradiogram represents regional brain protein synthesis. Optical densities of the cerebral regions were determined, and tissue radioactivities were calculated using appropriate autoradiography standards. Table values are the averages of two separate brain perfusion experiments.

Brain Slice Region	Free Leucine (TCA soluble) pCi/mg	Incorporated Leucine (TCA insoluble) pCi/mg
Anterior		
Gray	107	481
White	75	118
Midbrain		
Gray	257	299
White	21	96
Posterior		
Gray	11	363
White	43	86

Table 5. Uptake of L-[1-^{14}C]Leucine by Perfused Canine Brain During Soman-induced Seizure. The experimental details are described in Table 4 except that the L-[1-^{14}C]leucine infusion was started 1 min after arterial injection of 100 μg of soman. Optical densities of the cerebral regions were determined, and tissue radioactivities were calculated using appropriate autoradiography standards. Table values are the averages of two separate brain perfusion experiments.

Brain Slice Region	Free Leucine (TCA soluble) pCi/mg	Incorporated Leucine (TCA insoluble) pCi/mg
Anterior		
Gray	278	139
White	96	32
Midbrain		
Gray	342	150
White	107	43
Posterior		
Gray	310	289
White	86	53

Table 6. Regional Protein Synthesis in Perfused Canine Brain After Soman Exposure. The experimental details are described in Table 4. In the experiments with soman, L-[1-^{14}C]leucine infusion was started 1 min after arterial injection of 100 μg of soman. The percentages of L-[1-^{14}C]leucine incorporated into protein (TCA insoluble) were determined relative to the total L-[1-^{14}C]leucine uptake (total radioactivity) in regions of the cerebral cortex. Two control and two soman exposure experiments were performed, and the values from each are averaged.

Brain Slice Region	Control (%)	Soman Exposure (%)
Anterior		
Gray	89	32
White	69	23
Midbrain		
Gray	65	30
White	85	26
Posterior		
Gray	97	46
White	70	36

Table 7. Unidirectional Influx of Glucose. Dog brains were isolated and perfused as described in METHODS. Indicator dilutions were performed as described previously (44) after soman exposure (100 µg), carbachol treatment (1 µM), carbachol + soman treatment (1 µM and 100 µg, respectively), arecoline treatment (20 µM), or AF64a. Data are mean ± S.E.M. values.

Conditions	v'_{in} (µmol/g·min)
Control (n = 22)	0.64 ± 0.06
After soman exposure	
5 min (n = 3)	0.89 ± 0.12
30 min (n = 3)	1.07 ± 0.33
After carbachol exposure	
10 min (n = 2)	0.89
30 min (n = 2)	0.68
After carbachol + soman exposure	
5 min (n = 1)	1.12
20 min (n = 1)	1.09
After arecoline exposure	
10 min (n = 2)	0.59
30 min (n = 2)	0.40
During AF64a exposure (n = 1)	0.72

Table 8. Unidirectional Influx of Leucine. Dog brains were isolated and perfused as described in METHODS. Indicator dilutions were performed as described previously (44) after soman exposure (100 μg), carbachol treatment (1 μM), carbachol + soman treatment (1 μM and 100 μg, respectively), arecoline treatment (20 μM), or AF64a. Data are mean ± S.E.M. values.

Conditions	v'_{in} (nmol/g·min)
Control (n = 18)	15.01 ± 0.55
After soman exposure	
5 min (n = 3)	15.07 ± 3.28
30 min (n = 3)	23.44 ± 2.48
After carbachol exposure	
10 min (n = 2)	14.74
30 min (n = 2)	12.29
After carbachol + soman exposure	
5 min (n = 1)	13.78
20 min (n = 1)	12.43
After arecoline exposure	
10 min (n = 2)	14.71
30 min (n = 2)	16.94
During AF64a exposure (n = 1)	12.13

Table 9. Unidirectional Influx of Glycine. Dog brains were isolated and perfused as described in METHODS. Indicator dilutions were performed as described previously (44) after soman exposure (100 μg), carbachol treatment (1 μM), carbachol + soman treatment (1 μM and 100 μg, respectively), arecoline treatment (20 μM), or AF64a. Data are mean ± S.E.M. values.

Conditions	v'_{in} (nmol/g·min)
Control (n = 18)	4.05 ± 0.84
After soman exposure	
5 min (n = 2)	11.93
30 min (n = 3)	12.52 ± 4.17
After carbachol exposure	
10 min (n = 2)	7.78
30 min (n = 2)	4.35
After carbachol + soman exposure	
5 min (n = 1)	5.53
20 min (n = 1)	3.98
During AF64a exposure (n = 1)	3.90

Table 10. Unidirectional Influx of Choline. Dog brains were isolated and perfused as described in METHODS. Indicator dilutions were performed as described previously (44) after soman exposure (100 μg), carbachol treatment (1 μM), carbachol + soman treatment (1 μM and 100 μg, respectively), arecoline treatment (20 μM), or AF64a. Data are mean ± S.E.M values.

Conditions	v_{in} (nmol/g·min)
Control (n = 22)	0.61 ± 0.13
After soman exposure	
5 min (n = 3)	0.56 ± 0.07
30 min (n = 3)	0.61 ± 0.07
After carbachol exposure	
10 min (n = 2)	0.58
30 min (n = 2)	0.50
After carbachol + soman exposure	
5 min (n = 1)	0.50
20 min (n = 1)	0.43
After arecoline exposure	
10 min (n = 2)	0.54
30 min (n = 2)	0.56
During AF64a exposure (n = 1)	0.56

Table 11. Levels of Choline (Ch) and Acetylcholine (ACh) (nmol/g) in Tissue From Various Regions of Canine Brain.

Region		Nonperfused brain (n = 3)	Perfused brain: Recirculated 5 min (n = 2)	Perfused brain: Recirculated 90 min (n = 3)	Perfused brain: Nonrecirculated (n = 4)
Cortex	Ch	41 ± 1.2	168 ± 7	295 ± 71	183 ± 3[a]
	ACh	4.3 ± 0.4	5.1 ± 0.1	6.6 ± 1.2	4.7 ± 0.2
Brain stem	Ch	79 ± 1	108 ± 2	239 ± 6[b]	116 ± 18
	ACh	4.1 ± 0.1	2.9 ± 0.1	2.8 ± 0.2	2.9 ± 0.1
Hippocampus	Ch	67 ± 3	131 ± 9	264 ± 19[c]	141 ± 2
	ACh	1.2 ± 0.2	1.1 ± 0.2	0.8 ± 0.1	1.0 ± 0.1
Cerebellum	Ch	61 ± 4	101 ± 3	274 ± 22[b]	104 ± 2
	ACh	0.6 ± 0.1	0.4 ± 0.01	0.6 ± 0.1	0.5 ± 0.1

Data are mean ± S.E.M values.
[a] $p<0.05$ when compared with values for 5-min recirculated perfusate.
[b] $p<0.005$ when compared with values for 5-min recirculated perfusate.
[c] $p<0.01$ when compared with values for 5-min recirculated perfusate.

Table 12. Cerebral Metabolism Rates for Choline (CMRCh).

	Perfusate Ch (nmol/ml)	(A - V)F/W (nmol/g·min)
Nonrecirculated (n = 4)	2.9 ± 0.2	-1.1 ± 0.1
Recirculated (n = 5)	4.9 ± 1.1	-1.6 ± 0.4

The CMRCh (nmol/g·min) was calculated by the following equation: efflux = (A - F)F/W, in which A and V are the respective concentrations of Ch in the arterial and venous samples (nmol/ml), F is the blood flow rate (ml/min), and W is the brain weight (g). Samples for Ch analysis were collected at 5-min intervals over a maximal period of 55 min for nonrecirculation experiments and at 10-min intervals over a 30-min period for recirculation experiments. Data are mean ± S.E.M values.

Table 13. Unidirectional Influx of Choline (Ch).

Conditions	υ'_{in} (nmol/g·min)
Control (n = 9)	0.49 ± 0.07
After soman exposure	
10 min (n = 5)	0.48 ± 0.07
40 min (n = 6)	0.42 ± 0.09

Influx velocity was determined by the indicator dilution method (44) before and at two intervals after soman (100 μg) administration. In this method, velocity, υ'_{in}, is calculated by the following formula: $\upsilon'_{in} = E \times A \times F/W$, in which E is the maximal extraction, A is the plasma Ch concentration, F is the plasma net flow rate, and W is the brain weight. Data are mean ± S.E.M values. The plasma Ch concentration used for calculation was 4.9 nmol/ml (Table 12). The experiments were conducted with recirculation of perfusate.

Table 14. Effects of Soman and Sarin on Acetylcholine (ACh) Levels (nmol/g) in Various Regions of Isolated, Perfused Canine Brain.

		Treatment			
		Soman		Sarin	
Region	Control	5 min after	60 min after	5 min after	60 min after
Cortex	6.6 ± 1.2	67 ± 7[a]	40 ± 8[b]	22 ± 1[a]	25 ± 2[a]
Brain stem	2.8 ± 0.2	54 ± 1[a]	46 ± 8[a]	18 ± 2[a]	56 ± 2[a]
Hippocampus	0.8 ± 0.1	41 ± 5[a]	105 ± 7[a]	19 ± 1[a]	20 ± 1[a]
Cerebellum	0.6 ± 0.1	1.6 ± 0.8	5.3 ± 1.2[b]	1.0 ± 0.1	5.0 ± 0.6[a]

Data are mean ± S.E.M values for three experiments. Controls are the concentrations in untreated brain perfused for 90 min under recirculation conditions (Table 11).
[a] $p<0.01$ when compared with control values.
[b] $p<0.05$ when compared with control values.

Table 15. Effects of Soman and Sarin on Choline (Ch) Levels (nmol/g) in Various Regions of Isolated, Perfused Canine Brain.

		Treatment			
		Soman		Sarin	
Region	Control	5 min after	60 min after	5 min after	60 min after
Cortex	295 ± 71	500 ± 10	258 ± 67	500 ± 4[a]	328 ± 5
Brain stem	239 ± 6	839 ± 221	718 ± 52	716 ± 10[b]	517 ± 9[b]
Hippocampus	264 ± 19	580 ± 15[b]	422 ± 9[b]	614 ± 9[b]	525 ± 7[b]
Cerebellum	274 ± 22	736 ± 25[b]	452 ± 29[b]	626 ± 9[b]	374 ± 9[b]

Data are mean ± S.E.M values for three experiments. Controls are the concentrations in untreated brain perfused for 90 min under recirculation conditions (Table 11).
[a] $p<0.01$ when compared with control values.
[b] $p<0.05$ when compared with control values.

Table 16. Phospholipase D Activity and the Effects of Diisopropylfluorophosphate (DFP) on the Hydrolysis of 1,2 Dipalmitoyl-*sn*-glycero-3-phosphoryl[^{3}H]choline by Phospholipase D Activity in Subcellular Fractions from Canine Brain.

	Activity (nmol [^{3}H]choline released/hr/mg of protein)			
	Control		DIFP	
	A	B	A	B
Homogenate	2.25	2.56	2.15	2.83
Crude membrane fraction	1.72	1.6	1.57	1.6
Microsomes	3.6	3.46	3.47	3.23

A and B are separate experiments with subcellular fractions obtained from two brains. Values are averages of two determinations. The incubation medium in 0.25 ml contained 40 mM HEPES buffer, pH 7.4, 0.1% Triton-X 100, 132 µM ^{3}H choline-labeled phosphatidylcholine (3.3×10^5 dpm; specific activity 1×10^4 dpm/nmol) and brain subcellular fractions (200-500 µg protein). Test incubation mixtures contained 50 µg of DIFP in 5 µl of ethanol. Incubation mixtures were held at 37°C with shaking for 30 min. Reactions were stopped, and lipids were extracted and analyzed as described in Specific Aim 7.

Table 17. Effects of Detergents on Hydrolysis of 1,2-Dipalmitoyl-*sn*-glycero-3-phosphoryl-[^{3}H]choline by Microsomal Phospholipase D.

	Detergent concentration			
	0.2 mg/ml	0.4 mg/ml	1.0 mg/ml	2.0 mg/ml
	(Activity, % of control)			
Sodium deoxycholate	55	75	69	27
Sodium oleate	93	55	45	21
Sodium linoleate	82	76	75	76
CHAPS	79	118	95	121
Octylglucopyranoside	124	159	54	29
Triton X-100	110	141	287	340

Values are averages of two determinations with the control value considered to be 100%. Incubation medium in 0.25 ml contained 40 mM HEPES buffer, pH 7.4, 132 μM [^{3}H]choline-labeled phosphatidylcholine (3.3 x 10^5 dpm; specific activity 1 x 10^4 dpm/nmol), microsomal protein (275 μg protein), and detergents as listed. The incubation period was 30 min at 37°C with shaking. Reactions were stopped by adding methanol, and lipids were extracted and analyzed as described in Specific Aim 7.

Table 18. Effects of EDTA and Cations on the Hydrolysis of 1,2-Dipalmitoyl-*sn*-glycero-3-phosphoryl[^{3}H]choline by Microsomal Phospholipase D.

Additions	Activity (% of control)
No additions (Control)	100
EDTA	
1 mM	96
4 mM	97
Ca^{2+}	
0.5 mM	91
2 mM	76
4 mM	68
Mg^{2+}	
0.5 mM	91
2 mM	76
4 mM	73
Zn^{2+}	
0.5 mM	50
2 mM	22
4 mM	6

Values are the averages of two determinations. Incubations were as described in Table 17 and in the presence of 1 mg/ml Triton X-100.

Table 19. Blood-brain Transport of [^{3}H]Palmitic Acid. Approximately 1.2 mCi of [^{3}H]palmitate in ethanol, dried under nitrogen, and resuspended in 250 µl of saline were infused into the carotid cannulae at a constant rate over a 5-min period. The influx constant was determined from the relationship $K_{in} = C^*_{br}/_0\int^5 C^*_a\, dt$, in which C^*_{br} is the concentration (dpm/mg) of ^{3}H-labeled free fatty acid in brain, C^*_a is the concentration in perfusate plasma (dpm/ml), and t is the time (sec). Values are expressed as ml/g·sec·10^5. The K_{in} values are related to permeability x surface area (P x S) products by the following relationship: $K_{in} = F \times \ln(1 - e^{-PxS/F})$, in which F is the perfusate flow rate (mg/g·sec), P is the permeability (sec^{-1}), and S is the vascular surface area (cm^2/g). However, when P x S is very small, $K_{in} = P \times S$, and, therefore the K_{in} values in Tables 19 and 20 can also be expressed as the P x S product.

Brain regions	Control (n = 4)	Soman (n = 3)
Cortex		
Frontal	7.3 ± 3.4	13 ± 3
Parietal	7.1 ± 3.0	15 ± 4
Temporal	5.8 ± 2.5	11 ± 2
Occipital	9.9 ± 5.3	21 ± 6
Cerebellar cortex	7.3 ± 3.0	18 ± 3
Vermis	10.4 ± 6.1	16 ± 3
Pons	4.7 ± 2.4	9 ± 2
Colliculus inferior	7.1 ± 2.5	28 ± 10
Midbrain	5.1 ± 2.2	11 ± 2
Hippocampus		
Rostral	4.2 ± 1.5	9 ± 2
Caudal	4.3 ± 1.8	8 ± 1
Thalamus	7.7 ± 4.0	20 ± 11
Caudate nucleus	5.1 ± 2.0	17 ± 9
White matter	2.1 ± 0.8	6 ± 2
Pituitary	71 ± 40	101 ± 22

Table 20. Blood-brain Transport of [^{3}H]Oleic Acid. Approximately 1.2 mCi of [^{3}H]oleate in ethanol, dried under nitrogen and resuspended in 250 µl of saline, were infused into the carotid cannulae at a constant rate over a 5-min period. The influx constant was determined from the relationship $K_{in} = C^*_{br}/_0\int^5 C^*_a\, dt$, in which C^*_{br} is the concentration (dpm/mg) of ^{3}H-labeled free fatty acid in brain, C^*_a is the concentration in perfusate plasma (dpm/ml), and t is the time (sec). Values are expressed as ml/g·sec·10^5. K_{in} values are related to permeability x surface area (P x S) products by the relationship $K_{in} = F \times \ln(1 - e^{-PxS/F})$, in which F is the perfusate flow rate (mg/g·sec), P is the permeability (sec^{-1}), and S is the vascular surface area (cm^2/g). However, when P x S is very small, $K_{in} \approx P \times S$, and, therefore the K_{in} values in Tables 19 and 20 can also be expressed as the P x S product.

Brain regions	Control (n = 3)	Soman (n = 3)
Cortex		
Frontal	32 ± 7	28 ± 16
Parietal	43 ± 14	25 ± 12
Temporal	20 ± 2	23 ± 7
Occipital	20 ± 4	37 ± 26
Cerebellar cortex	19 ± 1	34 ± 26
Vermis	17 ± 2	28 ± 17
Pons	9 ± 0	15 ± 3
Colliculus inferior	31 ± 11	51 ± 38
Midbrain	37 ± 26	27 ± 21
Hippocampus		
Rostral	15 ± 5	15 ± 6
Caudal	18 ± 6	25 ± 12
Thalamus	24 ± 6	30 ± 12
Caudate nucleus	15 ± 4	27 ± 11
White matter	12 ± 2	4 ± 1
Pituitary	71 ± 8	96 ± 27

Table 21. Free Fatty Acid Concentrations in Perfusate. Plasma lipids were extracted, and free fatty acids were separated along with C17:0 fatty acid as the internal standard. The fatty acids were converted to methyl esters by reaction with diazomethane and were analyzed by gas liquid chromatography. Values are expressed as means ± S.D., n = 12.

Fatty acid	Concentration (μM)	Percent of total
Palmitic (16:0)	80 ± 18	25.8
Palmitoleic (16:1)	16 ± 9	5.2
Stearic (18:0)	41 ± 12	13.2
Oleic (18:1)	83 ± 30	26.0
Linoleic (18:2)	55 ± 30	17.7
Linolenic (18:3)	20 ± 11	6.5
Arachidonic (20:4)	15 ± 10	4.8

Table 22. [^{3}H]Palmitate Incorporated into Lipids.
Control values are means ± S.E.M. from three experiments.

Radioactivity incorporated (dpm x 10^{-3}/g·min) into control canine brain

Lipids	Cortex	Thalamus	Hypothalamus	Caudate	Hippocampus	Brain stem	Cerebellum
Sphingo-myelin	4.6 ± 0.1	2.7 ± 0.1	5.2 ± 1.7	7.5 ± 3.2	3.7 ± 0.9	6.5 ± 1.8	3.5 ± 0.5
Phosphatidyl-choline	15.0 ± 1.1	9.6 ± 0.5	15.0 ± 4.2	14.2 ± 1.9	8.6 ± 0.7	17.0 ± 4.1	14.0 ± 2.9
Phosphatidyl-inositol	1.1 ± 0.1	0.8 ± 0	1.1 ± 0.3	1.8 ± 0.7	0.8 ± 0.1	0.9 ± 0.1	1.2 ± 0.1
Phosphatidyl-serine	0.6 ± 0.1	0.3 ± 0	0.7 ± 0.1	1.2 ± 0.6	0.3 ± 0.1	0.6 ± 0	0.8 ± 0.3
Phosphatidyl-ethanolamine	1.1 ± 0.1	1.0 ± 1.1	1.0 ± 0.2	1.4 ± 0.8	1.0 ± 0.4	1.3 ± 0.1	1.4 ± 0.7
Others, incl. fatty acids	12 ± 1	8 ± 0.5	6 ± 0.2	8 ± 4	6 ± 0.8	6 ± 0.2	13 ± 3

Table 23. Effects of Soman on [^{3}H]Palmitate Incorporated into Lipids.
Values after soman (100 µg) exposure are means ± S.E.M. from three experiments.

Radioactivity incorporated (dpm x 10^{-3}/g·min) into soman-exposed canine brain

Lipids	Cortex	Thalamus	Hypothalamus	Caudate	Hippocampus	Brain stem	Cerebellum
Sphingo-myelin	0.9 ± 0.2[a]	0.5 ± 0.2[a]	0.6 ± 0.2[b]	0.4 ± 0.1[b]	0.4 ± 0.1[a]	0.4 ± 0.1[b]	0.8 ± 0.2[a]
Phosphatidyl-choline	6.4 ± 1.9[a]	6.8 ± 1.1	6.9 ± 0.7	6.6 ± 1.0[b]	4.7 ± 1.1[b]	7.3 ± 2.3	14.0 ± 5.2
Phosphatidyl-inositol	1.4 ± 0.2	0.9 ± 0.2	1.9 ± 0.2	0.9 ± 0.1	0.7 ± 0	0.8 ± 0.2	2.3 ± 0.5
Phosphatidyl-serine	0.3 ± 0.2	0.1 ± 0.1	0.3 ± 0.2	ND	ND	0.3 ± 0.1	0.2 ± 0.1
Phosphatidyl-ethanolamine	1.1 ± 0.4	1.4 ± 0.4	1.6 ± 0.4	0.8 ± 0.4	0.8 ± 0.3	1.4 ± 0.6	2.9 ± 0.3
Others, incl. fatty acids	38 ± 2[a]	35 ± 10[b]	26 ± 1[a]	42 ± 13	20 ± 7	25 ± 7[b]	39 ± 12

[a] $p < 0.01$
[b] $p < 0.05$
ND = not detected

Table 24. [^{3}H]Oleate Incorporated into Lipids.
Control values are means ± S.E.M. from three experiments.

Radioactivity incorporated (dpm x 10^{-3}/g·min) into control canine brain

Lipids	Cortex	Thalamus	Hypothalamus	Caudate	Hippocampus	Brain stem	Cerebellum
Sphingo-myelin	0.8 ± 0.2	1.0 ± 0.5	0.3 ± 0	0.4 ± 0.2	0.2 ± 0.2	0.3 ± 0	0.7 ± 0
Phosphatidyl-choline	11.0 ± 0.2	9.6 ± 1.2	6.9 ± 0.4	9.5 ± 0.3	6.4 ± 1.0	5.2 ± 0.6	9.6 ± 1.3
Phosphatidyl-inositol	2.3 ± 0.5	1.8 ± 0.2	1.2 ± 0.3	1.8 ± 0.3	1.3 ± 0.3	0.7 ± 0.1	2.2 ± 0.4
Phosphatidyl-serine	0.7 ± 0.3	0.5 ± 0.3	0.4 ± 0.1	0.6 ± 0.3	0.2 ± 0.2	0.2 ± 0.1	0.4 ± 0.1
Phosphatidyl-ethanolamine	5.5 ± 0.2	5.0 ± 0.9	3.2 ± 0.1	3.3 ± 0.1	2.3 ± 0.2	2.3 ± 0.4	4.5 ± 0.5
Others, incl. fatty acids	165 ± 45	101 ± 52	78 ± 22	152 ± 74	49 ± 17	39 ± 2	213 ± 185

Table 25. Effects of Soman on [^{3}H]Oleate Incorporated into Lipids.
Values after soman (100 µg) exposure are means ± S.E.M. from four experiments.

Radioactivity incorporated (dpm x 10^{-3}/g·min) into soman-exposed canine brain

Lipids	Cortex	Thalamus	Hypothalamus	Caudate	Hippocampus	Brain stem	Cerebellum
Sphingo-myelin	0.3 ± 0.3	0.1 ± 0.1	0.2 ± 0.2	0.1 ± 0.1	0.1 ± 0.1	0.1 ± 0.1[b]	0.2 ± 0.1[a]
Phosphatidyl-choline	3.6 ± 0.5[a]	4.8 ± 1.2[b]	4.3 ± 0.9	3.6 ± 0.7[a]	2.3 ± 0.4[b]	3.4 ± 0.4	6.3 ± 0.9
Phosphatidyl-inositol	1.1 ± 0.1	1.1 ± 0.4	1.0 ± 0.2	1.1 ± 0.3	0.5 ± 0.2	0.6 ± 0.2	1.5 ± 0.1
Phosphatidyl-serine	0.1 ± 0.1	0.3 ± 0.3	0.1 ± 0.1	0.1 ± 0.1	ND	0.1 ± 0.1	0.3 ± 0.1
Phosphatidyl-ethanolamine	1.2 ± 0.1[a]	1.9 ± 0.7[b]	1.8 ± 0.3[a]	1.0 ± 0.3[a]	0.4 ± 0.2[a]	1.5 ± 0.2	2.5 ± 0.3[b]
Others, incl. fatty acids	92 ± 58	135 ± 100	79 ± 69	147	31 ± 14	30 ± 18	97 ± 77

[a] $p < 0.01$
[b] $p < 0.05$
ND = not detected

Table 26. Biogenic Amine Levels in Canine Brain. Soman (100 µg) was injected after a 30-min control period. In separate experiments, propranolol (0.06 µM) or pimozide (2 µM) was added to the perfusate after a 30-min control period, and soman (100 µg) was injected after propranolol or pimozide treatment. Tissue samples from various regions of canine brain were dissected and analyzed by HPLC. Values are expressed as means (ng/g of tissue) ± S.E.M., with n = 8 for controls and n = 2 for soman, propranolol + soman, and pimozide + soman.

Dopamine	Perfused controls	Soman	Propranolol + Soman	Pimozide + Soman
Brain stem	87 ± 34	35	29	169
Cerebellum	18 ± 4	< 4	< 4	< 4
Cortex	22 ± 3	< 4	< 4	21
Motor cortex	43 ± 5	27	19	45
Hippocampus	29 ± 9	< 4	< 4	< 4
Hypothalamus	320 ± 77	129	178	367
Norepinephrine	**Perfused controls**	**Soman**	**Propranolol + Soman**	**Pimozide + Soman**
Brain stem	349 ± 53	507	285	582
Cerebellum	92 ± 12	608	112	298
Cortex	146 ± 18	572	168	320
Motor cortex	194 ± 11	586	209	333
Hippocampus	162 ± 9	460	167	210
Hypothalamus	1637 ± 459	838	388	783
Serotonin	**Perfused controls**	**Soman**	**Propranolol + Soman**	**Pimozide + Soman**
Brain stem	441 ± 107	203	293	366
Cerebellum	8 ± 2	< 4	8	10
Cortex	102 ± 17	82	64	98
Motor cortex	176 ± 37	152	93	137
Hippocampus	394 ± 76	214	212	340
Hypothalamus	1180 ± 169	803	553	901
5-Hydroxyindole-3-acetic acid	**Perfused controls**	**Soman**	**Propranolol + Soman**	**Pimozide + Soman**
Brain stem	1712 ± 380	623	889	1850
Cerebellum	44 ± 9	25	107	24
Cortex	101 ± 23	58	39	56
Motor cortex	77 ± 10	66	37	68
Hippocampus	732 ± 248	242	148	309
Hypothalamus	1412 ± 217	1076	549	753
Homovanillic acid	**Perfused controls**	**Soman**	**Propranolol + Soman**	**Pimozide + Soman**
Brain stem	1282 ± 491	346	313	1407
Cerebellum	86 ± 19	126	174	66
Cortex	66 ± 15	76	34	54
Motor cortex	183 ± 37	220	112	227
Hippocampus	596 ± 124	429	236	430
Hypothalamus	2210 ± 402	2255	986	2066

Table 27. Biogenic Amine and Metabolite Levels in Canine Brain. α-Methyl-*p*-tyrosine (α–MPT, 300 mg/l) was added to the perfusate after a 30-min control period. Soman (100 µg) was injected immediately after α-MPT treatment in the test experiments. Tissue samples from various regions of canine brain were dissected and analyzed with HPLC. Values are expressed as means (ng/g of tissue) ± S.E.M., with n = 8 for untreated controls, n = 5 for α-MPT-treated samples, and n = 4 for α-MPT- and soman-treated samples.

Dopamine	Perfused controls	α-MPT	α-MPT + Soman
Brain stem	87 ± 34	35 ± 13	59 ± 50
Cerebellum	18 ± 4	<4	<4
Cortex	22 ± 3	8 ± 9	<4
Motor cortex	43 ± 5	16 ± 9	4 ± 4
Hippocampus	29 ± 9	3 ± 4	15 ± 6
Hypothalamus	320 ± 77	152 ± 56	227 ± 107
Norepinephrine	**Perfused controls**	**α-MPT**	**α-MPT + Soman**
Brain stem	349 ± 53	708 ± 199	544 ± 112
Cerebellum	92 ± 12	551 ± 190	443 ± 76
Cortex	146 ± 18	456 ± 172	364 ± 114
Motor cortex	194 ± 11	418 ± 178	403 ± 92
Hippocampus	162 ± 9	342 ± 142	292 ± 109
Hypothalamus	1637 ± 77	793 ± 184	659 ± 112
Serotonin	**Perfused controls**	**α-MPT**	**α-MPT + Soman**
Brain stem	441 ± 107	957 ± 332	1167 ± 322
Cerebellum	8 ± 2	25 ± 10	84 ± 57
Cortex	102 ± 17	100 ± 21	92 ± 9
Motor cortex	176 ± 37	125 ± 29	152 ± 36
Hippocampus	394 ± 76	290 ± 58	477 ± 103
Hypothalamus	1180 ± 169	1066 ± 145	1061 ± 163
5-Hydroxyindole-3-acetic acid	**Perfused controls**	**α-MPT**	**α-MPT + Soman**
Brain stem	1712 ± 380	1900 ± 601	2622 ± 514
Cerebellum	44 ± 9	35 ± 14	55 ± 15
Cortex	101 ± 23	69 ± 13	97 ± 15
Motor cortex	77 ± 10	46 ± 11	87 ± 10
Hippocampus	732 ± 248	239 ± 40	357 ± 28
Hypothalamus	1412 ± 217	1119 ± 238	1318 ± 194
Homovanillic acid	**Perfused controls**	**α-MPT**	**α-MPT + Soman**
Brain stem	1282 ± 491	1378 ± 296	1721 ± 466
Cerebellum	86 ± 19	92 ± 39	97 ± 21
Cortex	66 ± 15	97 ± 38	70 ± 12
Motor cortex	183 ± 37	205 ± 46	217 ± 14
Hippocampus	596 ± 124	323 ± 103	430 ± 95
Hypothalamus	2210 ± 402	2293 ± 95	2941 ± 428

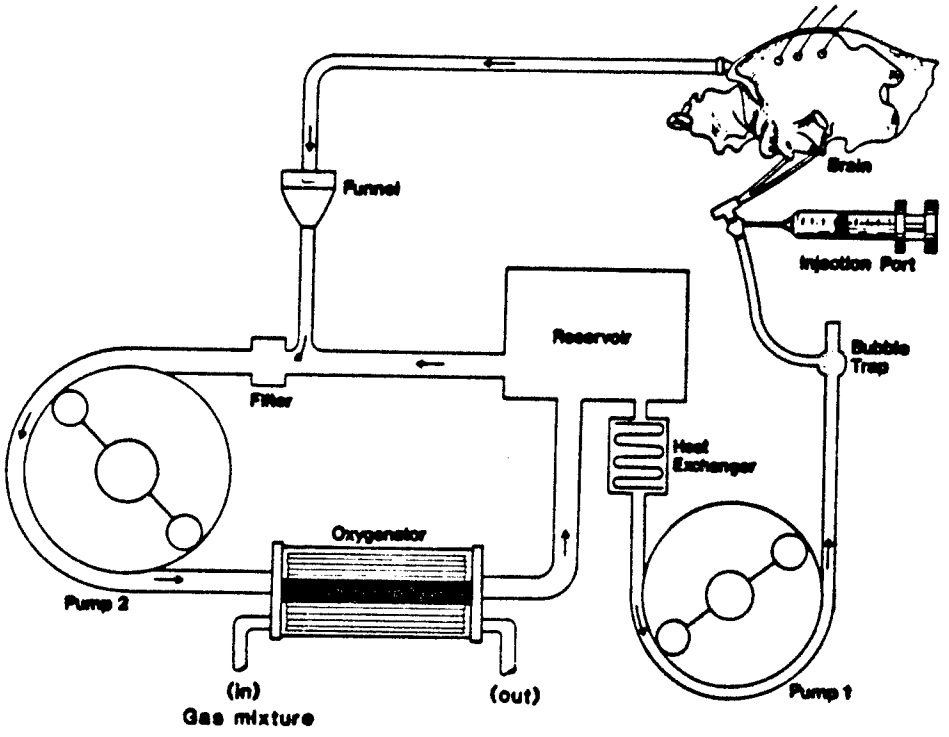

Fig. 1. Diagram of Brain Perfusion System. Artist's sketch of the side view of the isolated brain within the skull is shown in the upper right corner. Perfusate enters via the carotid arteries at the base of the skull. Venous blood returns to the perfusion system via a cannula inserted into the confluence of venous sinuses. Electrodes for EEG monitoring are attached to the bone. Perfusate in the reservoir is continuously oxygenated and filtered.

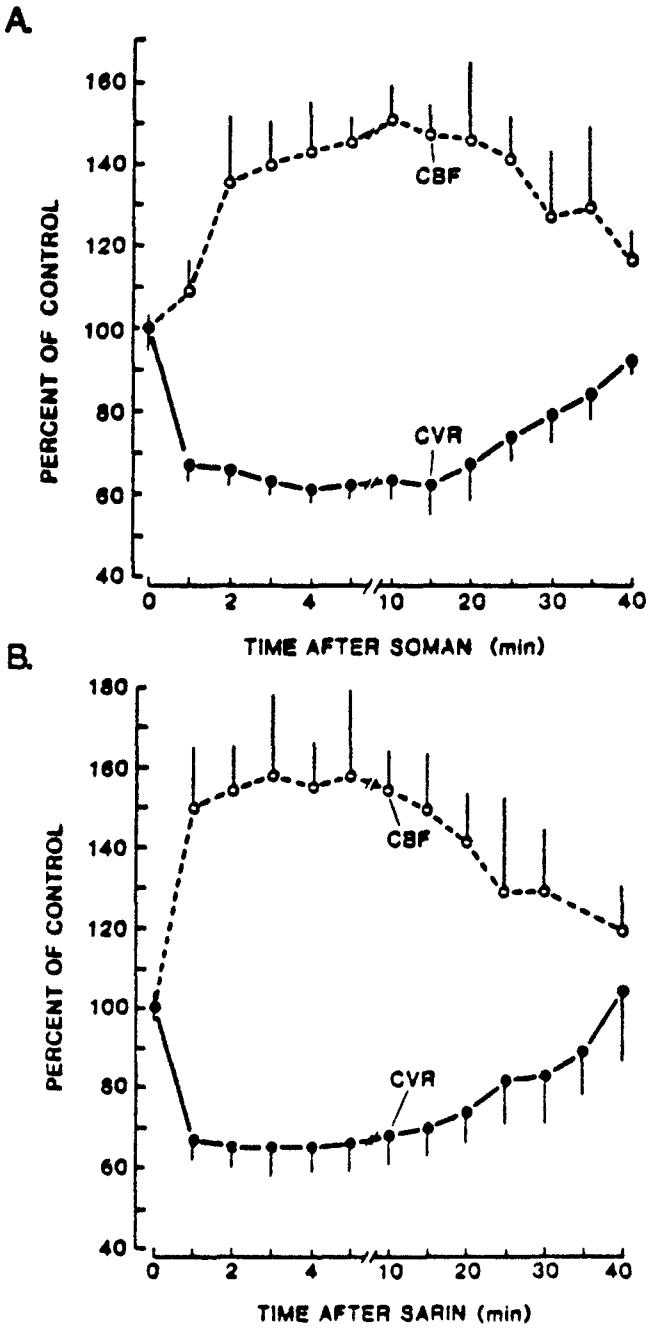

Fig. 2. Cerebral Vascular Resistance (CVR) and Cerebral Blood Flow (CBF) in Perfused Brain Under Constant Pressure Conditions After OP Treatment. The CVR and CBF are plotted as functions of time after arterial injection of either **A)** 100 µg of soman or **B)** 400 µg of sarin. The CVR or CBF at the time of injection is considered to be 100% of the control for each preparation. CVR is the ratio of pressure to flow. Data are expressed as means ± SEM. Average CVR before OP exposure was 169 ± 7 torr·g·min/ml, n = 5. The average CBF before OP exposure was 50.9 ± 1.6 ml/min, n = 5.

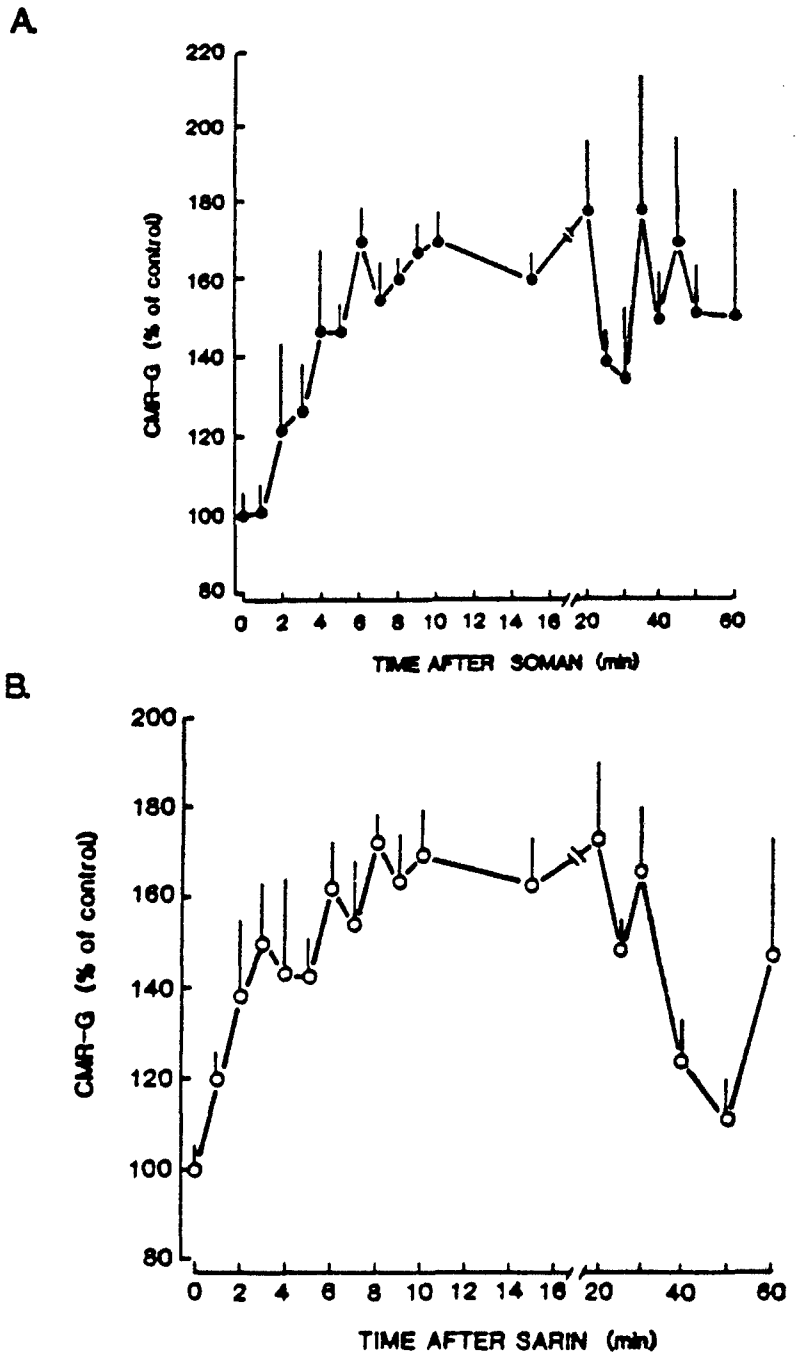

Fig. 3. Cerebral Glucose Metabolism (CMR-G) Under Constant Pressure Conditions After OP Exposure. The CMR-G, expressed as a percent of the CMR-G before OP exposure, is plotted as a function of time after administration of A) soman, 100 μg or B) sarin, 400 μg. The vertical bars represent standard errors. Data are means with n = 5. The average glucose consumption before OP exposure was 37.6 ± 2 μmol/100 g·min.

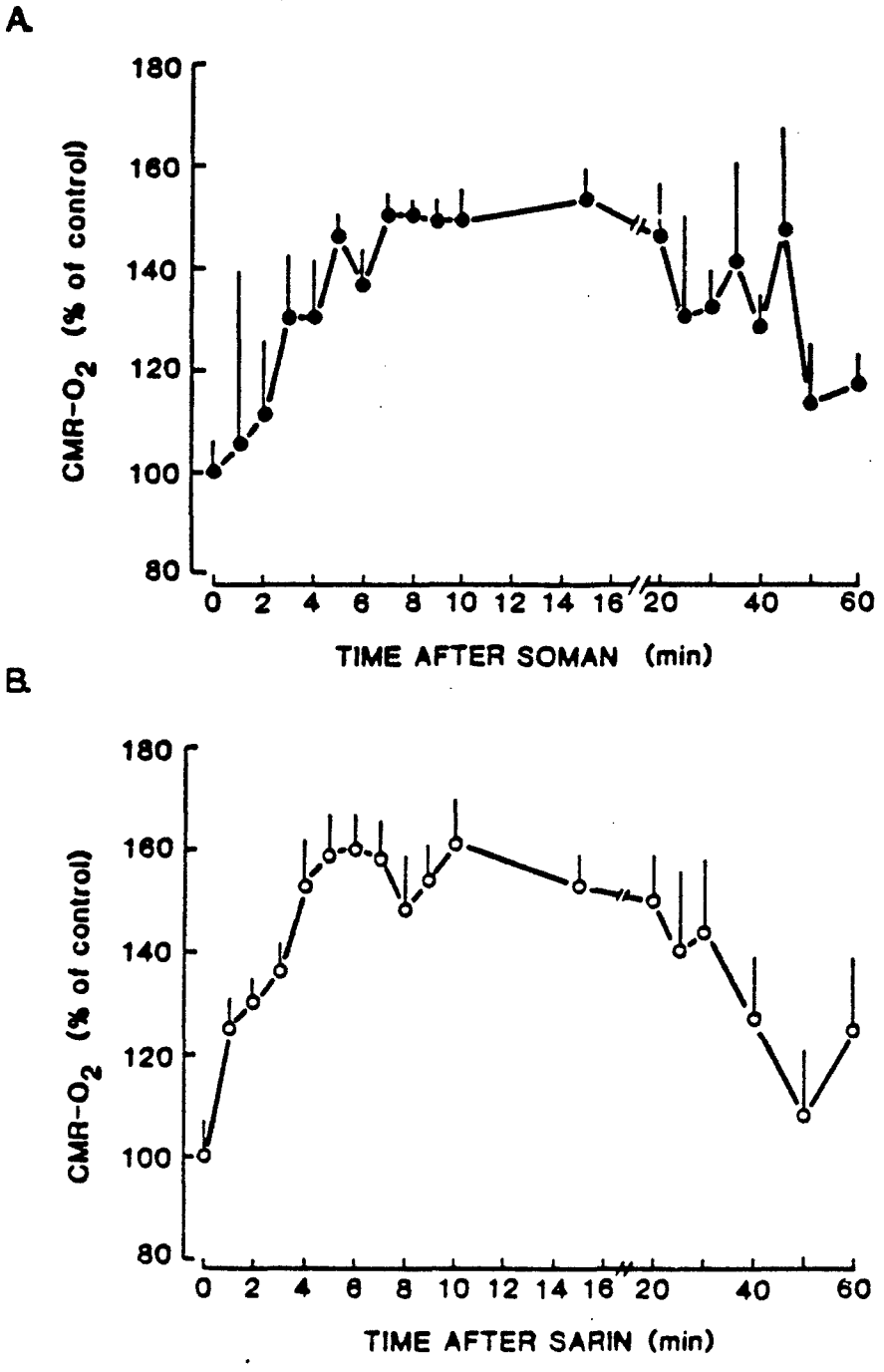

Fig. 4. Cerebral Oxygen Metabolism (CMR-O_2) Under Constant Pressure Conditions After OP Exposure. The CMR-O_2, expressed as a percent of the CMR-O_2 before OP exposure, is plotted as a function of time after administration of A) soman, 100 µg or B) sarin, 400 µg. The vertical bars represent standard errors. Data are means with n = 5, and the average O_2 consumption before OP exposure was 205 ± 14 µmol/100 g·min.

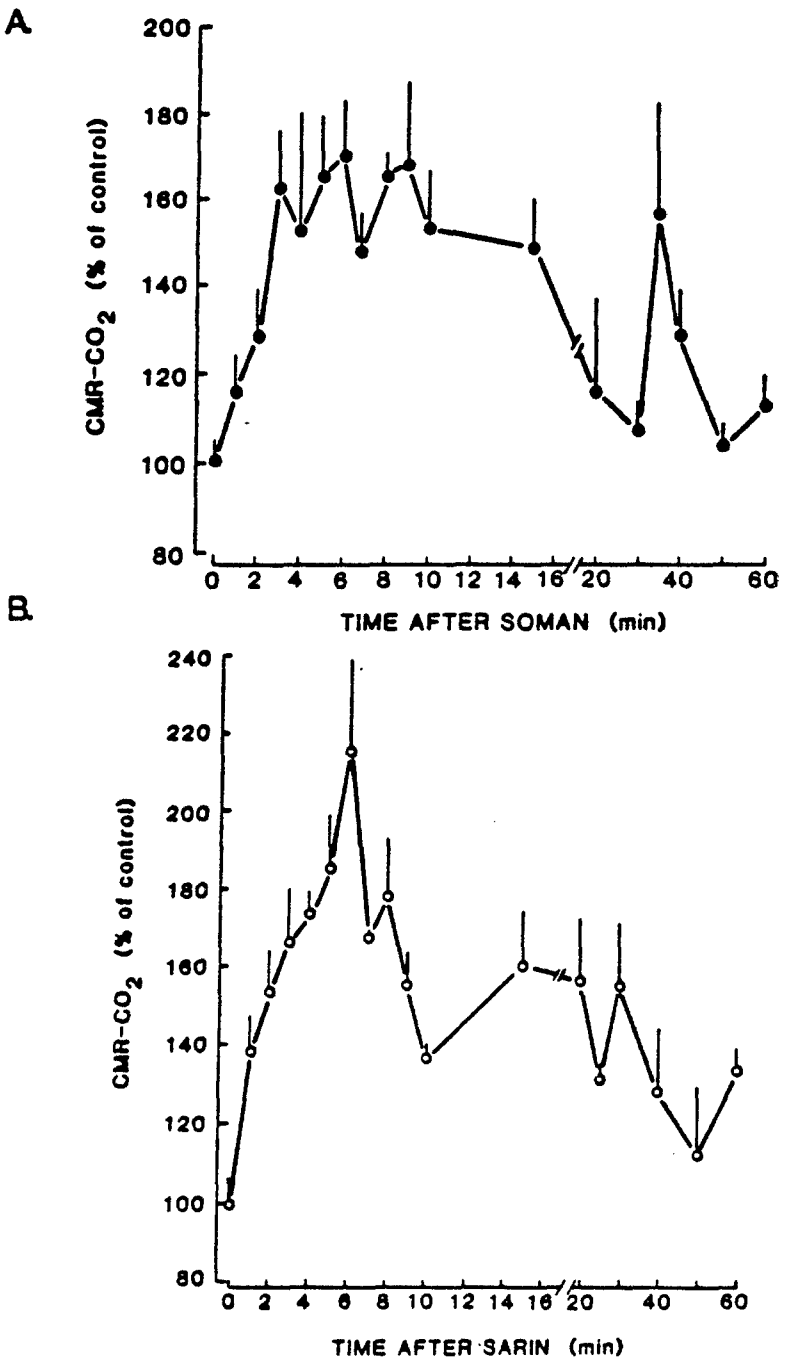

Fig. 5. Cerebral Carbon Dioxide Production ($CMR\text{-}CO_2$) Under Constant Pressure Conditions After OP Exposure. The $CMR\text{-}CO_2$, expressed as a percent of the $CMR\text{-}CO_2$ before OP exposure, is plotted as a function of time after administration of **A**) soman, 100 µg or **B**) sarin, 400 µg. The vertical bars represent standard errors. Data are means with n = 5, and the average CO_2 production before OP was -273 ± 15 µmol/100 g·min.

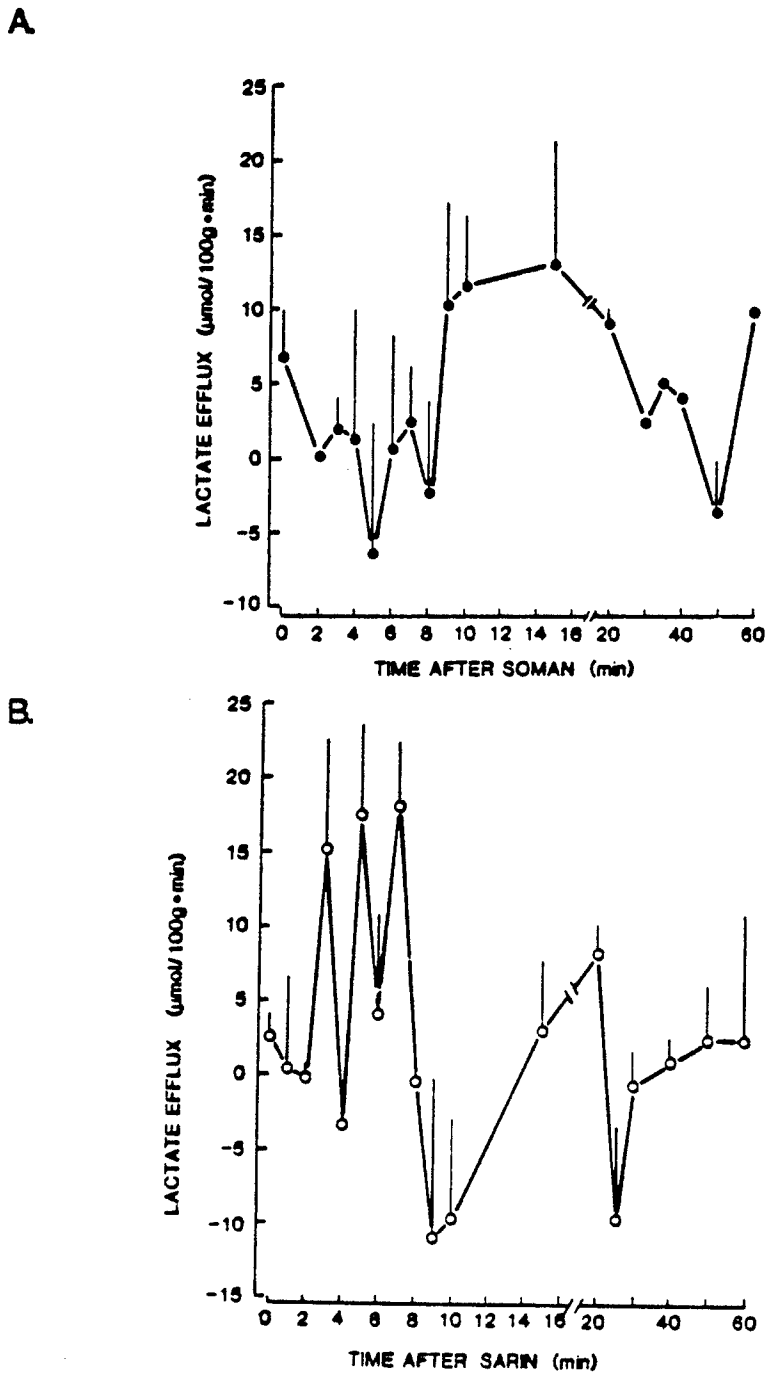

Fig. 6. Lactate Efflux from Brain Under Constant Pressure Conditions After OP Exposure. The cerebral metabolic rate for lactate (CMR-L) was determined for perfused brain before OP exposure and at pre-determined intervals for 1 hr after arterial injection of **A**) soman, 100 µg or **B**) sarin, 400 µg. Vertical bars represent standard errors. Data are means with n = 5, and the average lactate efflux before OP exposure was 4.6 ± 2.4 µmol/100 g·min.

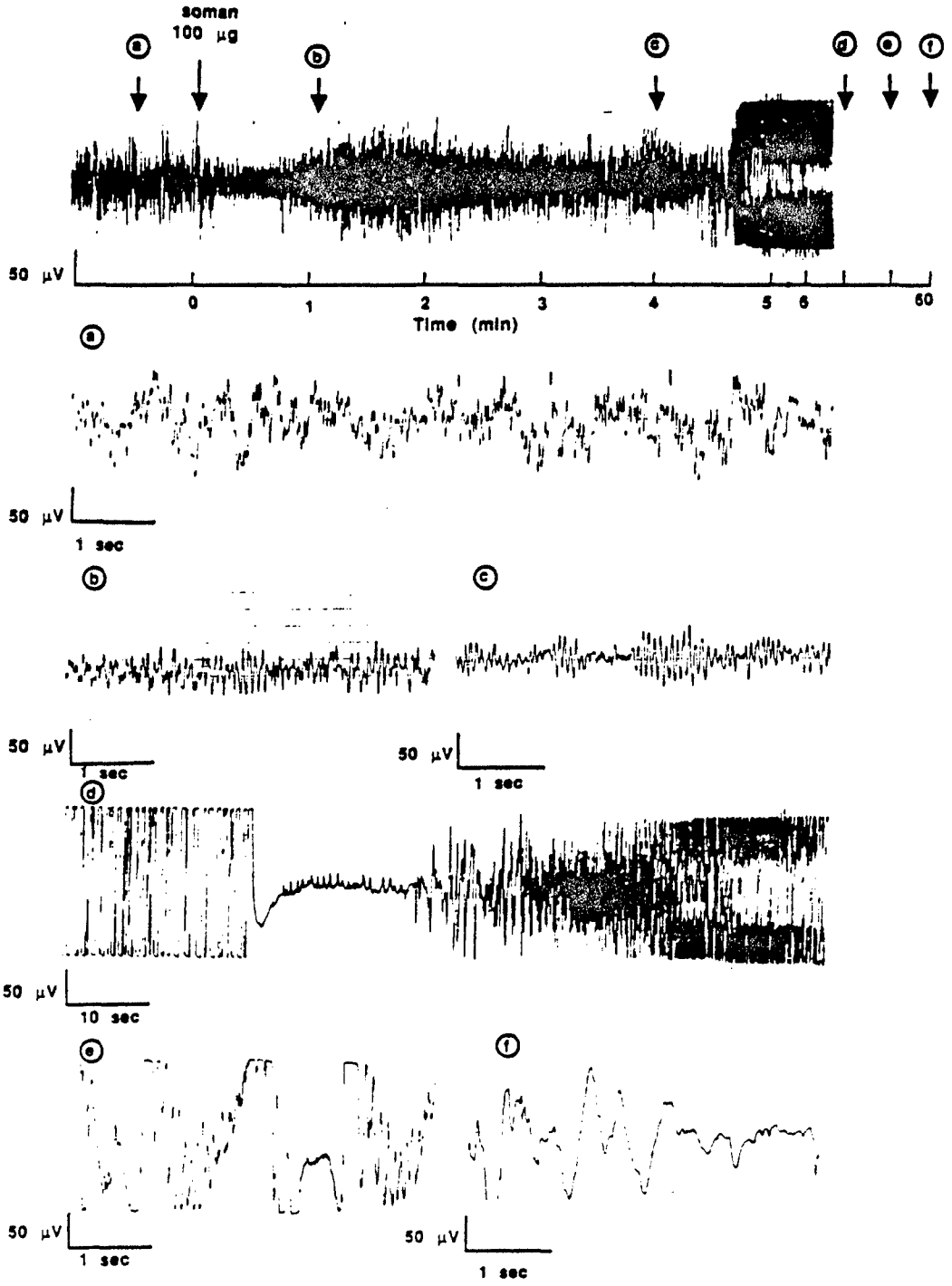

Fig. 7. EEG and Soman Exposure During Constant Pressure Conditions. The EEG was recorded from two electrodes placed over the parietal cortex about 2.5 cm apart. Soman (100 µg) was administered as described in Specific Aim 1. Appropriate scales are shown for each tracing.

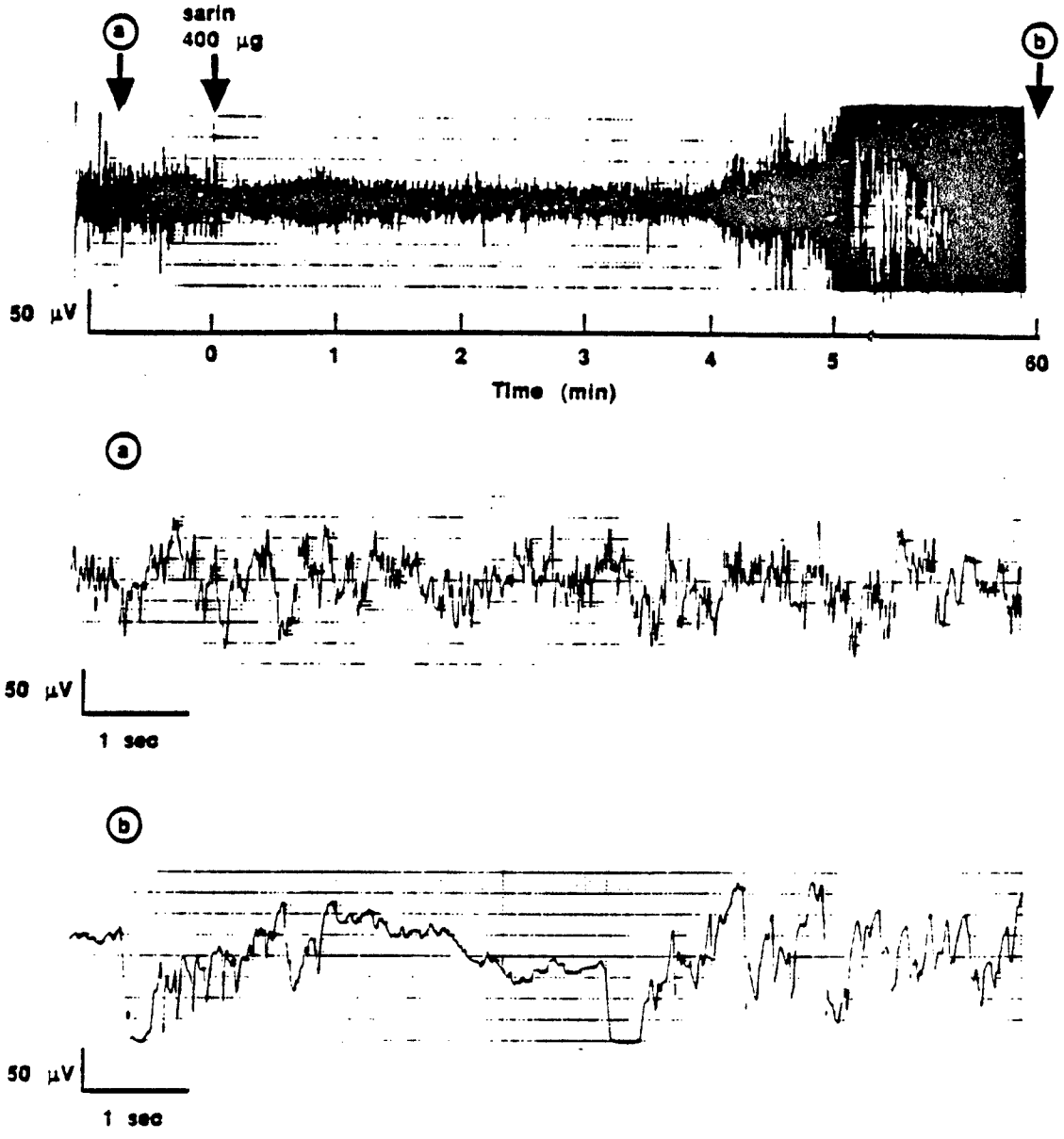

Fig. 8. EEG and Sarin Exposure During Constant Pressure Conditions. The EEG was recorded from two electrodes placed over the parietal cortex about 2.5 cm apart. Sarin (400 µg) was administered as described in Specific Aim 1. Appropriate scales are shown for each tracing.

Section Location

A. Frontal

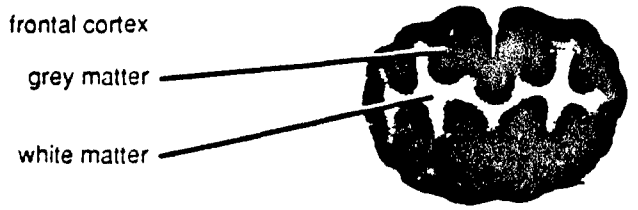

B. Medial

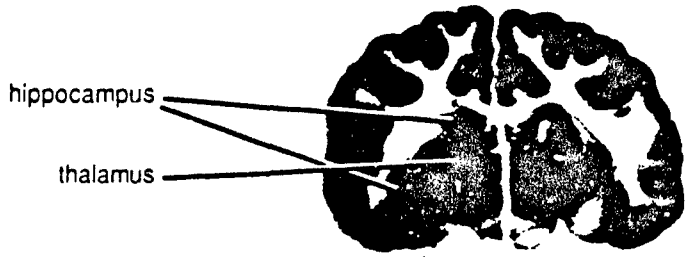

C. Occipital

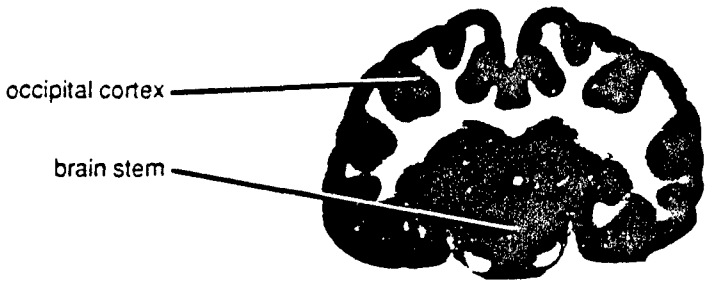

D. Cerebellum

Fig. 9. Regional Cerebral Blood Flow in the Isolated Canine Brain as Determined by [^{14}C]Iodoantipyrine Infusion and Autoradiography. [^{14}C]Iodoantipyrine (25 μCi) was infused over a period of 30 sec into the arterial perfusate. Flow was stopped instantly, and the brain was rapidly removed from the cranium, cut into ~1-cm thick slabs, and frozen. Coronal sections (20 μm) were then cut with a cryostat, dried, and subjected to autoradiography. Tissue samples (20-60 mg) from selected brain regions were also collected, weighed, and digested; the radioactivity levels were determined by scintillation spectrometry. Regional CBF was calculated as described in the Method section of Specific Aim 2. The autoradiograms are representative of five control experiments. Four experiments were conducted with soman (data not shown).

Fig. 10. Regional Glucose Metabolism in the Isolated Canine Brain. **A**) Autoradiograph of coronal brain section from the medial region after infusion of [6-^{14}C]D-glucose as described in the Specific Aim 3. **B**) Autoradiograph of cerebellar region.

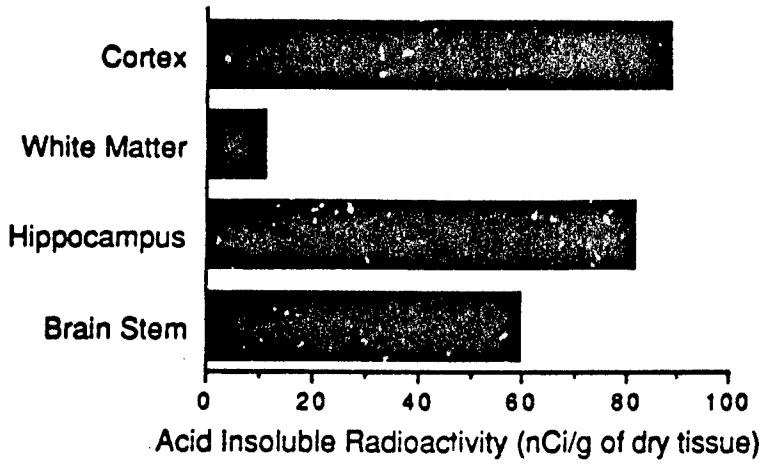

Fig. 11. Relative Protein Synthesis in Brain Regions. Brain sections were washed with TCA to remove free L-[1-^{14}C]leucine and then exposed to photosensitive film. Autoradiographic images obtained represent incorporation of L-[1-^{14}C]leucine into brain proteins.

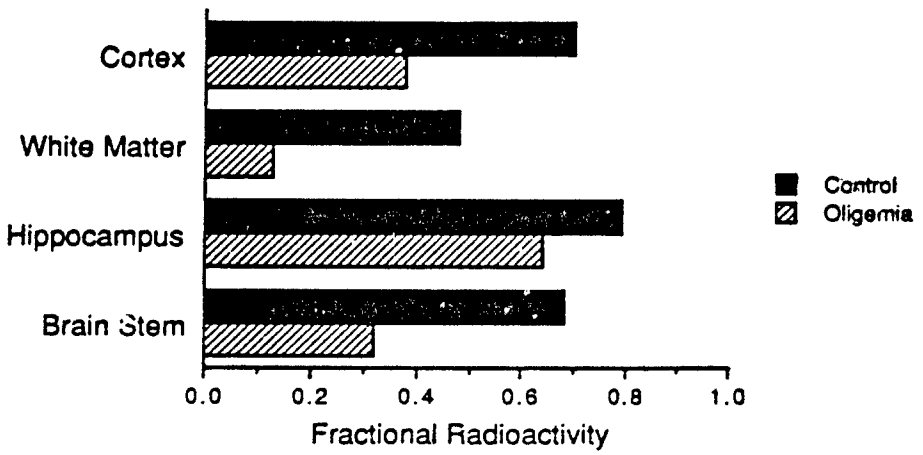

Fig. 12. Effects of Oligemia on Relative Protein Synthesis in Brain Regions. Oligemia was produced by reducing the pump flow until the EEG tracing showed significant changes in amplitude and frequency, corresponding to a 55% decrease in brain blood flow. Fractional radioactivity is acid insoluble radioactivity expressed as the percent of total radioactivity before TCA washout.

^{14}C Radioactivity

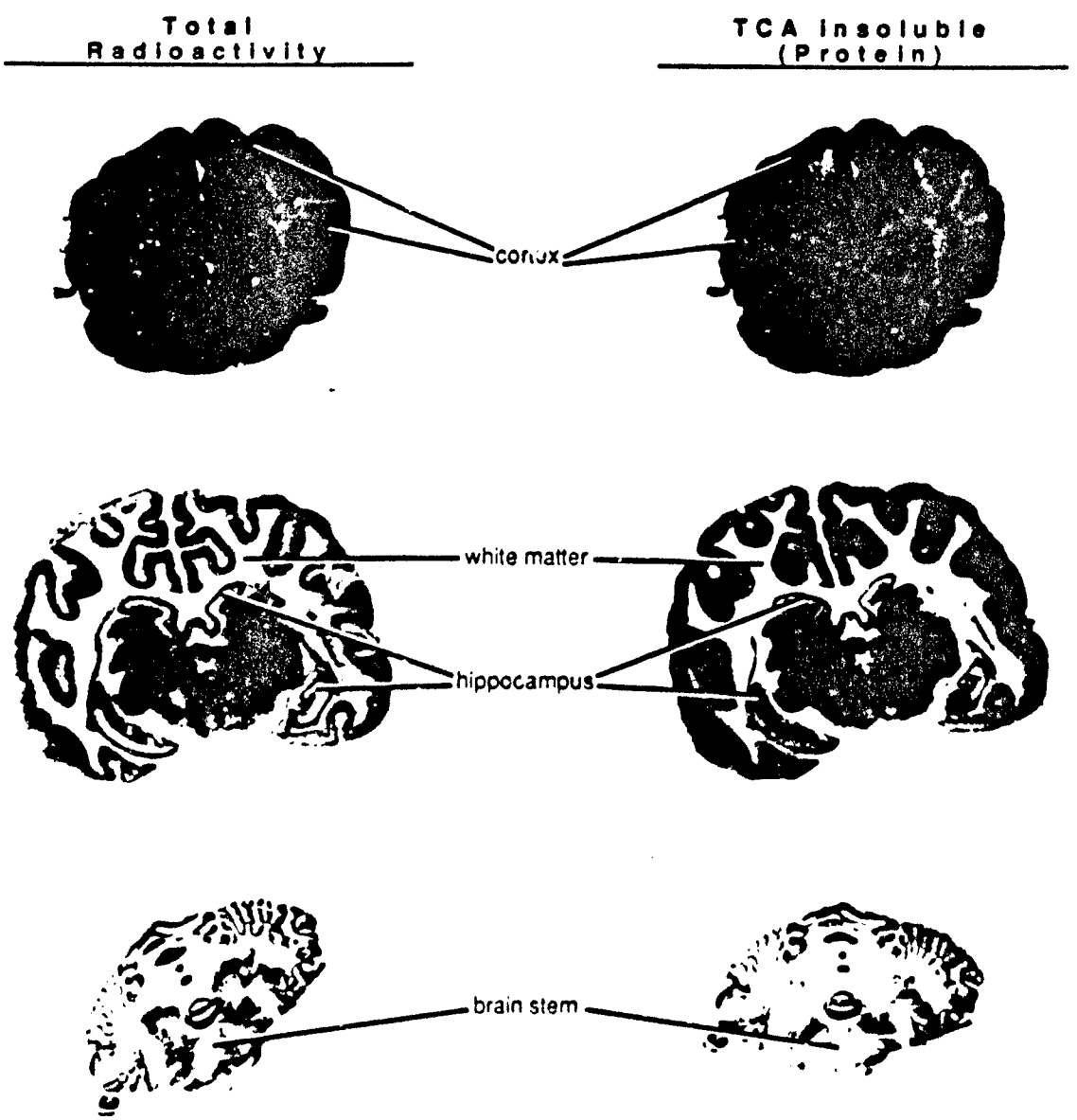

Fig. 13. Autoradiography of L-[1-^{14}C]leucine Uptake and Protein Synthesis in Brain Under Control Perfusion Conditions. Total radioactivity represents the total of free acid-soluble L-[1-^{14}C]leucine and L-[1-^{14}C]leucine incorporated into proteins. After TCA wash, the remaining radioactivity represents synthesized ^{14}C protein. Coronal brain sections from frontal brain, medial brain, and cerebellum were prepared and subjected to autoradiography. Experimental details are described in Specific Aim 4.

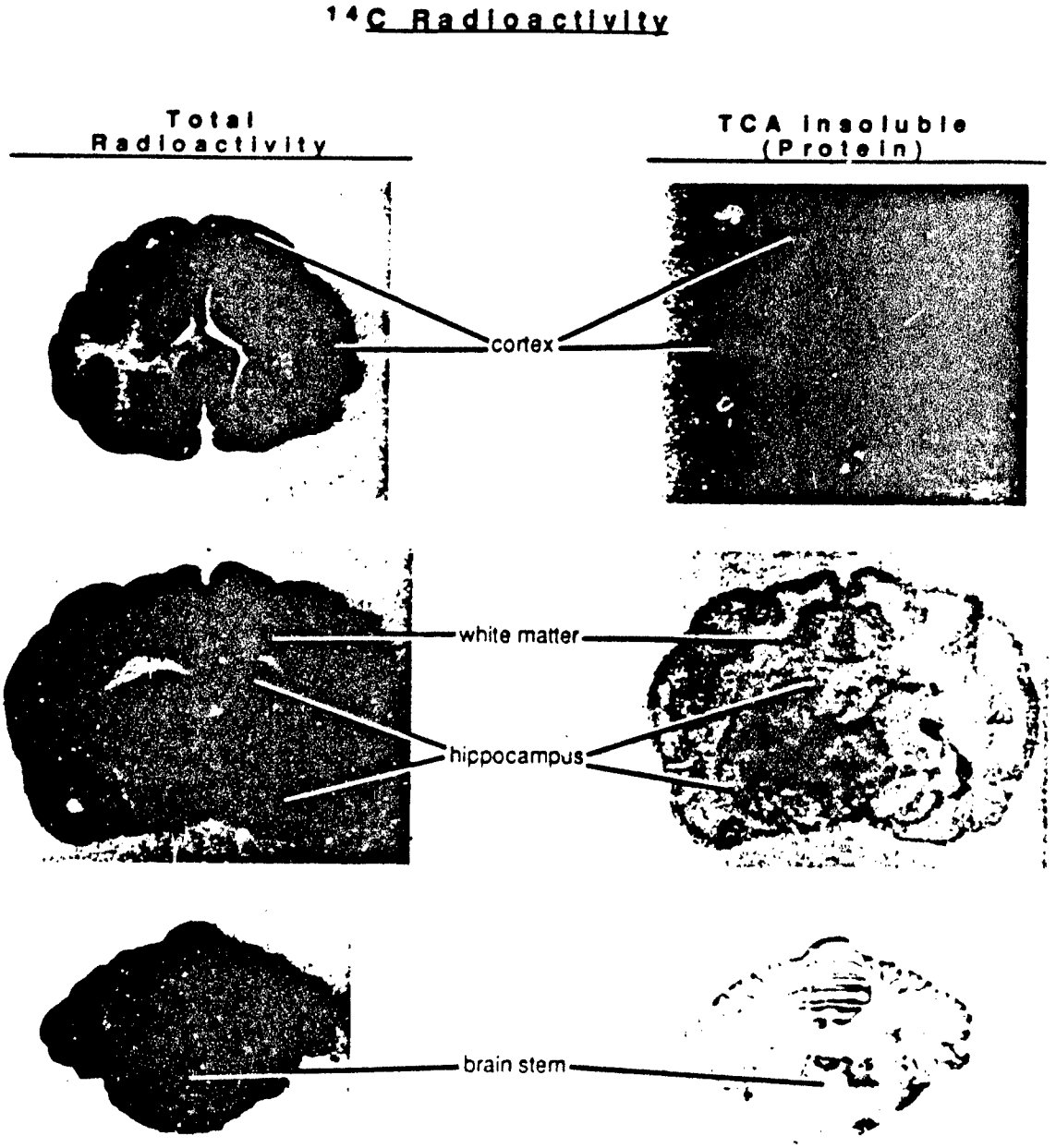

Fig. 14. Autoradiography of L-[1-^{14}C]leucine Uptake and Protein Synthesis in Brain Following OP (Soman, 100 µg) Exposure. Total radioactivity represents the total of free acid-soluble L-[1-^{14}C]leucine and L-[1-^{14}C]leucine incorporated into proteins. After TCA wash, the remaining radioactivity represents synthesized ^{14}C protein. Coronal brain sections from frontal brain, medial brain, and cerebellum were prepared and subjected to autoradiography. Experimental details are described in Specific Aim 4.

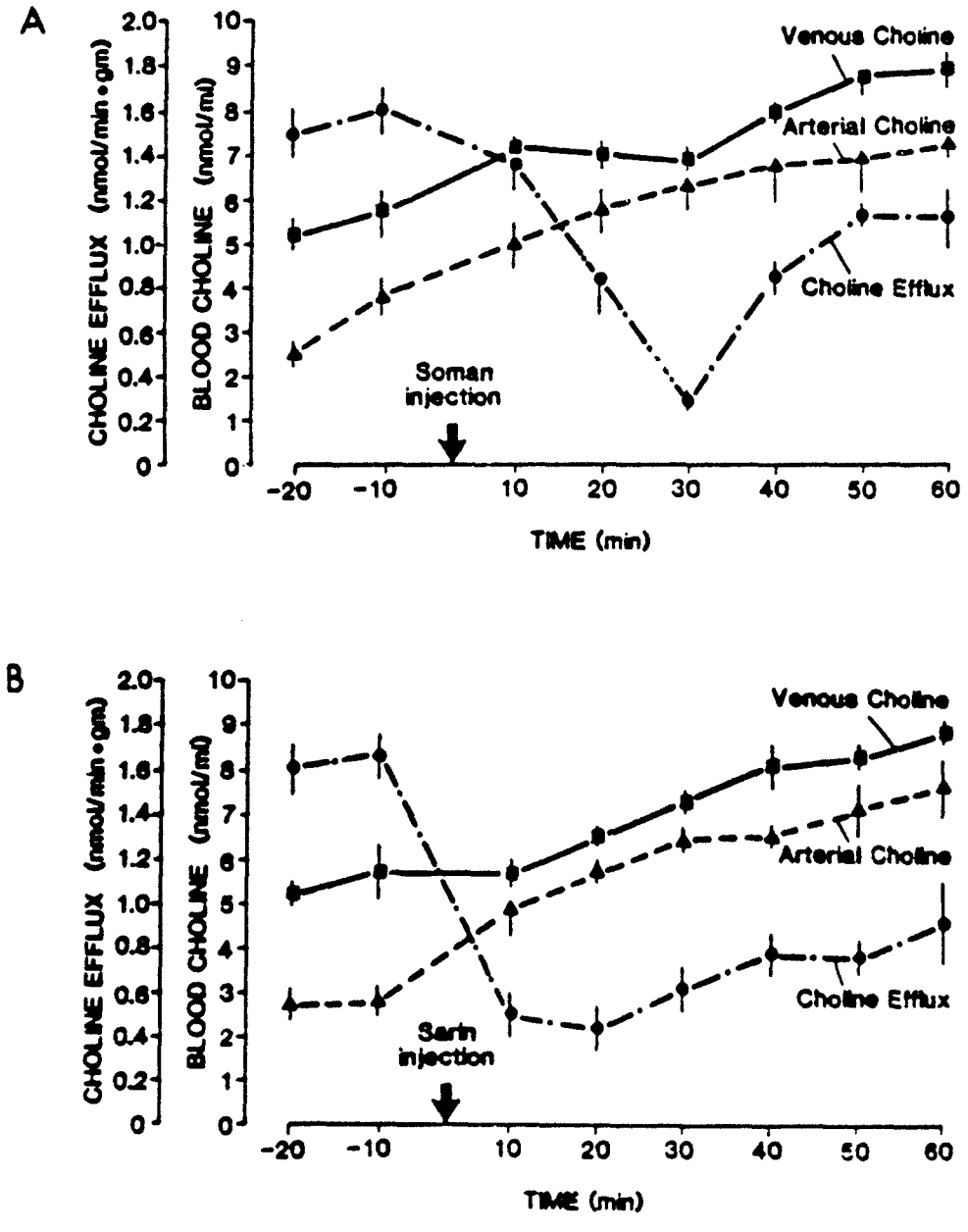

Fig. 15. Ch Efflux from A) Soman- and B) Sarin-treated Perfused Canine Brain. Arterial and venous perfusate samples were collected and analyzed for Ch content using a gas chromatography-mass spectrometry method. Ch efflux was then calculated from the arteriovenous differences as described in Specific Aim 6. The data for each treatment are from three experiments, and the vertical bars represent the S.E.M. values.

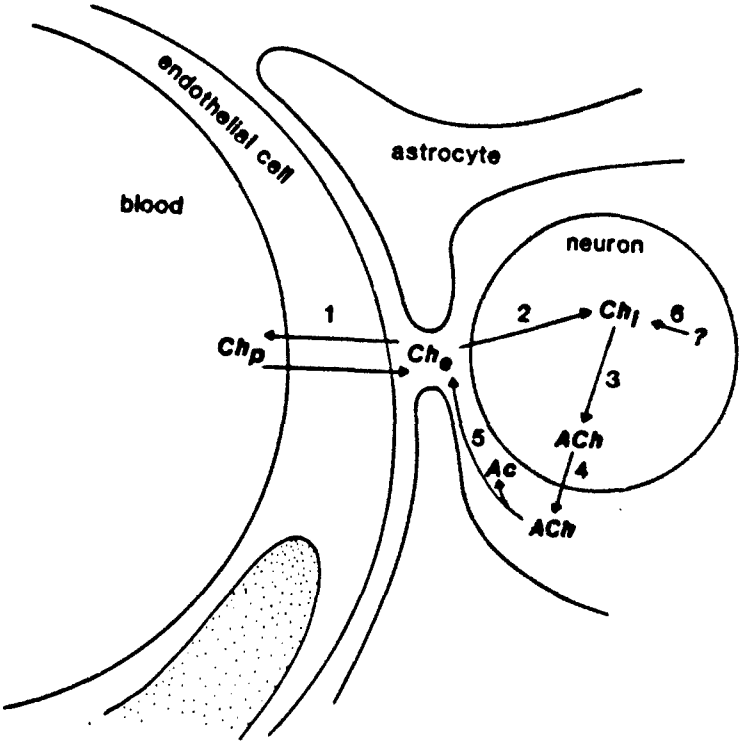

Fig. 16. Brain Ch Metabolism. Ch metabolism in brain involves at least six biochemical reactions. Equilibration of plasma Ch (Ch_p) and extracellular Ch (Ch_e) occurs via the Ch transporter (reaction **1**) of the endothelial cell. Transport into neurons (reaction **2**) occurs by a carrier-mediated process. ACh synthesis by Ch acetyltransferase (reaction **3**), ACh release (reaction **4**), and degradation by AChE (reaction **5**) are illustrated. Synthesis of intracellular Ch (Ch_i) may also occur from endogenous substrates (reaction **6**).

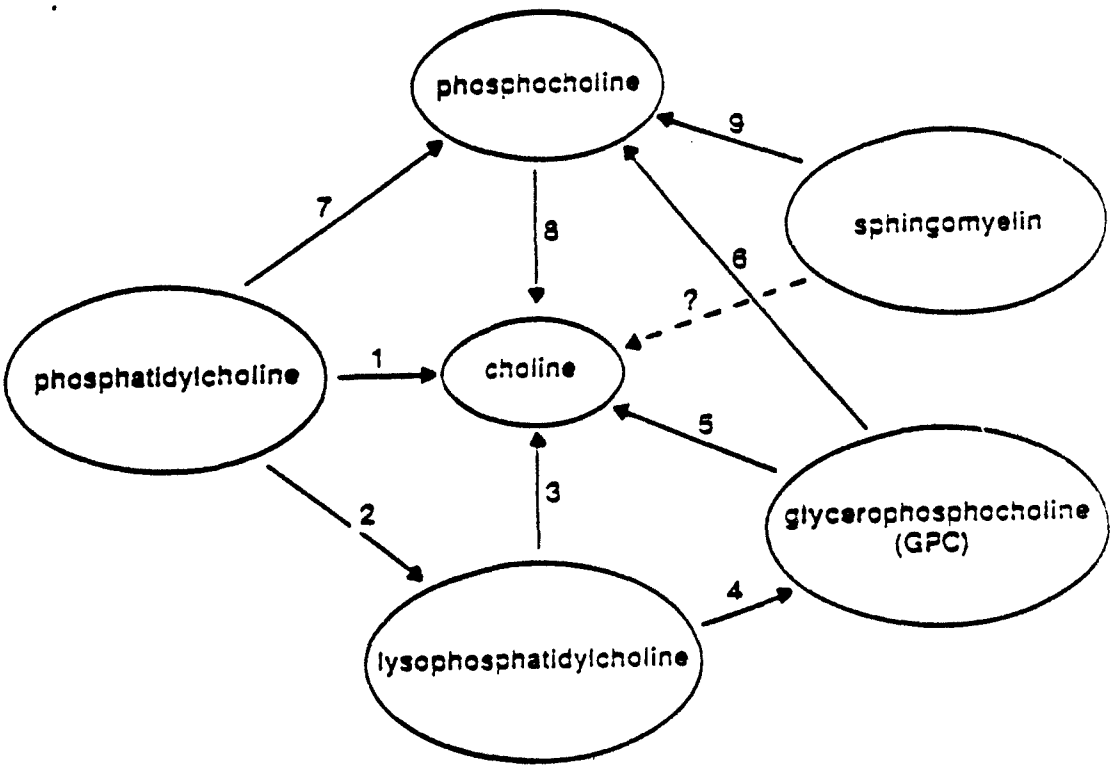

Fig. 17. Possible Pathways and Enzymes Involved in Choline Production. The numbers in the figure refer to enzymes as follows: **1**, phospholipase D; **2**, phospholipase A_2 or A_1; **3**, lysophospholipase D; **4**, lysophospholipase; **5**, glycerophosphocholine phosphodiesterase; **6**, glycerophosphocholine-cholinephosphodiesterase: **7**, phospholipase C; **8**, alkaline phosphatase; **9**, sphingomyelinase.

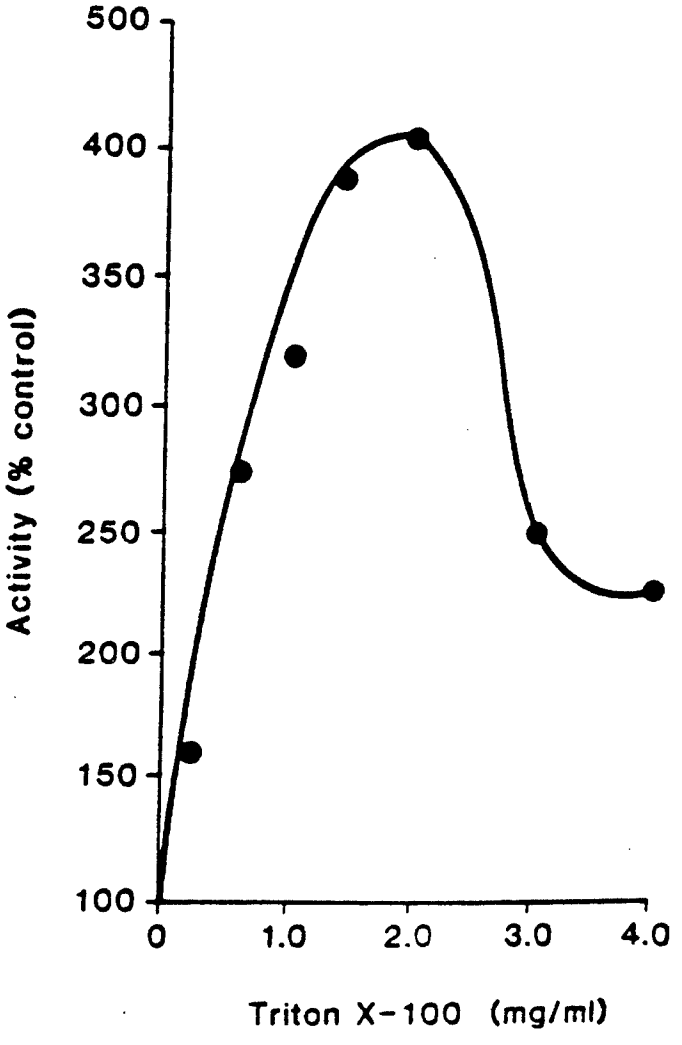

Fig. 18. Effects of Triton X-100 on the Hydrolytic Activity of Dog Brain Microsomal Phospholipase D. Incubations were carried out as described in Table 17. Triton X-100 was added to the reaction mixtures before the addition of enzyme. Data are the averages of two determinations, and control activity in the absence of Triton X-100 is considered to be 100%.

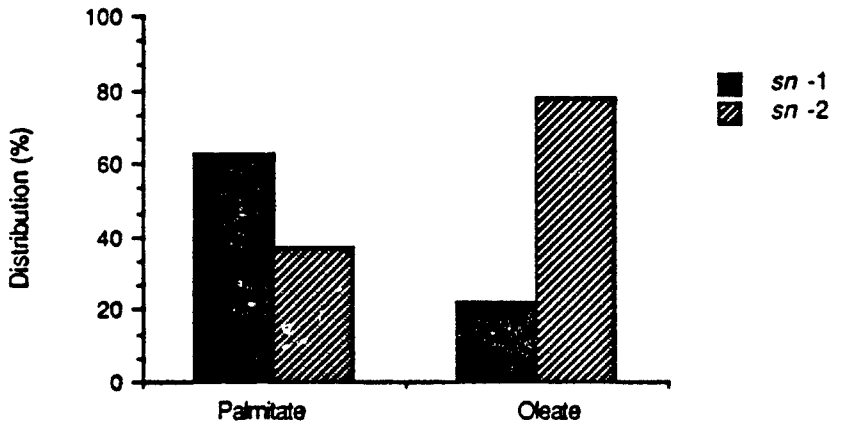

Fig. 19. Positional Distribution of Labeled Fatty Acids Incorporated into Phosphatidylcholine. Phosphatidylcholine from the lipid extracts was isolated using thin-layer chromatography (TLC) and was subjected to phospholipase A2 (*Ophiophagus hannah*) hydrolysis. The radioactivity levels associated with lysoPC (*sn*-1) and the free fatty acid released (*sn*-2) were determined after separation by TLC (silica gel H). The solvent for TLC was chloroform:methanol:water (65:35:5).

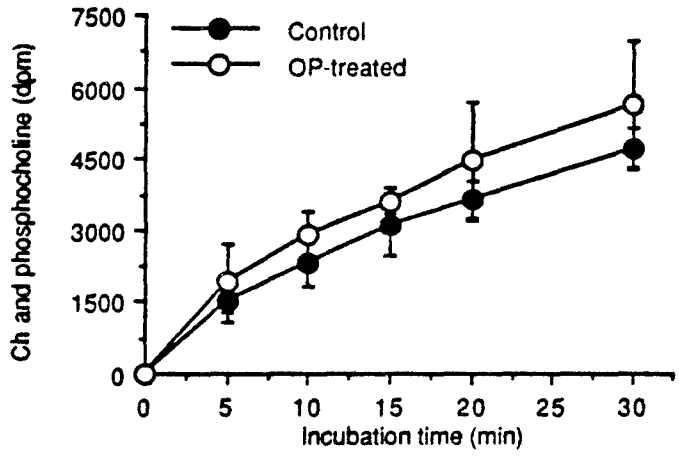

Fig. 20. Comparison of the Amounts of Choline (Ch) and Phosphocholine Released by Cerebral Cortex Synaptosomes Prepared from Control Dog Brains with the Amounts Released by Synaptosomes from Organophosphate-treated Brains. The perfusion experiments and assay procedures were carried out as described in Specific Aim 9. Values are the means ± S.D. of four separate experiments conducted in triplicate.

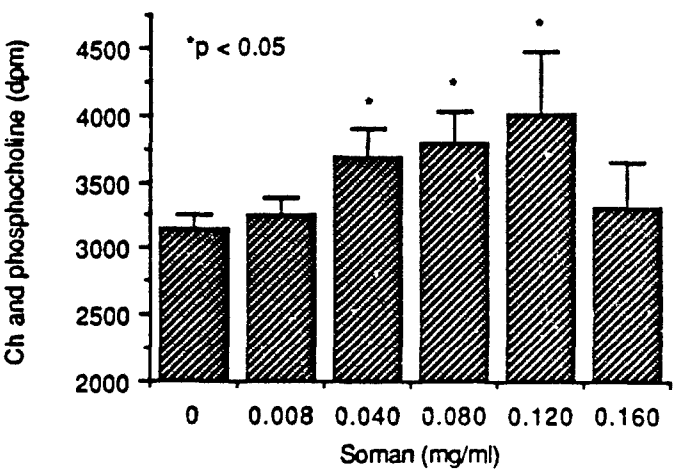

Fig. 21. Effects of *In Vitro* Addition of Soman on Choline (Ch) and Phosphocholine Release by Control Cerebral Cortex Synaptosomes. Various amounts of soman were added to incubation mixtures. The assay procedure was conducted as described in Specific Aim 9. Values are the means ± S.D. of three separate experiments conducted with four replicates.

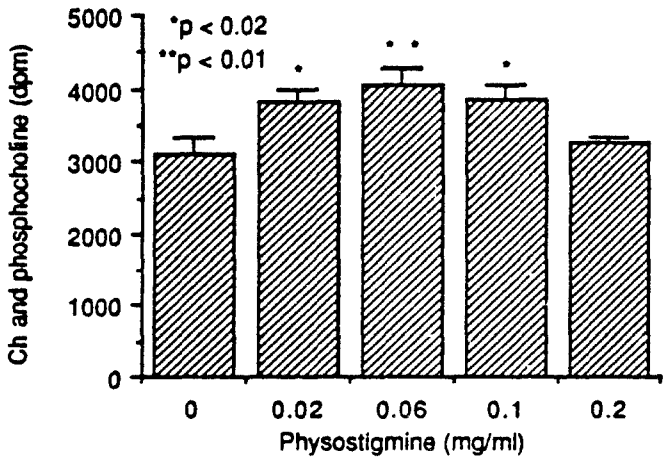

Fig. 22. Effects of Physostigmine on Choline (Ch) and Phosphocholine Release by Synaptosomes. Various amounts of physostigmine were added to incubation mixtures as described in Specific Aim 9. Values are the means ± S.D. of three separate experiments conducted in triplicate.

A.

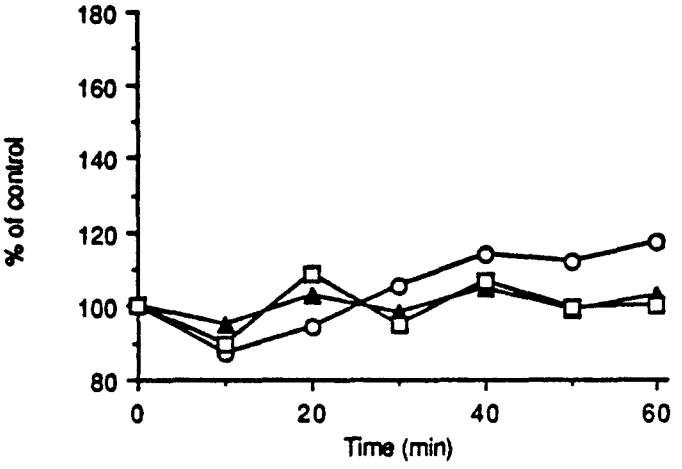

B.

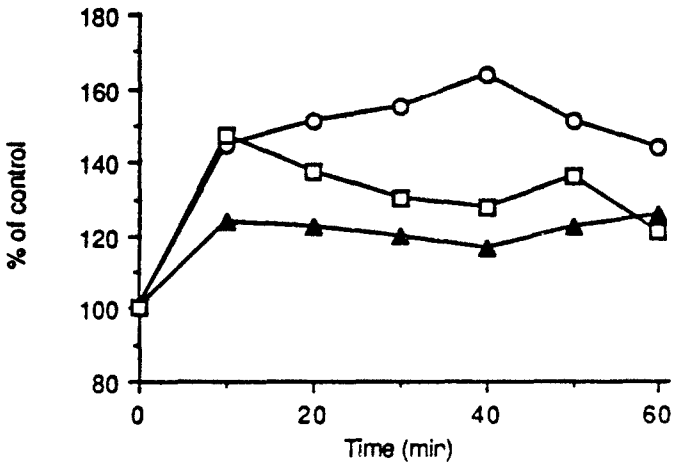

Fig. 23. Effects of α-Methyl-*p*-tyrosine on Cerebral Metabolism Rates (CMRs). Isolated brains were perfused for a 30-min control period. Then α-methyl-*p*-tyrosine (300 mg/L) was added to the perfusate and is indicated in the figure as 0 min. A) without OP and B) with soman treatment (100 µg). Standard error averaged <10% in A) n=5 and <12% in B) n=4. Key: CMR-Glucose (-O-); CMR-O_2 (-▲-); CMR-CO_2 (-□-).

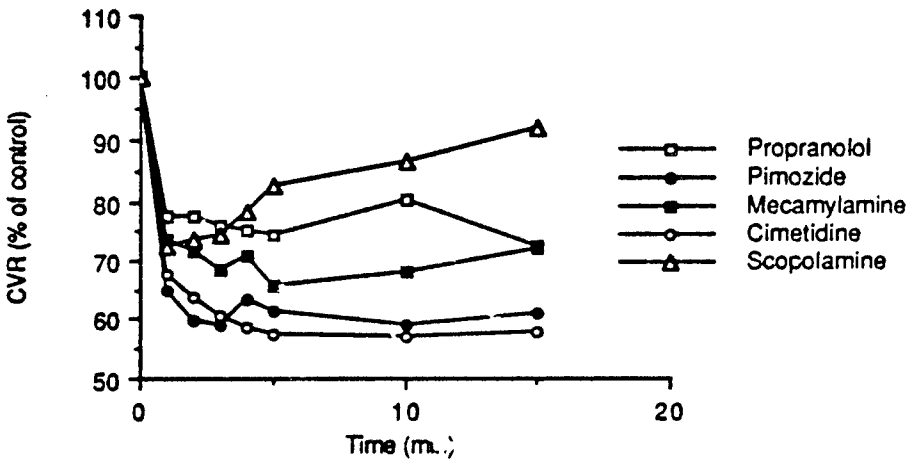

Fig. 24. Effects of Soman on Cerebrovascular Resistance (CVR) in Brains Pretreated with Specific Antagonists. Key: scopolamine (-△-); propranolol (-□-); mecamylamine (-■-); pimozide (-●-); cimetidine (-○-). After a 30- to 45-min control period, the specific antagonist was added to the perfusate. Soman (100 µg) was injected 15 min later, and cerebrovascular responses were calculated. The control value (100%) was 180±19 torr·g·min/ml. The data points are means of two experiments for propranolol and cimetidine and three experiments, in which the standard error averaged 8%, for scopolamine, mecamylamine, and pimozide.

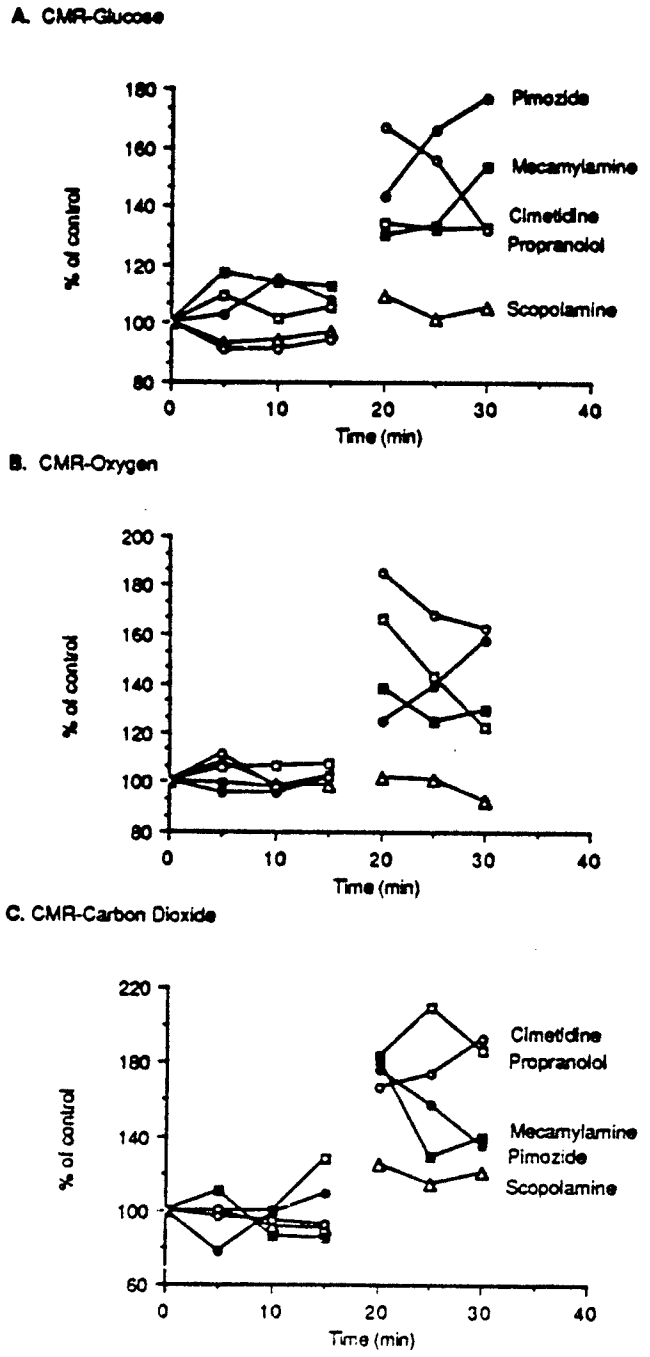

Fig. 25. Effects of Soman on Cerebral Metabolism Rates (CMRs) in Brains Pretreated with Specific Antagonists. Key: scopolamine (-△-); mecamylamine (-■-); pimozide (-●-); propranolol (-□-); cimetidine (-○-). Control values expressed in μmol/100 g·min were **A**, CMR-Glucose, 33±1; **B**, CMR-Oxygen, 171±4; and **C**, CMR-Carbon Dioxide, 247±17. The data points are means of two experiments for propranolol and cimetidine and three experiments, in which standard error averaged 10%, for scopolamine, mecamylamine, and pimozide.

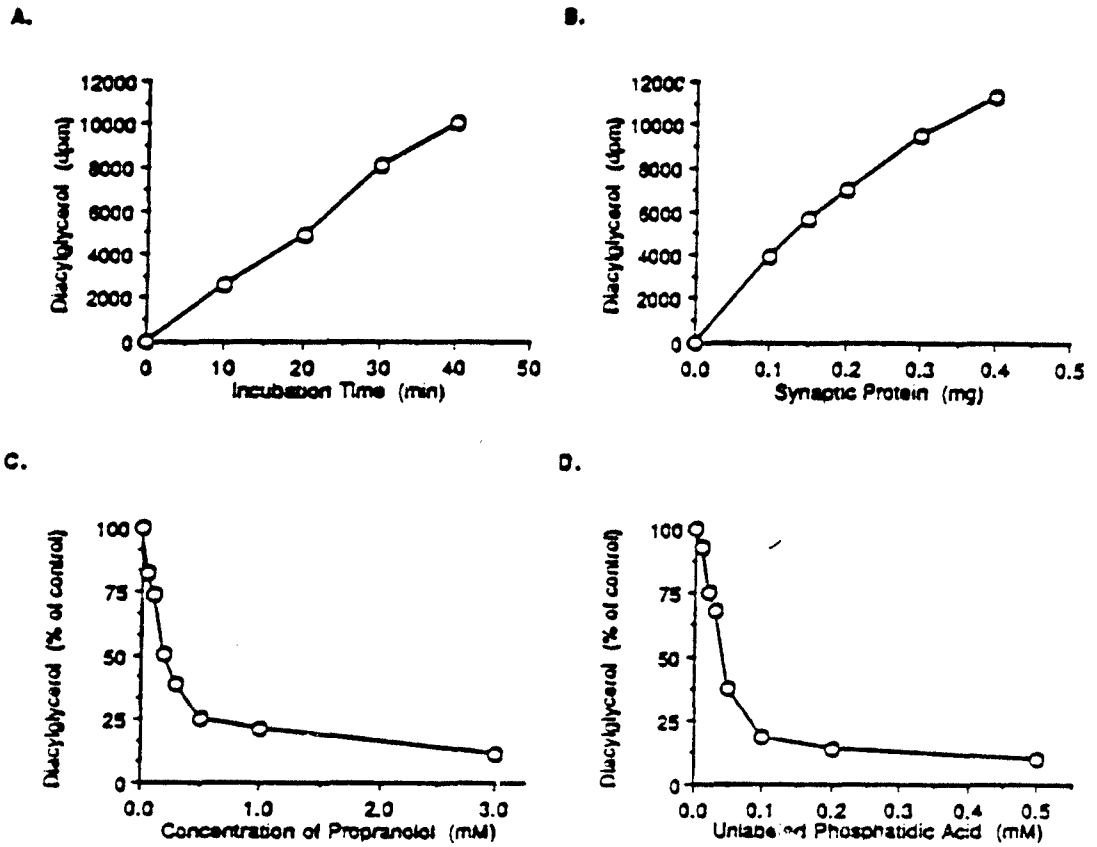

Fig. 26. Properties of PA Phosphatase in Synaptic Membranes of Canine Cerebral Cortex. Results shown are those of typical experiments. **A)** Time course of the enzyme reaction (150 µg of synaptic protein/reaction mixture); **B)** DAG formation as a function of synaptic protein concentration curve (20-min incubation); **C)** Effects of DL-propranolol on PA phosphatase activity (150 µg of protein/reaction mixture, 20-min incubation); **D)** Inhibition of nonradioactive-labeled exogenous PA on apparent enzyme activity (150 µg of protein/reaction mixture, 20-min incubation).

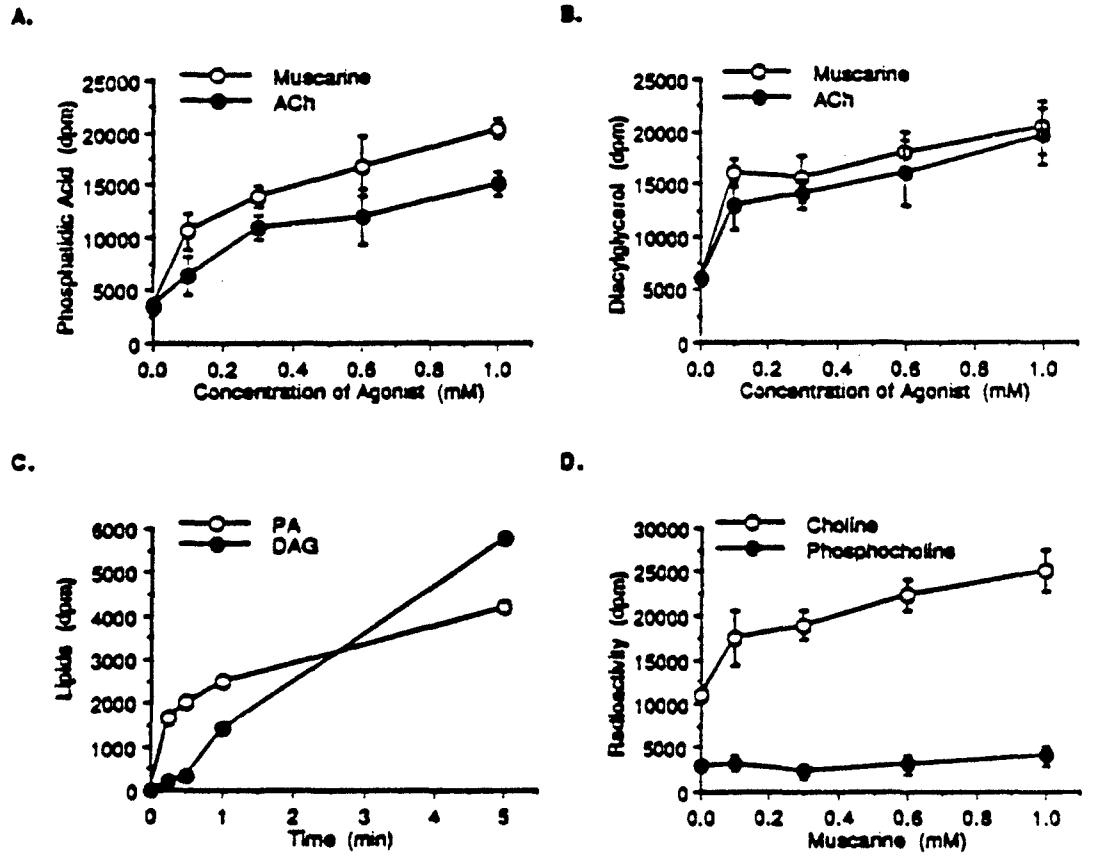

Fig. 27. Cholinergic Stimulation of [^{3}H]Phosphatidic Acid (PA) and [^{3}H]Diacylglycerol (DAG) Generation in Synaptic Membranes of Canine Cerebral Cortex. **A)** Cholinergic effects on conversion of [^{3}H]PC to [^{3}H]PA. Values are the means ± S.D. of three separate experiments conducted in duplicate. **B)** Accumulation of [^{3}H]DAG after ACh and muscarine stimulation. Values are the means ± S.D. of three separate experiments conducted in duplicate. **C)** Time course of [^{3}H]PA and [^{3}H]DAG generation after 1 mM ACh stimulation. At least three separate experiments were conducted in duplicate, and the results are from a typical experiment. **D)** [^{3}H]Choline and [^{3}H]phosphorylcholine formation after ACh stimulation in the synaptic membranes. The exogenous radioactive-labeled substrate 1,2-dipalmitoyl-*sn*-glycerol-3-phosphoryl[^{3}H]choline was used to replace 1-palmitoyl-2-[9,10-^{3}H]palmitoyl-L-3-phosphorylcholine in the incubation mixtures. Values are the means ± S.D. of three separate experiments conducted in triplicate.

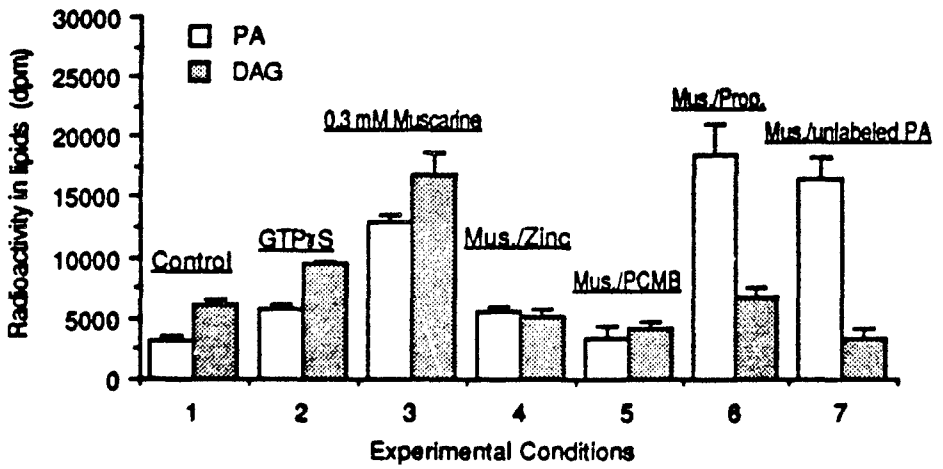

Fig. 28. Effects of Various Compounds on Muscarinic Stimulation of [^{3}H]PA and [^{3}H]DAG Generation in Synaptic Membranes. Radioactive PC, 1-palmitoyl-2-[9,10-^{3}H]palmitoyl-L-3-phosphorylcholine, was used as the exogenous substrate. The incubation conditions and assay procedures are as described in Specific Aim 13, except that GTPγS was omitted in the control and 0.3 mM muscarine was present in tests 3 to 7. The following compounds were added to the incubation mixtures where indicated: zinc, 2 mM; *p*CMB, 0.5 mM; DL-propranolol, 3 mM; and unlabeled PA, 0.2 mM. Values are the means ± S.D. of four separate experiments conducted in duplicate.

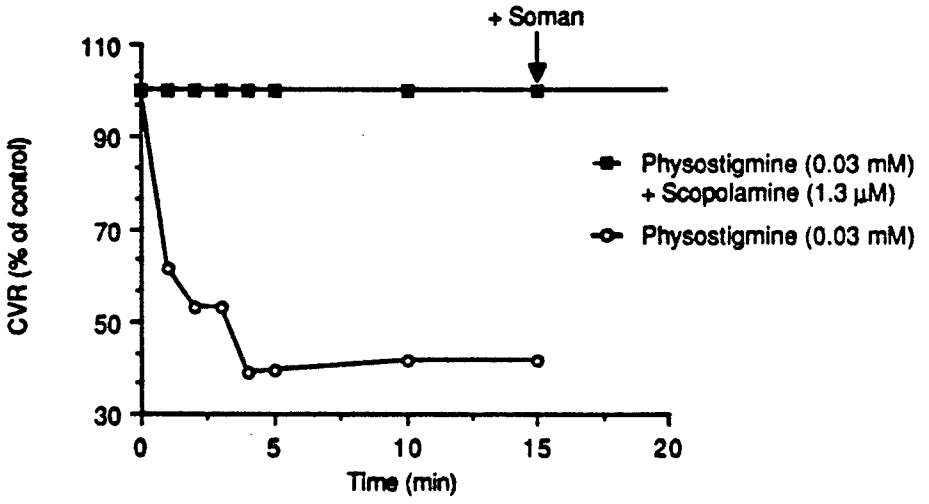

Fig. 29. Brain Vascular Response After Acetylcholinesterase Inhibition. In an experiment with physostigmine alone, the compound was added to the perfusate after a 30-min control period. In two other experiments, scopolamine preceded physostigmine, and soman (100 µg) was added at 45 min.

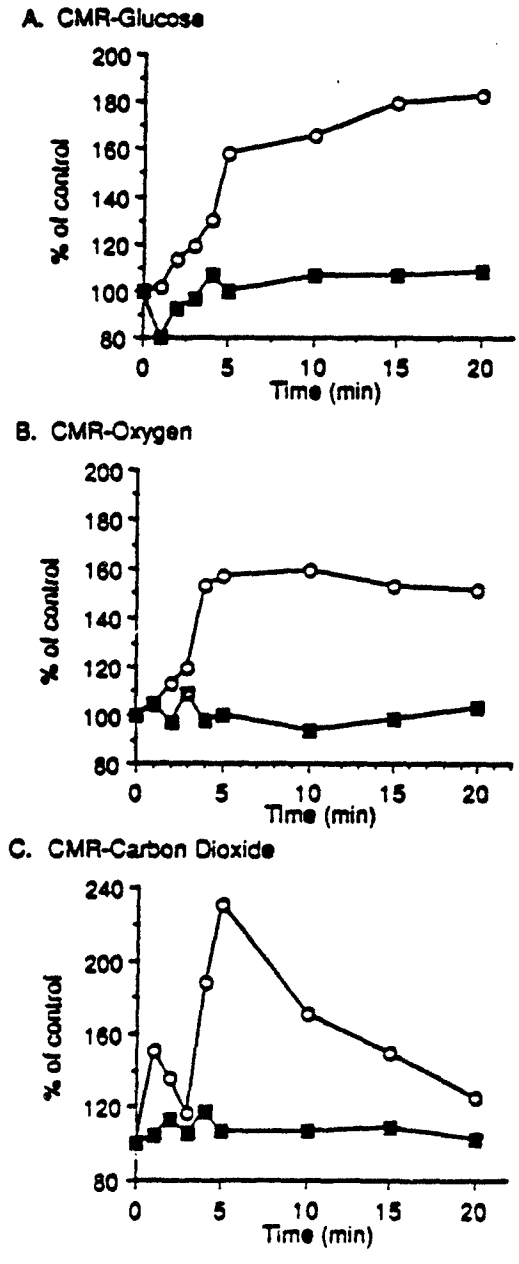

Fig. 30. Effects of Physostigmine on Cerebral Metabolism Rates (CMRs) in Brains Pretreated with Scopolamine. Scopolamine (1.3 μM) was added to the perfusate before addition of 0.03 mM physostigmine. Results are the averages of two experiments. Key: Physostigmine(-o-); Physostigmine + Scopolamine(-■-). Control values (100%) expressed in μmol/100 g·min were A) CMR-Glucose, 43±1; B) CMR-Oxygen, 210±13; and C) CMR-Carbon Dioxide, 330±10.

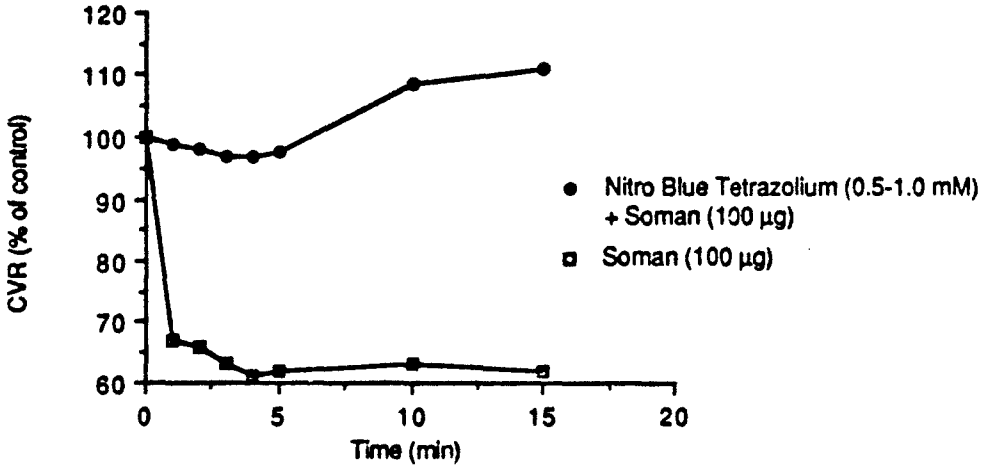

Fig. 31. Cerebrovascular Resistance (CVR) After Soman Treatment and After Soman Preceded by Nitro Blue Tetrazolium. Data are averages of two control and two test experiments.

REFERENCES

1. Grob, D. and Harvey, A. M. (1953) The effects and treatment of nerve gas poisoning. *Am. J. Med.* 14:52-63.

2. Karczmar, A. G. (1984) Acute and long lasting central actions of organophosphorus agents. *Fund. Appl. Toxicol.* 4(2, part 2):S1-S17.

3. Gilboe, D. D., Betz, A. L., and Drewes, L. R. (1975) Use of the isolated canine brain in studies of cerebral metabolism, metabolite transport, and cerebrovascular physiology, in *Research Methods in Neurochemistry* (Marks, N. and Rodnight, A., eds.) Plenum Press, New York, pp. 3-42.

4. Drewes, L. R. (1980) An improved apparatus for blood perfusion of the canine cerebral vasculature. *Neurochem. Res.* 5:551-560.

5. Wolthuis, O. L., Berends, F., and Meeter, E. (1981) Problems in therapy of soman poisoning. *Fund. Appl. Toxicol.* 1:183-192.

6. Burchfiel, J. S. and Duffy, F. H. (1982) Organophosphate neurotoxicity: chronic effects of sarin on the electroencephalogram of monkey and man. *Neurobehav. Toxicol. Teratol.* 4:767-778.

7. Drewes, L. R. and Singh, A. K. (June 1984) Cerebral metabolism and blood-brain transport: toxicity of organophosphorus compounds. *USAMRDC Annual Summary Report*, Ft. Detrick, Frederick, MD, Contract No. DAMD17-82-C-2136.

8. Drewes, L. R. and Singh, A. K. (1987) Cerebral metabolism and blood-brain transport: toxicity of organophosphorus compounds. *USAMRDC Final Summary Report*, Ft. Detrick, Frederick, MD, Contract No. DAMD17-82-C-2136.

9. Ingvar, M., Soderfeldt, B., Folbergrova, J., Kilimo, H., Olsson, Y., and Siesjö, B. K. (1984) Metabolic, circulatory, and structural alterations in the rat brain induced by sustained pentylenetetrazole seizures. *Epilepsia* 25:191-204.

10. Siesjö, B. K. (1978) *Brain Energy Metabolism* Wiley Press, Chichester.

11. Singh, A. K., Zeleznikar, R. J., Jr., and Drewes, L. R. (1983) Neurotoxic effects of acetylcholinesterase inhibitors on the isolated canine brain. *J. Neurochem.* 41:S9.

12. Estrada, C., Krause, D. N., and Scremin, O. (1983) Biochemical and physiological evidence for a cholinergic regulation of the cerebrovasculature. *J. Cereb. Blood Flow Metabol.* 3:S184-S185.

13. Brodersen, P., Paulson, O. B., Bolwig, T. G., Rogon, Z. E., Rafaelsen, O. J., and Lassen, N. A. (1973) Cerebral hyperemia in electrically induced epileptic seizure. *Arch. Neurol.* 28:334-338.

14. Plum, F. and Duffy, T. E. (1975) The couple between cerebral metabolism and blood flow during seizure, in *Brain Work* (Inguar, D. H. and Lassen, N. A., eds.) Manksgaard, Copenhagen, pp. 197-214.

15. Howse, D. C., Caronna, J. J., Duffy, T. E., and Plum, F. (1974) Cerebral energy metabolism, pH, and blood flow during seizures in the cat. *Am. J. Physiol.* 227:1444-1451.

16. Rubio, R. and Berne, R. M. (1975) Relationships of adenosine concentration, lactate levels and oxygen supply in rat brain, in *Blood Flow of Metabolism in the Brain* (Harper, A. M., et al., eds.) Churchill Livingstone, Edinburgh, pp. 3.23-3.29.

17. Meldrum, B. S. and Nilsson, B. (1976) Cerebral blood flow and metabolic rate early and late in prolonged epileptic seizures induced in rats by bicuculline. *Brain* 99:523-542.

18. Kreisman, N. R., Rosenthal, M., Sick, T. J., and LaManna, J. C. (1983) Oxidative metabolic responses during recurrent seizures are independent of convulsant, anesthetic, or species. *Neurol. (Cleveland)* 33:861-867.

19. Chapman, A. G., Meldrum, B. S., and Siesjö, B. K. (1977) Cerebral metabolic changes during prolonged epileptic seizures in rats. *J. Neurochem.* 28:1025-1035.

20. McDonough, J. H., Jr., Hackley, B. E., Cross, R. S., Samson, F., and Nelson, S. (1983) Brain regional glucose use during soman-induced seizures. *Neurotoxicol.* 4:203-210.

21. Pazdernik, T. L., Cross, R. S., Nelson, S., Samson, F., and McDonough, J. H., Jr. (1983) Soman-induced depression of brain activity in TAB-pretreated rats: 2-deoxyglucose study. *Neurotoxicol.*, 4:27-34.

22. Samson, F., Pazdernik, T. L., Cross, R. S., Giesler, M. P., Mewes, K., Nelson, S. R., and McDonough, J. H., Jr. (1984) Soman-induced changes in brain regional glucose use. *Fund. Appl. Toxicol.* 4:S173-S183.

23. Rehncrona, S., Rosen, I., and Siesjö, B. K. (1981) Brain lactic acidosis and ischemic cell damage: 1. Biochemistry and neurophysiology. *J. Cereb. Blood Flow Metabol.* 1:297-311.

24. Matin, M. A. and Siddiqui, R. A. (1982) Effect of diacetylmonoxime and atropine on malathion-induced changes in blood glucose level and glycogen content of certain brain structures of rats. *Biochem. Pharmacol.* 31:1801-1803.

25. Clement, J. G. and Lee, M. J. (1980) Soman-induced convulsions: significance of changes in levels of blood electrolytes, gases, glucose, and insulin. *Toxicol. Appl. Pharmacol.* 55:203-204.

26. Kalimo, H., Rehncrona, S., Soderfeldt, B., Olsson, Y., and Siesjö, B. K. (1981) Brain lactic acidosis and ischemic cell damage: 2. Histopathology. *J. Cereb. Blood Flow Metabol.* 1:313-327.

27. Kreisman, N. R., Sick, T. J., and Rosenthal, M. (1983) Importance of vascular responses in determining cortical oxygenation during recurrent paroxysmal events of varying duration and frequency of repetition. *J. Cereb. Blood Flow Metabol.* 3:330-338.

28. Drewes, L. R. and Reddy, P.V. (15 June 1989) Metabolism, seizures, and blood flow in brain following organophosphate exposure: mechanisms of action and possible therapeutic agents. *USAMRDC Annual Summary Report*, Ft. Detrick, Frederick, MD, Contract No. DAMD17-86-C-6036.

29. Kety, S. S. (1960) Measurement of local flow by the exchange of an inert diffusible substance. *Methods Med. Res.* 8:228-236.

30. Drewes, L. R. and Singh, A. K. (1985) Perfused canine brain: metabolism and blood-brain transport during altered metabolic states, in *Oxygen Transport to Tissue-VI* (Bruley, D., Bicher, H. I., and Reneau, D., eds.) Plenum Press, New York, pp. 141-152.

31. Hawkins, R. A., Mans, A. M., Davis, D. W., Vina, J. R., and Hibbard, L. S. (1985) Cerebral glucose use measured with [^{14}C]glucose labeled in the 1, 2, or 6 position. *Am. J. Physiol.* 248:C170-C176.

32. Sokoloff, L., Reivich, M., Kennedy, C., Des Rosiers, M. H., Patlak, C. S., Pettigrew, K. D., Sakurada, O., and Shinohara, M. (1977) The [^{14}C]deoxyglucose method for the measurement of local cerebral glucose utilization: theory, procedure, and normal values in the conscious and anesthetized albino rat. *J. Neurochem.* **28**:897-916.

33. Gjedde, A. (1982) Calculation of cerebral glucose phosphorylation from uptake of glucose analogues in vivo: a re-examination. *Brain Res. Reviews* **4**:237-252.

34. Pardridge, W. M., Crane, P. D., Mietus, L. J., and Oldendorf, W. H. (1982) Nomogram for 2-deoxyglucose lumped constant for rat brain cortex. *J. Cereb. Blood Flow Metabol.* **2**:197-206.

35. Bodsch, W. and Hossmann, K.-A. (1983) A quantitative regional analysis of amino acids involved in rat brain protein synthesis by high performance liquid chromatography. *J. Neurochem.* **40**:371-382.

36. Bodsch, W. and Hossmann, K.-A. (1983) The double-label method of local protein synthesis: autoradiography and protein biochemistry of *in vivo* labeled proteins. *J. Cereb. Blood Flow Metabol.* **3**:S468-S469.

37. Kiessling, M., Xie, Y., and Kleihues, P. (1983) Regional protein synthesis in the rat brain during severe hypoglycemia. *J. Cereb. Blood Flow Metabol.* **3**:S472-S473.

38. Doebler, J. A., Bocan, T., Moore, R. A., Shih, T. -M., and Anthony, A. (1983) Brain neuronal RNA metabolism during acute soman toxication: effects of antidotal pretreatments. *Neurochem. Res.* **8**:997-1011.

39. Sterri, S. H., Lyngaas, S., and Fonnum, F. (1981) Toxicity of soman after repetitive injection of sublethal doses in guinea pig and mouse. *Acta Pharm. Toxicol.* **49**:8-13.

40. Fonnum, F. and Sterri, S. H. (1981) Factors modifying the toxicity of organophosphorus compounds including soman and sarin. *Fund. Appl. Toxicol.* **1**:143-147.

41. Bodsch, W., Takahashi, K., Barbier, A., Grosse-Ophoff, B., and Hossmann, K. -A. (1985) Cerebral protein-synthesis and ischemia. *Prog. Brain Res.* **63**:197-210.

42. Yoshimine, T., Hayakawa, T., Kato, A., Yamada, K., Matsumoto, K., Ushio, Y., and Mogami, H. (1987) Autoradiographic study of regional protein synthesis in focal ischemia with TCA wash and image subtraction techniques. *J. Cereb. Blood Flow Metabol.* **7**:387-393.

43. Xie, Y., Mies, G., and Hossmann, K. -A. (1989) Ischemic threshold of brain protein synthesis after unilateral carotid artery occlusion in gerbils. *Stroke* **20**:620-626.

44. Betz, A. L., Gilboe, D. D., Yudilevich, D. L., and Drewes, L. R. (1973) Kinetics of unidirectional glucose transport into the isolated dog brain. *Am. J. Physiol.* **225**:586-592.

45. Zeisel, S. H. (1981) Dietary choline: biochemistry, physiology, and pharmacology. *Ann. Rev. Nutr.* **1**:95-121.

46. Blusztajn, J. K. and Wurtman, R. J. (1983) The synthesis of choline and acetylcholine in brain, in *Handbook of Neurochemistry*, Vol. 5, (Lajtha, A., ed.) Plenum Press, New York, pp. 295-310.

47. Blusztajn, J. K., Zeisel, S. H., and Wurtman, R. J. (1979) Synthesis of lecithin (phosphatidylcholine) from phosphatidylethanolamine in bovine brain. *Brain Res.* **179**:319-327.

48. Ansell, G. B. and Spanner, S. (1971) Studies on the origin of choline in the brain of the rat. *Biochem. J.* **122**:741-750.

49. Illingworth, D. R. and Portman, W. O. (1972) The uptake and metabolism of plasma lysophosphatidylcholine *in vivo* by the brain of squirrel monkeys. *Biochem. J.* 130:557-567.

50. Comford, E. M., Braun, L. D., and Oldendorf, W. H. (1978) Carrier-mediated blood-brain transport of choline and certain choline analogs. *J. Neurochem.* 30:299-308.

51. Shih, T.-M. (1982) Time-course effects of soman on acetylcholine and choline levels in six discrete areas of the rat brain. *Psychopharmacol.* 78:170-175.

52. Flynn, C. J. and Wecker, L. (1986) Elevated choline levels in brain: a non-cholinergic component of organophosphate toxicity. *Biochem. Pharmacol.* 35:3115-3121.

53. Ladinsky, H., Consolo, S., and Peri, G. (1974) Effect of oxotremorine and physostigmine on choline levels in mouse whole brain, spleen and cerebellum. *Biochem. Pharmacol.* 23:1187-1193.

54. Lundgren, G., Karlen, B., and Holmstedt, B. (1977) Acetylcholine and choline in mouse brain - influence of peripherally acting cholinergic drugs. *Biochem. Pharmacol.* 26:1607-1612.

55. Singh, A. K. and Drewes, L. R. (1985) Improved analysis of acetylcholine and choline in canine brain and blood samples by capillary gas chromatography-mass spectrometry. *J. Chromatogr.* 339:170-174.

56. Steel, R. G. D. and Torrie, J. H. (1960) *Principles and Procedures in Statistics* McGraw-Hill, New York, pp. 188-190.

57. Khandelwal, J., Szilagyi, L. A., Barker, L. A., and Green, J. P. (1981) Simultaneous measurement of acetylcholine and choline in brain by pyrolysis-gas chromatography-mass spectrometry. *Eur. J. Pharmacol.* 76:145-156.

58. Haug, P., Suzuki, M., Moritz, J., Nitsch, C., Wagner, A., Wunn, W., and Hassler, R. (1980) Changes in acetylcholine in caudate nucleus tissue isolated *in situ* detected by gas chromatography-mass spectrometry selected ion monitoring. *Biomed. Mass Spectrom.* 7:533-536.

59. Howard, S. G. and Garcia-Rill, E. (1983) Effects of electrical stimulation on acetylcholine synthesis in cat caudate nucleus. *Brain Res. Bulletin* 10:437-440.

60. Siniscalchi, A., Veratti, E., Bianchi, C., and Beani, L. (1985) Effect of morphine on acetylcholine content of electrically stimulated brain slices. *Pharmacol. Res. Commun.* 17:165-176.

61. Thakurta, S. G. and Bhattacharya, S. (1984) Regional activity of acetylcholinesterase and its relationship with acetylcholine concentration in the brain of the goat, *Capra capra*. *Comp. Physiol. Ecol.* 9:405-408.

62. McCandless, D. W., Looney, G. A., Modak, A. T., and Stavinoha, W. B. (1985) Cerebral acetylcholine and energy metabolism changes in acute ammonia intoxication in the lower primate *Tupaia glis*. *J. Lab. Clin. Med.* 106:183-186.

63. Gilboe, D. D. (1982) Perfusion of the isolated brain, in *Handbook of Neurochemistry, Vol. 2* (Lajtha, A., ed.) Plenum Press, New York, pp. 301-330.

64. Dross, K. and Kewitz, H. (1972) Concentration and origin of choline in the rat brain. *Naunyn Schmiedebergs Arch. Pharmacol.* 274:91-106.

65. Zeisel, S. H. (1985) Formation of unesterified choline by rat brain. *Biochim. Biophys. Acta* 835:331-343.

66. Choi, R. L., Freeman, J. J., and Jenden, D. J. (1975) Kinetics of plasma choline in relation to turnover of brain choline and formation of acetylcholine. *J. Neurochem.* 24:735-741.

67. Aquilonius, S. -M., Ceder, G., Lying-Tunell, U., Malmlund, H. O., and Schuberth, J. (1975) The arteriovenous difference of choline across the brain of man. *Brain Res.* 99:430-433.

68. Spanner, S., Hall, R. C., and Ansell, G. B. (1976) Arterio-venous differences of choline and choline lipids across the brain of rat and rabbit. *Biochem. J.* 154:133-140.

69. Pardridge, W. M., Cornford, E. M., Braun, L. D., and Oldendorf, W. H. (1979) *Nutrition and the Brain,* Vol. 5 (Barbeau, A., Growdon, J. H., and Wurtman, R. J., eds.) Raven Press, New York, pp. 25-34.

70. Wurtman, R. J. (1979) Precursor control of transmitter synthesis, in *Nutrition and the Brain, Vol. 5: Choline and Lecithin in Brain Disorders* (Barbeau, A., Growdon, J. H., and Wurtman, R. J., eds.) Raven Press, New York, pp. 1-12.

71. Cohen, E. and Wurtman, R. J. (1975) Brain acetylcholine: increase after systemic choline administration. *Life Sci.* 16:1095-1102.

72. Haubrich, D. R., Wan, P. F. L., Clody, D. E., and Wedeking, P. W. (1975) Increase in rat brain acetylcholine induced by choline or deanol. *Life Sci.* 17:957-980.

73. Jope, R. S. (1982) Effects of phosphatidylcholine administration to rats on choline in blood and choline and acetylcholine in brain. *J. Pharmacol. Exptl. Ther.* 220:322-328.

74. Tucek, S. (1985) Regulation of acetylcholine synthesis in the brain. *J. Neurochem.* 44:11-24.

75. Singh, A. K., Zeleznikar, R. J., Jr., and Drewes, L. R. (1986) Protection from quinidine or physostigmine against *in vitro* inhibition by sarin of acetylcholinesterase activity. *Life Sci.* 38:165-172.

76. Drewes, L. R. and Singh, A. K. (1985) Transport, metabolism and blood flow in brain during organophosphate induced seizures. *Proc. West. Pharmacol. Soc.* 28:191-195.

77. Bazán, N. G., Jr., De Bazán, H. E. P., Kennedy, W. G., and Joel, C. D. (1971) Regional distribution and rate of production of free fatty acids in rat brain. *J. Neurochem.* 18:1387-1393.

78. Yoshida, S., Ikeda, M., Busto, R., Santiso, M., Martinez, E., and Ginsberg, M. D. (1986) Cerebral phosphoinositide, triacylglycerol, and energy metabolism in reversible ischemia: origin and fate of free fatty acids. *J. Neurochem.* 47:744-757.

79. Ikeda, M., Yoshida, S., Busto, R., Santiso, M., and Ginsberg, M. D. (1986) Polyphosphoinositides as a probable source of brain free fatty acids accumulated at the onset of ischemia. *J. Neurochem.* 47:123-132.

80. Sun, G. Y. and Foudin, L. L. (1984) On the status of lysolecithin in rat cerebral cortex during ischemia. *J. Neurochem.* 43:1081-1086.

81. Estrada, C., Hamel, E., and Krause, D. N (1983) Biochemical evidence for cholinergic innervation of intracerebral blood vessels. *Brain Res.* 266:261-270.

82. Armstrong, D. M. (1986) Ultrastructural characterization of choline acetyltransferase-containing neurons in the basal forebrain of rat: evidence for a cholinergic innervation of intracerebral blood vessels. *J. Comp. Neurol.* 250:81-92.

83. Drewes, L. R. and Singh, A. K. (1988) Choline transport and metabolism in soman- or sarin-intoxicated brain. *J. Neurochem.* 50:868-875.

84. Ansell, G. B. and Spanner, S. (1975) The origin and metabolism of brain choline, in *Cholinergic Mechanisms* (Waser, P. G., ed.) Raven Press, New York, pp. 117-129.

85. Wykle, R. L. and Schremmer, J. M. (1974) A lysophospholipase D pathway in the metabolism of ether-linked lipids in brain microsomes. *J. Biol. Chem.* 249:1742-1746.

86. Wykle, R. L., Krammer, W. F., and Schremmer, J. M. (1980) Specificity of lysophospholipase D. *Biochim. Biophys. Acta* 619:58-67.

87. Linder, R. and Bernheimer, A. W. (1978) Effect of sphingomyelin-containing liposomes of phospholipase D from *Corynebacterium ovis* and the cytolysin from *Stoichactis helianthus*. *Biochim. Biophys. Acta* 530:236-246.

88. Whittaker, V. P. and Barker, L. A. (1972) The subcellular fractionation of brain tissue with special reference to the preparation of synaptosomes and their component organelles, in *Methods of Neurochemistry*, Vol. 2 (Friede, R., ed.) Marcel Dekker, New York, pp. 1-52.

89. Natarajan, V., Schmid, P. C., Reddy, P. V., Zuzarte-Augustin, M. L., and Schmid, H. H. O. (1983) Biosynthesis of N-acylethanolamine phospholipids by dog brain preparations. *J. Neurochem.* 41:1303-1312.

90. Lowry, O. H., Rosebrough, N. J., Farr, A. L., and Randall, R. J. (1951) Protein measurement with the Folin-phenol reagent. *J. Biol. Chem.* 193:265-275.

91. Bligh, E. G. and Dyer, W. J. (1959) A rapid method of total lipid extraction and purification. *Can. J. Biochem. Physiol.* 37:911-917.

92. Choy, P. C., Lim, P. H., and Vance, D. E. (1977) Purification and characterization of CTP: choline phosphate cytidyltransferase from rat liver. *J. Biol. Chem.* 252:7673-7677.

93. Chalifour, R. and Kanfer, J. N. (1982) Fatty acid activation and temperature perturbation of rat brain microsomal phospholipase D. *J. Neurochem.* 39:299-302.

94. Drewes, L. R. and Reddy, P. V. (18 September 1989) Metabolism, seizures, and blood flow in brain following organophosphate exposure: mechanisms of action and possible therapeutic agents. *Annual Summary Report*, USAMRDC Contract No. DAMD17-86-C-6036.

95. Qian, Z., Reddy, P. V., and Drewes, L. R. (1990) Guanine nucleotide-binding protein regulation of microsomal phospholipase D activity of canine cerebral cortex. *J. Neurochem.* 54:1632-1638.

96. Blasberg, R. G., Fenstermacher, J. D., and Patlak, C. S. (1983) Transport of α-aminoisobutyric acid across brain capillary and cellular membranes. *J. Cereb. Blood Flow Metabol.* 3:8-32.

97. Skipski, V. P. (1972) Lipid composition of lipoproteins in normal and diseased states, in *Blood Lipids and Lipoproteins: Quantitation, Composition, and Metabolism* (Nelson, G. J., ed.) John Wiley & Sons, Inc., New York, pp. 471-583.

98. Irving, H. R. and Exton, J. H. (1987) Phosphatidylcholine breakdown in rat liver plasma membranes. *J. Biol. Chem.* 262:3440-3443.

99. Lindmar, R., Loffelholz, K., and Sandmann, J. (1988) On the mechanism of muscarinic hydrolysis of choline phospholipids in the heart. *Biochem. Pharmacol.* 37:4689-4695.

100. Qian, Z. and Drewes, L. R. (1989) Muscarinic acetylcholine receptor regulates phosphatidylcholine phospholipase D in canine brain. *J. Biol. Chem.* **264**:21720-21724.

101. Feldberg, W. and Sherwood, S. L. (1954) Injection of drugs into the lateral ventricle of the cat. *J. Physiol.* **123**:148-167.

102. Jones, B. J. and Roberts, D. J. (1968) The effects of intracerebro-ventricularly administered noradnamine and other sympathomimetic amines upon leptazol convulsions in mice. *Brit. J. Pharmacol.* **34**:27-31.

103. Crunelli, V., Cervo, L., and Samarin, R. (1981) *Neurotransmitters, Seizures, Epilepsy* (Morselli, P. L., et al., eds.) Raven Press, New York.

104. Banister, E. W. and Singh, A. K. (1979) The time course of blood and brain catecholamines, ammonia and amino acids in rats convulsed by oxygen at high pressure. *Can. J. Physiol. Pharmacol.* **57**:390-395.

105. Lehmann, A. (1967) Audiogenic seizure data in mice supporting new theories of biogenic amine mechanisms in the central nervous system. *Life Sci.* **6**:1423-1431.

106. Prockop, D. J., Shore, P. A., and Brodie, B. B. (1959) Anticonvulsant properties of monoamine oxidase inhibitors. *Ann. N. Y. Acad. Sci.* **80**:643-651.

107. Schlesinger, K., Boggan, W., and Freedman, D. X. (1968) Genetics of audiogenic seizure: II. Effects of pharmacological manipulation of brain serotonin, norepinephrine and GABA. *Life Sci.* **7**:437-447.

108. Lassin, A. W. and Parkes, M. W. (1959) The effect of reserpine and other agents upon leptazol convulsions in mice. *Brit. J. Pharmacol.* **14**:108-111.

109. Pfeifer, A. K. and Galambos, E. (1967) Effect of reserpine, α-methyl-*m*-tyrosine, phenylalanine and guanethidine on metrazol convulsions and brain monoamine levels in mice. *Arch. Int. Pharmacodyn.* **165**:201-211.

110. De Schaepdryver, A. F., Plette, Y., and Delaunois, A. L. (1962) Brain amines and electroshock threshold. *Arch. Int. Pharmacodyn.* **140**:350-367.

111. Faiman, M. D., Mehl, R. G., and Myers, M. B. (1971) Brain norepinephrine and serotonin in central oxygen toxicity. *Life Sci.* **10**:21-34.

112. Boggan, W O. and Seiden, L. S. (1971) Dopa reversal of reserpine enhancement of audiogenic seizure susceptibility in mice. *Physiol. Behav.* **2**:215-217.

113. Browning, R. A. and Maynert, E. W. (1971) Role of body temperature in the monoamine induced facilitation of seizures. *Fed. Proc.* **20**:589.

114. Chen, G., Ensor, C. R., and Bohner, B. (1968) Drug effects on the disposition of active biogenic amines in the CNS. *Life Sci.* **7**:1063-1074.

115. Cox, B. and Lomax, P. (1976) Brain amines and spontaneous epileptic seizure in mongolian gerbil. *Pharmacol. Biochem. Behav.* **4**:263-267.

116. MacKenzie, E. T., McCulloch, J., and Harper, A. M. (1976) Influence of endogenous norepinephrine on cerebral blood flow and metabolism. *Am. J. Physiol.* **231**:489-494.

117. Brodie, B. B., Costa, E., Dlabac, A., Neff, N. H., and Smookler, H. H. (1966) Application of steady state kinetics to the estimation of synthesis rate and turnover time of tissue catecholamines. *Exp. Ther.* **154**:493-499.

118. Triguero, D., Lopez de Pablo, A. L., Gomez, B., and Estrada, C. (1988) Regional differences in cerebrovascular cholinergic innervation in goats. *Stroke* **19**:736-740.

119. Reddy, P. V., Banjac, B., and Drewes, L. R. (1987) Cholinergic agonists and organophosphate-induced metabolic and physiologic alterations in brain. *USAMRDC: Proc. 6th Medical Chemical Defense Biosci. Rev.*, pp. 417-420.

120. Drewes, L. R. and Singh, A. K. (1985) Cerebral metabolism and blood-brain transport: toxicity of organophosphorus compounds. *USAMRDC: Proc. 5th Medical Chemical Defense Biosci. Rev.*, pp. 427-437.

121. Edvinsson, L., Owman, Ch., and Sjöberg, N. -O. (1976) Autonomic nerves, mast cells, and amine receptors in human brain vessels. A histochemical and pharmacological study. *Brain Res.* **115**:377-393.

122. Edvinsson, L., Falck, B., and Owman, Ch. (1977) Possibilities for a cholinergic action on smooth musculature and on sympathetic axons in brain vessels mediated by muscarinic and nicotinic receptors. *J. Pharmacol. Exptl. Ther.* **200**:117-126.

123. Edvinsson, L. and Owman, Ch. (1974) Pharmacological characterization of adrenergic alpha and beta receptors mediating the vasomotor responses of cerebral arteries *in vitro*. *Circ. Res.* **35**:835-849.

124. Ekstrom-Jodal, B., von Essen, C., and Haggendal, E. (1974) Effects of noradrenaline on the cerebral blood flow in the dog. *Acta Neurol. Scand.* **50**:11-26.

125. Lowe, R. F. and Gilboe, D. D. (1971) Demonstration of alpha and beta adrenergic receptors in canine cerebral vasculature. *Stroke* **2**:193-200.

126. Winquist, R. J., Webb, R. C., and Bohr, D. F. (1982) Relaxation to transmural nerve stimulation and exogenously added norepinephrine in porcine cerebral vessels. A study utilizing cerebrovascular intrinsic tone. *Circ. Res.* **51**:769-776.

127. McCulloch, J. and Harper, A. M. (1977) Cerebral circulation: effect of stimulation and blockade of dopamine receptors. *Am. J. Physiol.* **233**:H222-H227.

128. Rönnberg, A. -L., Edvinsson, L., Larsson, L. -I., Nielsen, K. C., and Owman, Ch. (1973) Regional variation in the presence of mast cells in the mammalian brain. *Agent Action* **3**:191.

129. Drewes, L. R. and Reddy, P. V. (25 August 1989) Metabolism, seizures, and blood flow in brain following organophosphate exposure: mechanisms of action and possible therapeutic agents. *Annual Summary Report*, USAMRDC Contract No. DAMD17-86-C-6036.

130. Nishizuka, Y. (1984) Turnover of inositol phospholipids and signal transduction. *Science* **225**:1365-1370.

131. Kikkawa, U. and Nishizuka, Y. (1986) The role of protein kinase C in transmembrane signalling. *Ann. Rev. Cell Biol.* **2**:149-178.

132. Berridge, M. J. and Irvine, R. F. (1984) Inositol lipids trisphosphate, a novel second messenger in cellular signal transduction. *Nature* **312**:315-321.

133. Majerus, P. W., Neufeld, E. J., and Wilson, D. B. (1984) Production of phosphoinositide-derived messengers. *Cell* **37**:701-703.

134. Bocckino, S. B., Blackmore, P. F., and Exton, J. H. (1985) Stimulation of 1,2-diacylglycerol accumulation in hepatocytes by vasopressin, epinephrine, and angiotensin II. *J. Biol. Chem.* **260**:14201-14207.

135. Exton, J. H. (1988) Mechanisms of action of calcium-mobilizing agonists: some variations on a young theme. *FASEB J.* **2**:2670-2676.

136. Pelech, S. L. and Vance, D. E. (1989) Signal transduction via phosphatidylcholine cycles. *Trends in Biol. Sci.* **14**:28-30.

137. Cabot, M. C., Welsh, C. J., Cao, H. -T., and Chabbott, H. (1988) The phosphatidylcholine pathway of diacylglycerol formation stimulated by phorbol diesters occurs via phospholipase D activation. *FEBS Lett.* **233**:153-157.

138. Martin T. W. (1988) Formation of diacylglycerol by a phospholipase D-phosphatidate phosphatase pathway specific for phosphatidylcholine in endothelial cells. *Biochim. Biophys. Acta* **962**:282-296.

139. Besterman, J. M., Duronio, V., and Cuatrecasas, P. (1986) Rapid formation of diacylglycerol from phosphatidylcholine: a pathway for generation of a second messenger. *Proc. Natl. Acad. Sci. USA* **83**:6785-6789.

140. Slivka, S. R., Meier, K. E., and Insel, P. A. (1988) α_1-Adrenergic receptors promote phosphatidylcholine hydrolysis in MDCK-D1 cells. *J. Biol. Chem.* **263**:12242-12246.

141. Daniel, L. W., Waite, M., and Wykle, R. L. (1986) A novel mechanism of diglyceride formation. *J. Biol. Chem.* **261**:9128-9132.

142. Cotman, C. W., McCaman, R. F., and Dewhurst, S. A. (1971) Synaptosomal distribution of enzymes involved in the metabolism of lipids. *Biochim. Biophys. Acta* **249**:395-405.

143. Billah, M. M., Lapetina, E. G., and Cuatrecasas, P. (1981) Phospholipase A_2 activity specific for phosphatidic acid. *J. Biol. Chem.* **256**:5399-5406.

144. Dixon, J. F. and Hokin, L. E. (1984) Secretogogue-stimulated phosphatidylinositol breakdown in the exocrine pancreas liberates arachidonic acid, stearic acid, and glycerol by sequential actions of phospholipase C and diglyceride lipase. *J. Biol. Chem.* **259**:14418-14425.

145. Domino, S. E., Bocckino, S. B., and Garbers, D. L. (1989) Activation of phospholipase D by the fucose-sulfate glycoconjugate that induces an acrosome reaction in spermatozoa. *J. Biol. Chem.* **264**:9412-9419.

146. Koul, O. and Hauser, G. (1987) Modulation of rat brain cytosolic phosphatidate phosphohydrolase: effect of cationic amphiphilic drugs and divalent cations. *Arch. Biochem. Biophys.* **253**:453-461.

147. Abdel-Latif, A. and Smith, J. P. (1976) Effects of DL-propranolol on the synthesis of glycerolipids by rabbit iris muscle. *Biochem. Pharmacol.* **25**:1697-1704.

148. Brindley, D. N. and Bowley, M. (1975) Drugs affecting the synthesis of glycerides and phospholipids in rat liver. *Biochem. J.* **148**:461-469.

149. Eichberg, J., Shein, H. M., Schwartz, M., and Hauser, G. (1973) Stimulation of $^{32}P_i$ incorporation into phosphatidylinositol and phosphatidylglycerol by catecholamines and β-adrenergic receptor blocking agents in rat pineal organ cultures. *J. Biol. Chem.* **248**:3615-3622.

150. Taki, T., Nishimura, K., and Matsumoto, M. (1973) Incorporation of ethanolamine into phosphatidylethanolamine in mouse liver by exchange reaction. *Jpn. J. Exptl. Med.* **43**:87-105.

151. Taki, T. and Kanfer, J. N. (1979) Partial purification and properties of a rat brain phospholipase D. *J. Biol. Chem.* **254**:9761-9765.

152. Qian, Z. and Drewes, L. R. (1990) A novel mechanism for acetylcholine to generate diacylglycerol in brain. *J. Biol. Chem.* **265**:3607-3610.

153. Kikkawa, U., Takai, Y., Minakuchi, R., Inohara, S., and Nishizuka, Y. (1982) Calcium-activated, phospholipid-dependent protein kinase from rat brain. *J. Biol. Chem.* **257**:13341-13348.

154. McLeod, C. G., Jr., and Wall, H. G. (1987) Pathology of experimental nerve agent poisoning, in *Neurobiology of Acetylcholine* (Dun, M. J. and Perlman, R., eds.) Plenum Press, New York, pp. 427-435.

155. Lemercier, G., Carpentier, P., Sentenac-Roumanou, H., and Morelis, P. (1983) Histological and histochemical changes in the central nervous system of the rat poisoned by an irreversible anticholinesterase organophosphorus compound. *Acta Neuropathol. (Berl.)* **61**:123-129.

156. Nold, J. B. (February 1990) OP-induced pathology, introduction and overview. *Proceedings of the Workshop on Convulsions and Related Brain Damage Induced by Organophosphorus Agents*, pp. 11-17.

157. Bruni, J. and Wilder, B. J. (1979) Valproic acid. Review of a new antiepileptic drug. *Arch. Neurol.* **36**:393-398.

158. Abbott, F. S. and Acheampong, A. A. (1988) Quantitative structure-anticonvulsant activity relationships of valproic acid, related carboxylic acids and tetrazoles. *Neuropharmacol.* **27**:267-294.

159. Chapman, A., Keane, P. E., Meldrum, B. S., Simiand, J., and Vernieres, J. C. (1982) Mechanism of anticonvulsant action of valproate. *Prog. Neurobiol.* **19**:315-359.

160. Slater, G. E. and Johnston, D. (1978) Sodium valproate increases potassium conductance in Aplysia neurons. *Epilepsia* **19**:379-384.

161. Coult, D. B. and Marsh, D. J. (1966) Dealkylation studies on inhibited acetylcholinesterase. *Biochem. J.* **98**:869-873.

162. Meeter, E. and Wolthuis, O. L. (1968) The spontaneous recovery of respiration and neuromuscular transmission in the rat after anticholinesterase poisoning. *Eur. J. Pharmacol.* **2**:377-386.

163. Sidell, F. R. (1974) Soman and sarin:clinical manifestations and treatment of accidental poisoning by organophosphate. *Clin. Toxicol.* **7**:1-17.

164. Oldiges, H. and Schoene, K. (1970) Pyridinium and imidozolinium salze als antidote gegenuber soman und paraoxonvergiftung bei mausen. *Arch. Toxikol.* **26**:293-305.

165. Boskovic, B., Tadic, V., and Kusic, R. (1980) Reactivating and protective effects of Pro-2-PAM in mice poisoned with paraoxon. *Toxicol. Appl. Pharmacol.* 55:32-36.

166. Heffron, P. F. and Hobbiger, R. (1980) Does reactivation of phosphorylated AChE in the brain enhance the antidotal actions of pyridinium aldoximes? *Brit. J. Pharmacol.* 69:313-314.

167. Lundy, P. M. and Shih, T. -M. (1983) Examination of the role of central cholinergic mechanisms in the therapeutic effects of HI-6 in organophosphate poisoning. *J. Neurochem.* 40:1321-1328.

168. Kirsch, D., Hauser, W., and Weger, M. (1981) Effect of the bis-pyridinium oximes HGG 12 and HGG 42 and ganglionic blocking agent on synaptic transmission and NAD(P)H fluorescence in the superior cervical ganglion of the rat after soman poisoning *in vitro*. *Fund. Appl. Toxicol.* 1:169-176.

169. Amitai, G., Kloog, Y., Balderman, D., and Sokolovsky, M. (1980) The interaction bis-pyridinium oximes with mouse brain muscarinic receptors. *Biochem. Pharmacol.* 29:483-488.

170. Berry, W. K. and Davis, D. R. (1970) Use of carbamates and atropine in protection of animals against poisoning by 1,2,2,-trimethylpropyl methylphosphonofluoridate. *Biochem. Pharmacol.* 19:927-934.

171. Koster, R. (1946) Synergism and antagonism between physostigmine and diisopropyl-fluorophosphate in cats. *J. Pharmacol. Ther.* 88:39-46.

172. Gordon, J. J., Leadbeater, L., and Maidment, M. P. (1978) Protection of animals against organophosphate poisoning by a carbamate pretreatment. *Toxicol. Appl. Pharmacol.* 43:207-216.

173. Dirnhuber, P., French, M. C., Green, D. M., Leadbeater, L., and Stratton, J. A. (1979) Protection of primates against soman poisoning by pretreatment with pyridostigmine. *J. Pharm. Pharmacol.* 31:295-299.

174. Harris, L. W., Heyl, W. C., Stitcher, D. L., and Moore, R. D. (1978) Effect of atropine and/or physostigmine on cerebral acetylcholine in rats poisoned with soman. *Life Sci.* 22:907-910.

175. Drewes, L. R. (3 January 1991) Metabolism, seizures, and blood flow in brain following organophosphate exposure: mechanisms of action and possible therapeutic agents. *Annual Summary Report*, USAMRDC Contract No. DAMD17-86-C-6036.

176. Furchgott, R. F. (1983) The obligatory role of endothelium in response of vascular smooth muscle. *Circ. Res.* 53:557-573.

177. Marshall, J. J., Wei, E. P., and Kontos, H. A. (1988) Independent blockade of cerebral vasodilation from acetylcholine and nitric oxide. *Am. J. Physiol.* 255: H847-H854.

178. Rees, D. D., Palmer, R., Hodson, H. F., and Moucada, S. (1989) A specific inhibitor of nitric oxide formation from L-arginine attenuates endothelium-dependent relaxation. *Br. J. Pharmacol.* 96:418-424.

179. Ignarro, L. J., Byrns, R. E., Buga, G. M., and Wood, K. S. (1987) Mechanisms of endothelium-dependent vascular smooth muscle relaxation elicited by bradykinin and VIP. *Am. J. Physiol.* 253:H1074-H1082.

180. Standen, N. B., Quayle, J. M., Davies, N. W., Brayden, J. E., Huang, Y., and Nelson, M. T. (1989) Hyperpolarizing vasodilators activate ATP-sensitive K^+ channels in arterial smooth muscle. *Science* 245:177-180.

List of Publications[1] Supported by U. S. Army Medical Research and Development Command
Contract No. DAMD17-82-C-2136 (15 April 1982 - 20 October 1985) and
Contract No. DAMD17-86-C-6036 (21 October 1985 - 20 July 1990)

1. Drewes, L. R. and Singh, A. K. (1985) Perfused canine brain: metabolism and blood-brain transport during altered metabolic states. *Oxygen Transport to Tissue-VI* (Bruley, D., Bicher, H. I., and Reneau, D., eds.) Plenum Publishing Corp., New York, pp. 141-152.

2. Singh, A. K., Zeleznikar, R. J., Jr., and Drewes, L. R. (1985) Analysis of soman and sarin in blood utilizing a sensitive gas chromatography—mass spectrometry method. *J. Chromatogr.* **324**:163-172.

3. Singh, A. K. and Drewes, L. R. (1985) Improved analysis of acetylcholine and choline in canine brain and blood samples by capillary gas chromatography—mass spectrometry. *J. Chromatogr.* **339**:170-174.

4. Drewes, L .R. and Singh, A. K. (1985) Transport, metabolism and blood flow in brain during organophosphate induced seizures. *Proc. West. Pharmacol. Soc.* **28**:191-195.

5. Singh, A. K., Zeleznikar, R. J., Jr., and Drewes, L. R. (1986) Protection from quinidine or physostigmine against in vitro inhibition by sarin of acetylcholinesterase activity. *Life Sci.* **38**:165-172.

6. Drewes, L. R. and Singh, A. K. (1988) Choline transport and metabolism in soman- or sarin-intoxicated brain. *J. Neurochem.* **50**:868-875.

7. Qian, Z. and Drewes, L. R. (1989) Muscarinic acetylcholine receptor regulates phosphatidylcholine phospholipase D in canine brain. *J. Biol. Chem.* **264**:21720-21724.

8. Qian, Z. and Drewes, L. R. (1990) A novel mechanism for acetylcholine to generate diacylglycerol in brain. *J. Biol. Chem.* **265**:3607-3610.

9. Qian, Z., Reddy, P. V., and Drewes, L. R. (1990) Guanine nucleotide-binding protein regulation of microsomal phospholipase D activity of canine cerebral cortex. *J. Neurochem.* **54**:1632-1638.

10. Qian, Z. and Drewes, L. R. (1991) Cross-talk between receptor-regulated phospholipase D and phospholipase C in brain. *FASEB J.* **5**:315-319.

[1] Abstracts presented at scientific meetings are not included.

List of Personnel Supported by U. S. Army Medical Research and Development Command
Contract No. DAMD17-86-C-6036 (21 October 1985 - 20 July 1990)

Lester R. Drewes, Ph.D.
Padala V. Reddy, Ph.D.
David Z. Gerhart, Ph.D.
Margaret Broderius, M.A.
Borislav Banjac, M.D.
Steven Olson, B.S.
Zhuo Qian (granted doctorate degree April 1990)
Karrin Helgerson (graduate student one quarter)
Quynh Nguyen (summer worker)
Sandra Geegan (summer worker)
Deborah Pomroy-Petry
Gary Madison
William Bailey
Otmar Kloiber (visiting postdoctoral research associate)
Undergraduate student workers (dishwashing)

DISTRIBUTION LIST

1 copy:	Commander US Army Medical Research and Development Command ATTN: SGRD-RMI-S Fort Detrick Frederick, MD 21702-5012
5 copies:	Commander US Army Medical Research and Development Command ATTN: SGRD-PLE Fort Detrick Frederick, MD 21702-5012
2 copies:	Administrator Defense Technical Information Center ATTN: DTIC-FDAC Cameron Station Alexandria, VA 22314
1 copy:	Superintendent Academy of Health Sciences, US Army ATTN: AHS-COM Fort Sam Houston, TX 78234
1 copy:	Dean, School of Medicine Uniformed Services University of the Health Sciences 4301 Jones Bridge Road Bethesda, MD 20014